

Screening of seabed geological conditions for the offshore wind farm area North Sea I and the adjacent cable corridor area

Desk study for Energinet

Niels Nørgaard-Pedersen,
Thomas Vangkilde-Pedersen & Steen Lomholt

Screening of seabed geological conditions for the offshore wind farm area North Sea I and the adjacent cable corridor area

Desk study for Energinet

Niels Nørgaard-Pedersen, Thomas Vangkilde-Pedersen & Steen Lomholt

Content

1.	Dansk resumé	4
2.	Summary	6
3.	Introduction	8
4.	Available data	10
4.1	GEUS shallow seismic and sediment core archives	10
5.	Geological setting	12
5.1	Framework	12
5.2	Pre-Quaternary deposits	14
5.3	Quaternary deposits	15
5.4	Stratigraphic model and geological evolution of screening area	20
6.	Geological conditions of screening area	23
6.1	Bathymetry	23
6.2	Seabed surface sediments	24
6.3	Sediment cores	25
6.4	Seismic data	29
6.5	Geological/seismic units	29
7.	North Sea I OWF area	31
7.1	Seismic type profiles	31
7.2	Mapped seismic units	33
7.3	Conceptual geological model of OWF area	37
8.	Cable corridor area	39
8.1	Seismic type profiles	39
8.2	Seabed geological map	45
8.3	Mobile sand layer	45
9.	Key geological conditions	48
10.	Relative sea level changes and archaeological interests	52
10.1	Relative sea level changes	52
10.2	Archaeological implications	56
11.	Conclusions	58
12.	References	60

12.1	Background reports	61
12.2	Supplementary papers	62

Appendices

A. Maps

- A1: Screening area
- A2: Bathymetry
- A3: Seafloor sediment
- A4: Seismic lines and sediment core sites
- A5: Location of selected seismic profiles
- A6: OWF area - Holocene unit (isopach)
- A7: OWF area - Base Holocene unit (m below sea level)
- A8: OWF area - Weichsel Meltwater Unit (isopach)
- A9: OWF area - Eemian unit (isopach)
- A10: OWF area - Top Saale unit (m below sea floor)
- A11: OWF area - Top Saale unit (m below sea level)
- A12: Cable corridor – Geologic units below mobile sand
- A13: OWF and cable corridor key geological units

B. OWF area: Selected long seismic sections (1-6) with interpretation

C. Cable corridor area: Selected long seismic sections (7-14) with interpretation

D. Table with available sediment cores (with link to description)

1. Dansk resumé

Der er udført en detaljeret screening af de overfladenære geologiske forhold i Nordsøen i havmøllepark området og det tilgrænsende kystnære område hvor kabelkorridorer måtte planlægges. Området er karakteriseret ved en relativt god datatæthed med hensyn til dækning af shallow seismiske linjer og kortere vibrocore borer.

Nordsø I området er relativt lavvandet (15-38 m) og de øvre 50 m af havbunden består af kvartære glaciale og interglaciale aflejringer med vekslende sandede og lerede sedimenter. Under de kvartære enheder findes miocæne aflejringer også af sandet til leret sammensætning. Den centrale til østlige del af området er karakteriseret ved store kvartære begravede dale eller kanaler, der eroderer 300-400 m ned i miocæne aflejringer.

Kortlægning af de kvartære enheders basis/top og tykkelse har afsløret, at glaciale aflejringer fra Saale (forrige istid) eller ældre glacial periode findes meget tæt på havbunden i den centrale til sydlige del af Nordsø I området. De glaciale sedimenter kan forventes at være af heterogen sammensætning og overkonsolideret på grund af tidligere isbelastning og perioder med mellemliggende tørlægning. Sedimenterne består af lerholdige eller sandede moræner med variabelt stenindhold, deformerede glaciofluviale sedimentlag (sand, grus og ler) og stedvist med glaciotehtonisk forstyrrede flager af miocæne aflejringer (sand og ler). Lignende forhold med højtliggende deformerede til udeformerede glaciale enheder er observeret ved tidligere undersøgelser af Horns Rev 2, dele af Horns Rev 3 og Thor OWF områderne.

Glaciofluviale sedimenter fra både sen Saale og Weichsel istiderne forekommer som kanalelementer og som udbredte enheder, der delvist har udjævnet det ældre glaciale landskab. De ukonsoliderede glaciofluviale og glaciolakustrine sedimenter varierer mellem sandede og bløde silt-lerholdige underenheder. Bløde marine lerede sedimenter fra sidste mellemistid Eem er begrænset til den østlige del af området, hvor enheden når en tykkelse på omkring 5-10 m. Denne lerenhed kendes også fra den østlige del af Thor og Horns Rev 3 OWF områderne.

De øvre marine holocæne aflejringer består for det meste af fint til mellemkornet sand, men bløde siltede-lerede eller gyttje-lignende sedimenter optræder i udfyldte lavninger i den centrale til sydøstlige del af området. Tørvelag er kun observeret i et begrænset antal sedimentkerner, og typisk kun af få decimeters tykkelse.

Kabelkorridorområdet viser fra nord til syd ret forskellige sedimentenheder tæt på havbunden. Den nordøstlige del indeholder et glacialt kompleks med højtliggende glaciotehtonisk deformerede miocæne leraflejringer, hvorimod den sydlige del er domineret af Eem leraflejringer og kanaliserede holocæne aflejringer. I den vestlige del af området dominerer sandede glaciofluviale aflejringer fra sen Weichsel. Sen-holocæne mobile sandområder med store bundformer på toppen findes overvejende i den nordlige del af kabelkorridorområdet.

Der er foretaget en vurdering af relevante kulstof-14 dateringer af marint og terrestrisk materiale og eksisterende kurver for relativt havniveau af den Holocæne transgression af området. Det konkluderes, at forløbet af transgressionen af området må antages at have ligget

tæt på den globale havniveaukurve og den velunderbyggede havniveaustigningskurve for det nordvestlige Tyskland. I Nordsø I-området og den dybere del af kabelkorridorområdet kan der generelt kun forventes fund fra ældre stenalder. På grund af det generelt høje energiniveau af bølger og strøm, anses muligheden for fund fra yngre kulturer på lavt vand i kystzonen for at være ret lav.

2. Summary

Screening of the surface-near geological conditions in North Sea I offshore wind farm area and the adjacent near coast cable corridor area has led to a detailed understanding of the composition and structure of major Quaternary geological units and the general geological development. The area is covered by a quite dense network of shallow seismic data and sediment cores, sufficient for a general evaluation of the variability of soil conditions and suitability for OWF foundation and cable corridor location.

The North Sea I area is relatively shallow (15-38 m) and flat and the upper c. 50 m or more of the sub bottom is characterised by Quaternary glacial and interglacial deposits composed of interbedded sandy and clayey units. Below the Quaternary units, Miocene deposits also of sandy to clayey composition are found. The central to eastern part of the area is characterised by major Quaternary buried valleys or channels eroding 300-400 m into the Miocene sequence.

Mapping of the Quaternary unit's base/top and thickness has revealed that Saalian (penultimate glacial) or older glacial deposits are found very close to the seabed in the central to southern part of the North Sea I area. The glacial sediments can be expected to be of heterogeneous composition and over-consolidated, due to prior ice-loading and subaerial exposure. The sediments consist of clayey or sandy till with variable stone content, deformed glaciofluvial sediment layers (sand, gravel and clay) and locally glaciotectionally disturbed floes of Miocene sediments (sand and clay). A similar setting with high-lying Saalian deformed to undeformed glacial units was observed by earlier investigations of the Horns Rev 2 OWF area and parts of the Horns Rev 3 and Thor OWF areas.

Glaciofluvial sediments from both the late Saalian (penultimate) glacial period and the Weichselian (last) glacial period occur as channel elements and as major sheets, which have partly levelled the older glacial landscape. The unconsolidated glaciofluvial and -glaciolacustrine sediments are varying between sandy and soft silty-clayey subunits. Soft Eemian (last interglacial) marine clayey sediments are confined to the eastern part of the area where the unit reaches a thickness of about 5-10 m. This clay unit is also known from the eastern part of Thor and Horns Rev 3 OWF.

The uppermost marine Holocene unit is mostly composed of fine to medium grained sand but soft silty and clayey or even gyttja like sediments, possibly early Holocene, appear in filled-in depressions in the central to southeastern part of the area. Peat layers have only been observed in a limited number of sediment cores, and typically only a few decimetres in thickness.

Based on the mapping results of the North Sea I area and settings of nearby OWF's, it is concluded that North Sea I in general is suitable for foundation of wind turbines. However, the area exhibits different characters with respect to the level of the glacial surface, the occurrence of several hundred-meter-deep buried valleys and composition and thickness of surficial sediment units composed mostly of sandy or clayey deposits. The occurrence of soft marine clays with up to 10-20 m in total thickness in the eastern part of the area, as well as

minor areas in the western part, is a point of attention, as these areas may be less suitable for wind turbine foundation. The same clay unit was identified by Thor and Horns Rev 3 OWF integrated geological model studies and geotechnical parameters from these projects may thus serve as a guide for potential challenges and foundation solutions.

The cable corridor area shows from north to south quite different sediment units close to the sea floor. The northeastern part contains a glacial complex with high-lying glaciotectonically deformed Miocene clay deposits, whereas the southern part is dominated by Eemian clayey deposits and channelised Holocene deposits. In the western part of the area, Weichselian sandy glaciofluvial deposits dominate. Late Holocene mobile sand areas with large bedforms on top are predominantly found in the northern part of the cable corridor area.

An assessment has been made of existing relative sea level (RSL) curves for the Holocene transgression of the area and relevant dates of marine and terrestrial material. It is concluded that the RSL rise for the area has been very close to the global sea level curve and the well-constrained RSL curve for north-western Germany. In the North Sea I area and the deeper part of the cable corridor area, generally only finds from the older Stone Age can be expected. Due to the generally high energy level of waves and currents, the possibility for finds from younger cultures in shallow water in the coastal zone must be considered as quite low.

3. Introduction

Energinet has asked GEUS to perform a geological desktop screening study of the offshore wind farm (OWF) area North Sea I and the potential cable corridor area to the east of the wind farm area, along the central west coast of Jutland, Denmark. The results are to be used as background for evaluation of the suitability for wind farm sites and cable laying to land. This report compiles results of a previous screening of the OWF area (GEUS Rep. 2022-7) and extend this with available data and knowledge from the cable corridor area.

The OWF area extends from c. 20 km west of Ringkøbing Fjord along the west coast of Jutland and c. 30 km further west in the north and c. 60 km further west in the south. It covers an area of 2193 km². The adjacent cable corridor area between the OWF area and the shore-line covers an area of 1021 km² (Figure 3.1).

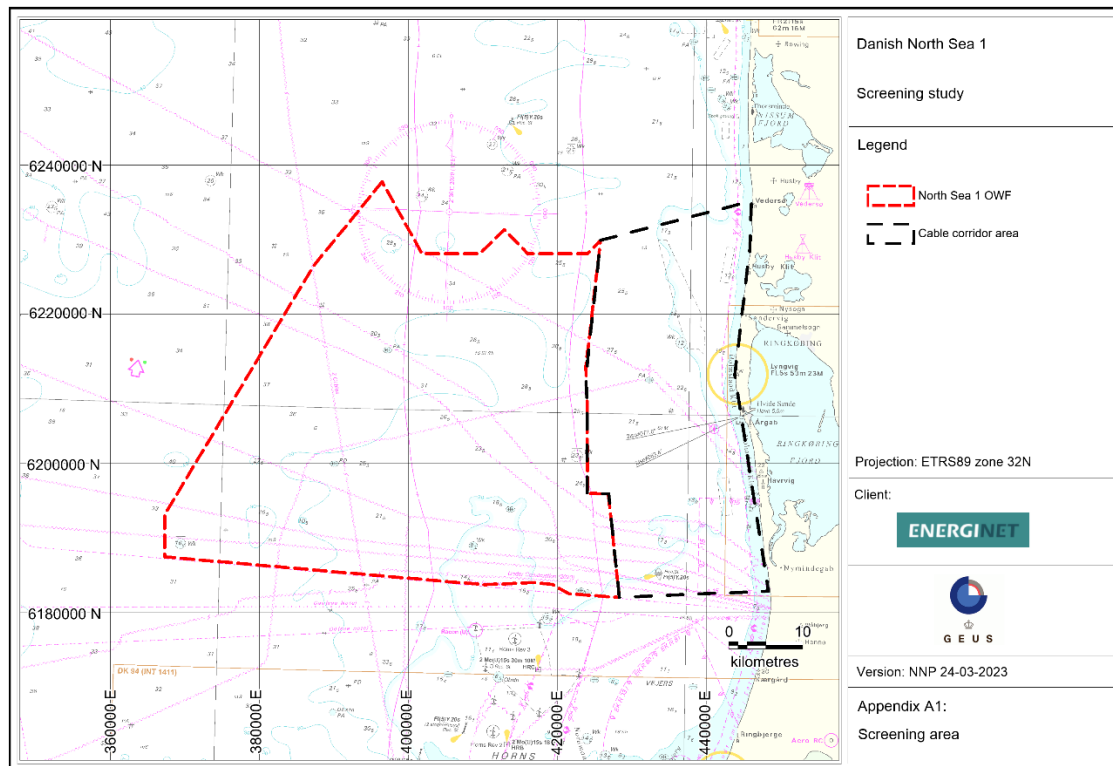


Figure 3.1. Screening area consisting of potential windfarm area (North Sea 1 OWF) with adjacent cable corridor area.

The screening study is based on existing data and include a description of the regional geological development of the Danish North Sea area and the establishment of a conceptual geological model for the understanding of the local geological conditions and possible implications for geotechnical conditions and archaeological interests.

The work is based on a combination of published reports, publications and archive seismic and sediment core data and includes detailed seismic mapping of specific surface-near geological units in the OWF area prepared for GEUS Rep. 2022-7 as well as new integrated

mapping of seismic data and sediment cores from the cable corridor area. The mapping results for the OWF area are presented as maps of thickness (isopach) and depth below sea level and sea floor of the identified main stratigraphic units. Moreover, selected interpreted seismic profiles with indicated stratigraphic/seismic units are presented. For the cable corridor area, selected interpreted seismic profiles are presented as well, and geological units immediately below the thin cover of mobile Holocene sand have been mapped out.

4. Available data

A combination of published work and GEUS' archive data have been used as a basis for this desktop screening study. The publications include technical reports from the Danish Energy Agency, the Danish Environmental Protection Agency (EPA), Energinet, GEO, GEUS as well as selected scientific publications on stratigraphy and relative sea level changes. The written material have been used together with shallow seismic data and vibrocore data from the [GEUS Marta database](#) (Figure 4.1).

4.1 GEUS shallow seismic and sediment core archives

The Marine raw material database (Marta) hosted by GEUS is developed in cooperation with the EPA and holds seismic data from raw material investigations, Natura-2000 area mapping, offshore windfarm projects, cable and bridge alignments in Danish waters. The database also links to information about sediment cores and grab samples in GEUS' borehole database (Jupiter) and to relevant reports from primarily raw material studies since 1980, but also from other studies.



Figure 4.1. Shallow seismic lines and sediment core/grab sites in the screening area in the Danish North Sea (from GEUS' Marta database).

The seismic data include both older analogue data and newer data in digital format. Most of the seismic lines can be downloaded directly from the web portal of the Marta database in SEG-Y file format.

The MARTA database further contains information on mapped raw material resource areas. This information is based on the results of processing and interpretation by GEUS of all reported raw material surveys and include the locations of the resource areas as well as the quality of the raw material deposits: resource type, geological formation type and resource certainty parameters (proven, probable, or speculative).

5. Geological setting

The screening area is situated off the central Danish west coast at water depths of about 0-30 m (Figure 5.1). Water depths in the OWF area is about 20-30 m, with the shallowest parts in the southern area north of Horns Rev.

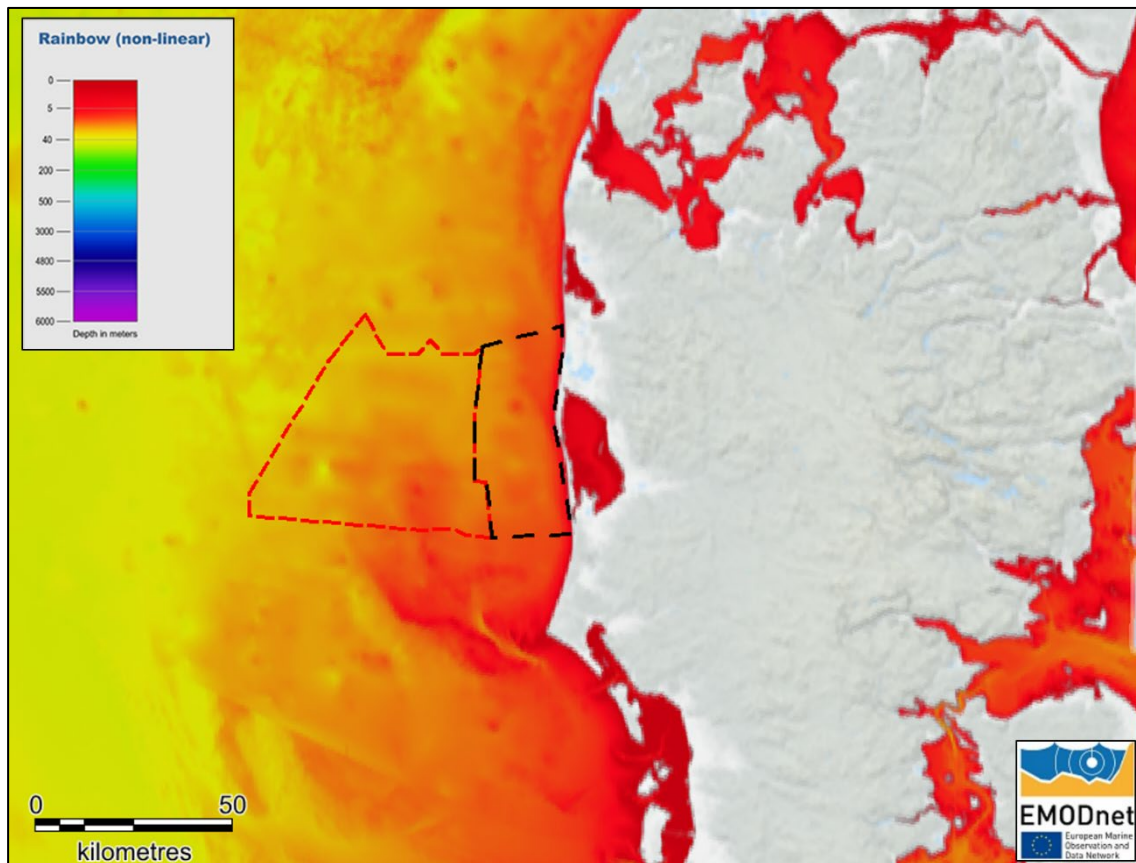


Figure 5.1 Bathymetrical map of the Danish North Sea with screening area Nordsøen I (red polygon) and adjacent potential cable corridor (black polygon) indicated (Bathymetry: EMODnet).

5.1 Framework

About 150 million years ago during the Jurassic and Cretaceous periods, the rifting that formed the northern part of the Atlantic Ocean, caused tectonic uplift of the British Isles. Since then, a shallow sea has almost continuously existed between the highs of the Fennoscandian Shield and the British Isles, growing and shrinking with the rise and fall of eustatic sea level during geological time. The deep tectonic structures in the North Sea area are dominated by the Ringkøbing-Fyn basement high and graben structures formed by rifting associated with the Alpine orogeny to the south.

The screening area is situated over the southern rim of the Danish Basin on the Ringkøbing-Fyn basement high and with the Horn Graben to the west (Figure 5.2). The area appears to

be very calm in terms of seismicity from earthquakes, especially compared to the area just north of the screening area (Figure 5.3).

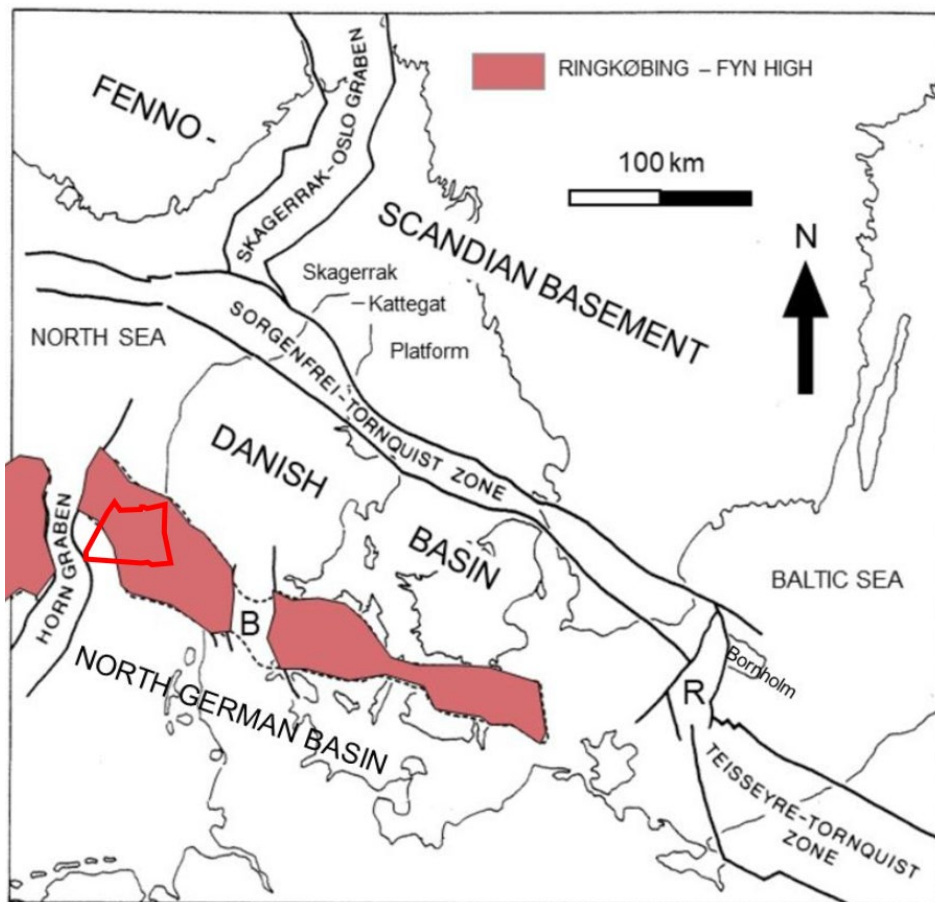


Figure 5.2 Structural elements of the Danish subsurface showing the Ringkøbing-Fyn High (red color) and the Horn Graben (from Gravesen et al., 2021). North Sea I area including cable corridor is indicated by red polygon.

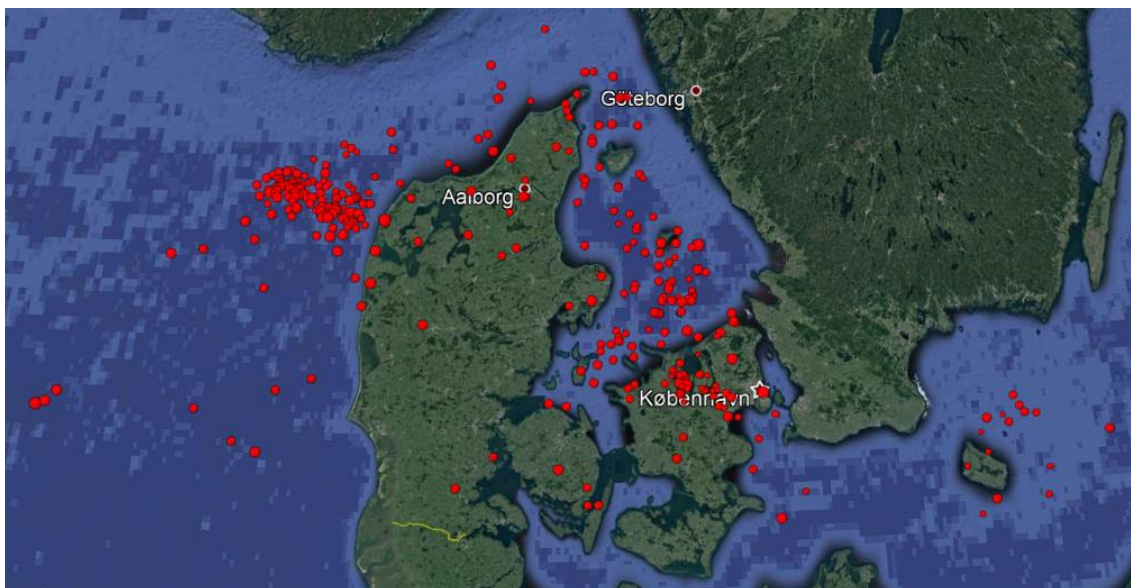


Figure 5.3 Seismicity in Denmark for the period 1930-2018 from GEUS earthquake database. Red dots show earthquake epicenters all determined using data from a minimum of three seismic stations. In addition to earthquakes the map may show data related to explosions which have not been removed (GEUS, 2018).

5.2 Pre-Quaternary deposits

Pre-Quaternary deposits in the screening area consists of Miocene sand and clay (Figure 5.4). Below the several hundred-meter-thick Miocene succession, Palaeogene and thick Cretaceous deposits are found. The oldest deposits in the screening area are probably sandstones and claystones of Lower Permian age to the north and sandstones, claystones and shales of Triassic age to the south. No, or only thin, Zechstein salt deposits are expected in the screenings area and no salt structures are expected. In contrast, further north, in the central parts of the Danish Basin, salt deposits are common and may show large variations in thickness due to salt movements into salt diapirs and salt pillows (Peryt et al., 2010).

During the Paleogene and the early part of the Neogene, sediment transport from the Scandinavian area into the North Sea basin from northeast and east was dominating. Onshore, west of the screening area, three phases of shoreline progradation into the basin in the Miocene gave rise to deposition of the sand-rich Billund, Bastrup and Odderup Formations, intercalated with the clayey and silty marine Vejle Fjord, Klintinghoved and Arnum Formations (Rasmussen et al., 2010).

Later in the Neogene, about 5 million years ago, the source of sediment transport into the North Sea changed to more southern areas. These include the Eridanos delta-system sourced from the Baltic Sea area and the later palaeo-Elbe system (Overeem et al., 2001; Ottesen et al., 2018).

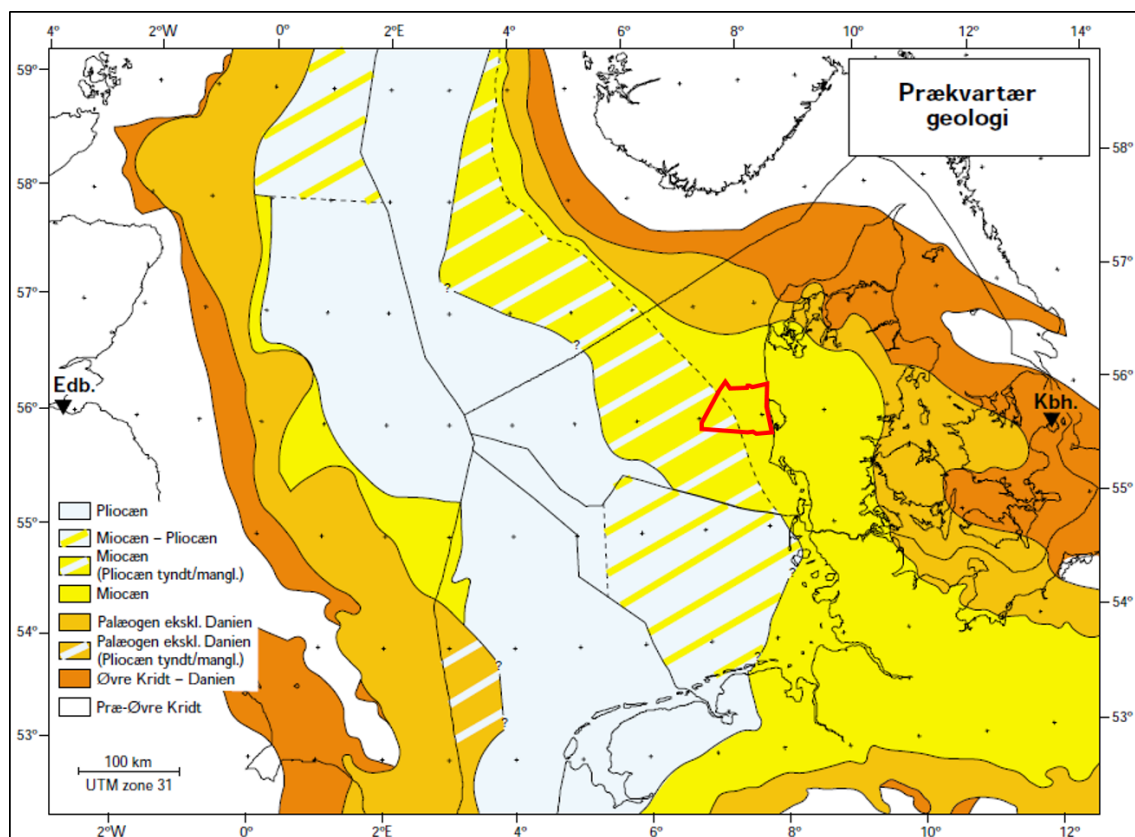


Figure 5.4. Pre-Quaternary geological units found below the base quaternary unconformity in the North Sea. (Japsen, 2000). North Sea I area including cable corridor is indicated by red polygon.

5.3 Quaternary deposits

The Quaternary deposits in the North Sea are mostly of glacial origin and deposited in pro- or subglacial environments intercalated with marine sediments from the warmer interglacial periods with high relative sea level.

The base of the Quaternary forms a marked erosional surface and is relatively shallow in the eastern part of the North Sea. Here, the thickness of the Quaternary deposits is typically only some tens of metres but increasing to the west and up to more than 1000 m in the Central Graben (Nielsen et al., 2008), see Figure 5.5.

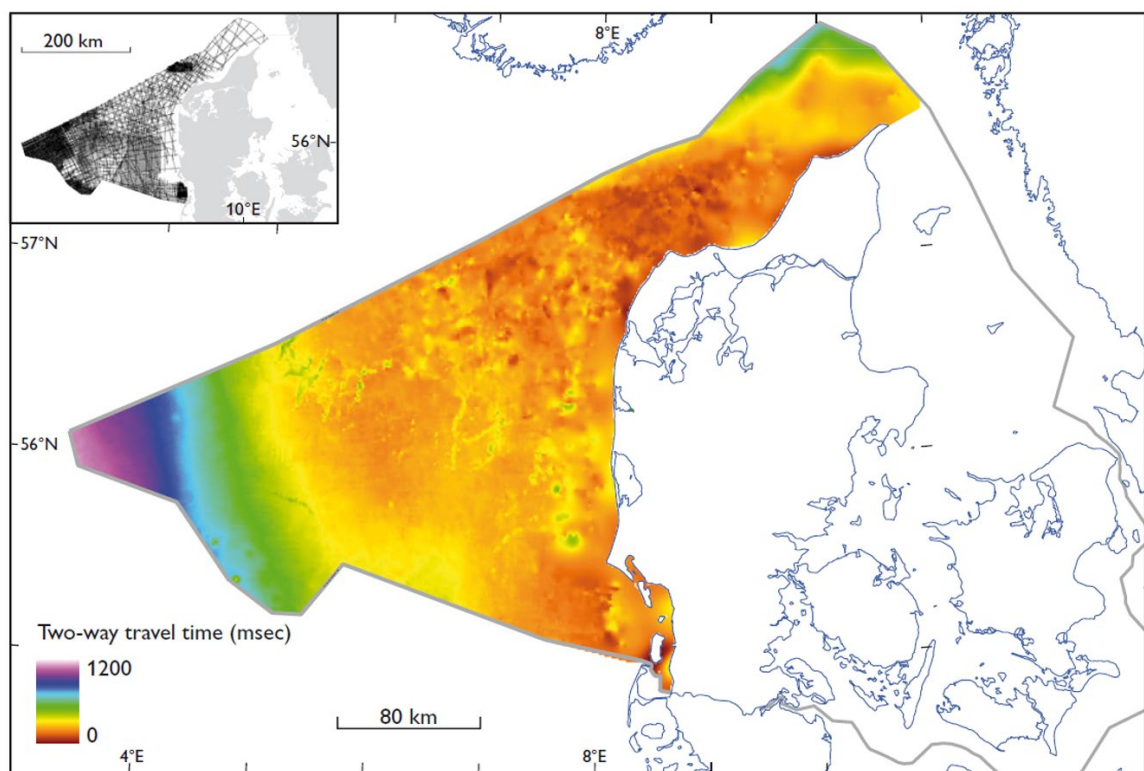


Figure 5.5. The depth to the base Quaternary surface in the Danish North Sea shown in seismic two-way travel time in milliseconds below sea surface (from Nielsen et al., 2008).

The North Sea was covered by the Scandinavian and British Ice Sheet several times during the Quaternary with the oldest traces of glaciations from c. 2,6 million years ago (Menapian, Elsterian, Saalian and Weichselian ice ages), see Figure 5.6. During the glaciations clayey and sandy till with stones and boulders was deposited as well as large volumes of sand in meltwater rivers and clay and silt in ice-dammed lakes. Till deposits from the Saalian glaciation occur at the seabed surface west of Horns Rev and northwest of Ringkøbing Fjord forming remnants of glacial hill islands (bakkeøer).

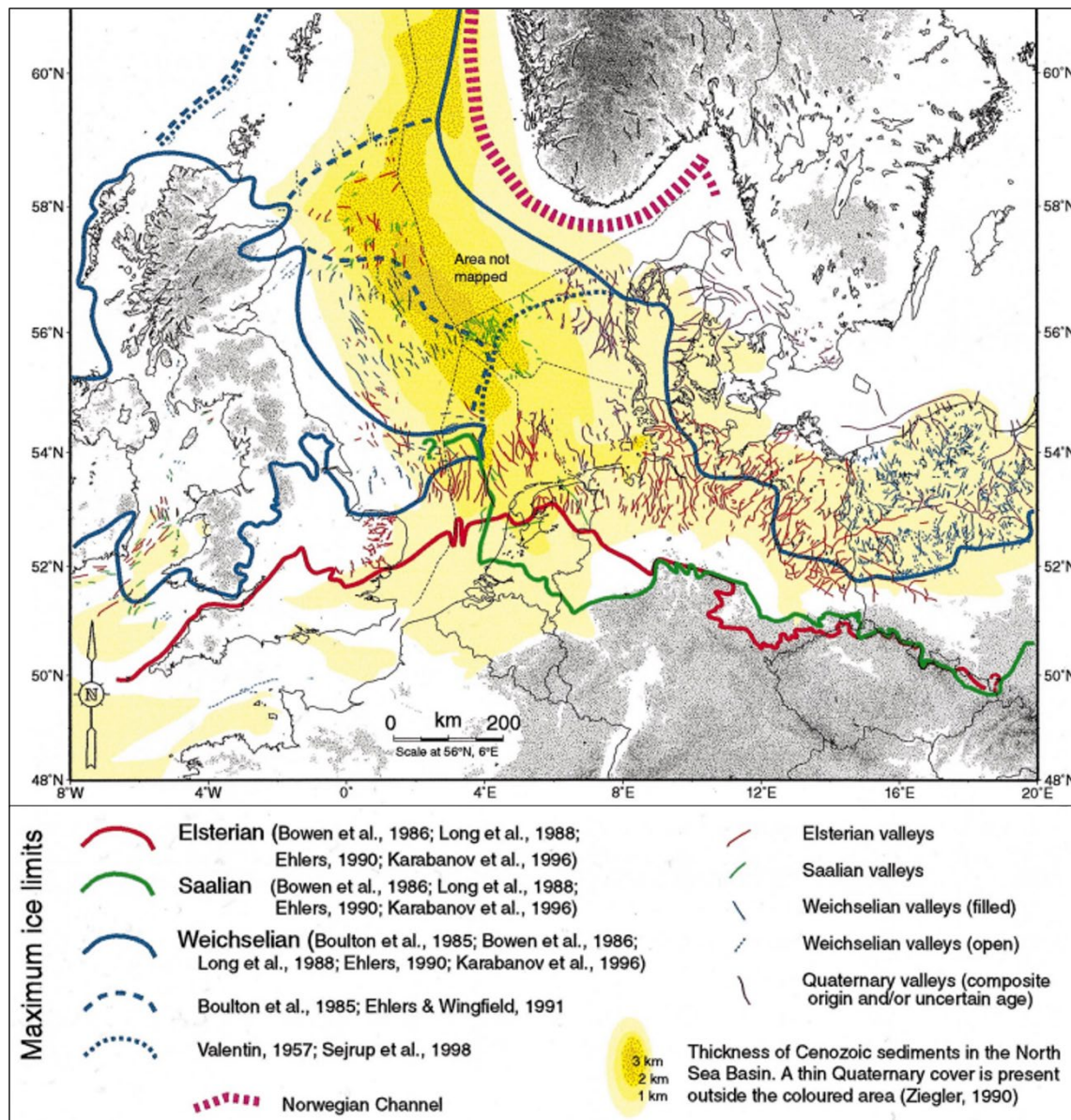


Figure 5.6. Estimated maximum ice sheet limits and mapped buried valley systems of the last three major glacial periods in the North Sea (from Huuse & Lykke-Andersen, 2000).

Between the ice ages, interglacial periods occurred (Cromerian, Holsteinian and Eemian) with a mild climate and high sea levels leading to deposition of marine sediments in the North Sea. Last interglacial Eemian marine sand, silt and clay appear in many areas and deposits from the older interglacials have also been found. Marine Eemian deposits have been verified in a number of sediment cores from the Wadden Sea area, Horns Rev and west of Ringkøbing Fjord, and in some parts the Eemian unit is exposed at the seabed (Figure 5.7). The Eemian unit forms a characteristic low amplitude transparent seismic unit, which has been identified in a number of seismic surveys within and near to the OWF area (Miljøstyrelsen 2019-2020 raw material mapping, Horns Rev 3 OWF, Thor OWF).

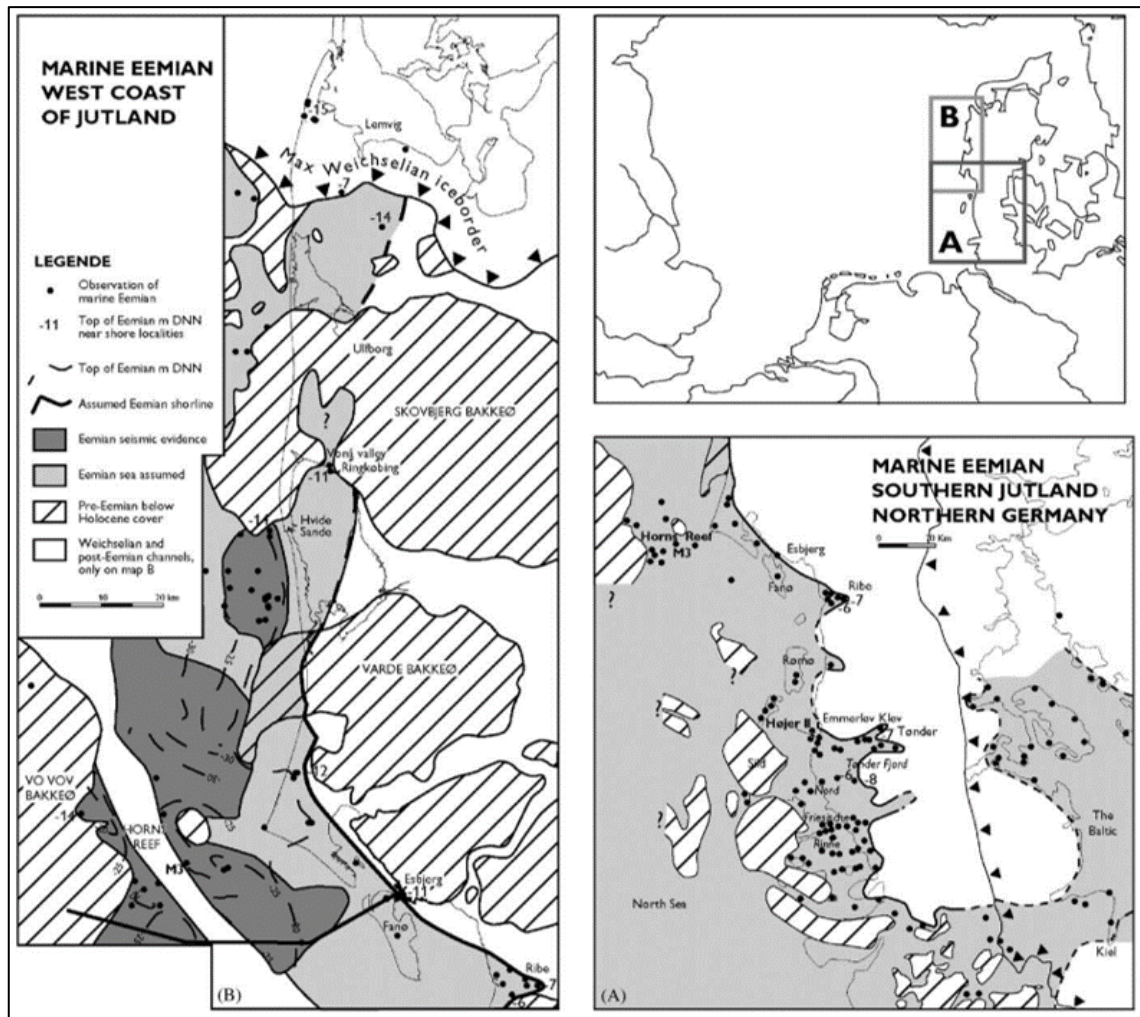


Figure 5.7. Occurrence of Eemian deposits on- and offshore the Danish west coast (Konradi et al., 2005).

Drainage of meltwater from the ice sheets formed large and widespread tunnel valleys and channel systems in the North Sea area often eroded deeply into the underlying pre-Quaternary formations (Huuse et al., 2001; Prins et al., 2020), and later filled with sediments and now appearing as so-called buried Quaternary valleys or palaeo-channels, see Figure 5.8. The buried valleys are primarily interpreted as subglacial tunnel valleys, although some have also been identified as subaerial river systems (Gaffney et al., 2007; Cotteril et al., 2017). Tunnel valleys are assumed to drain towards the ice margin and are therefore used to interpret maximum ice sheet extent during glaciations. Detailed 3D-seismic studies have confirmed that the tunnel valley systems are often of composite nature, with rejuvenation of parts of the systems during subsequent glaciations. The sediment infill of the buried valleys is generally heterogeneous and can vary from till to well sorted sand and gravel and lacustrine-marine clay deposits (O Cofaigh, 1996), while the deposits in the fluvial channels can also vary, but often contain well sorted, coarse-grained clastics (Gibling, 2006) and in places peat deposits rich in organic material (Coughlan et al., 2018; Hepp et al., 2017).

Huuse & Lykke-Andersen (2000) mapped out the extension of buried Quaternary valleys in the eastern part of the Danish North Sea. The valleys can typically be followed over tens of kilometres, are about 1-5 km wide and incised to more than 300 m below present sea level.

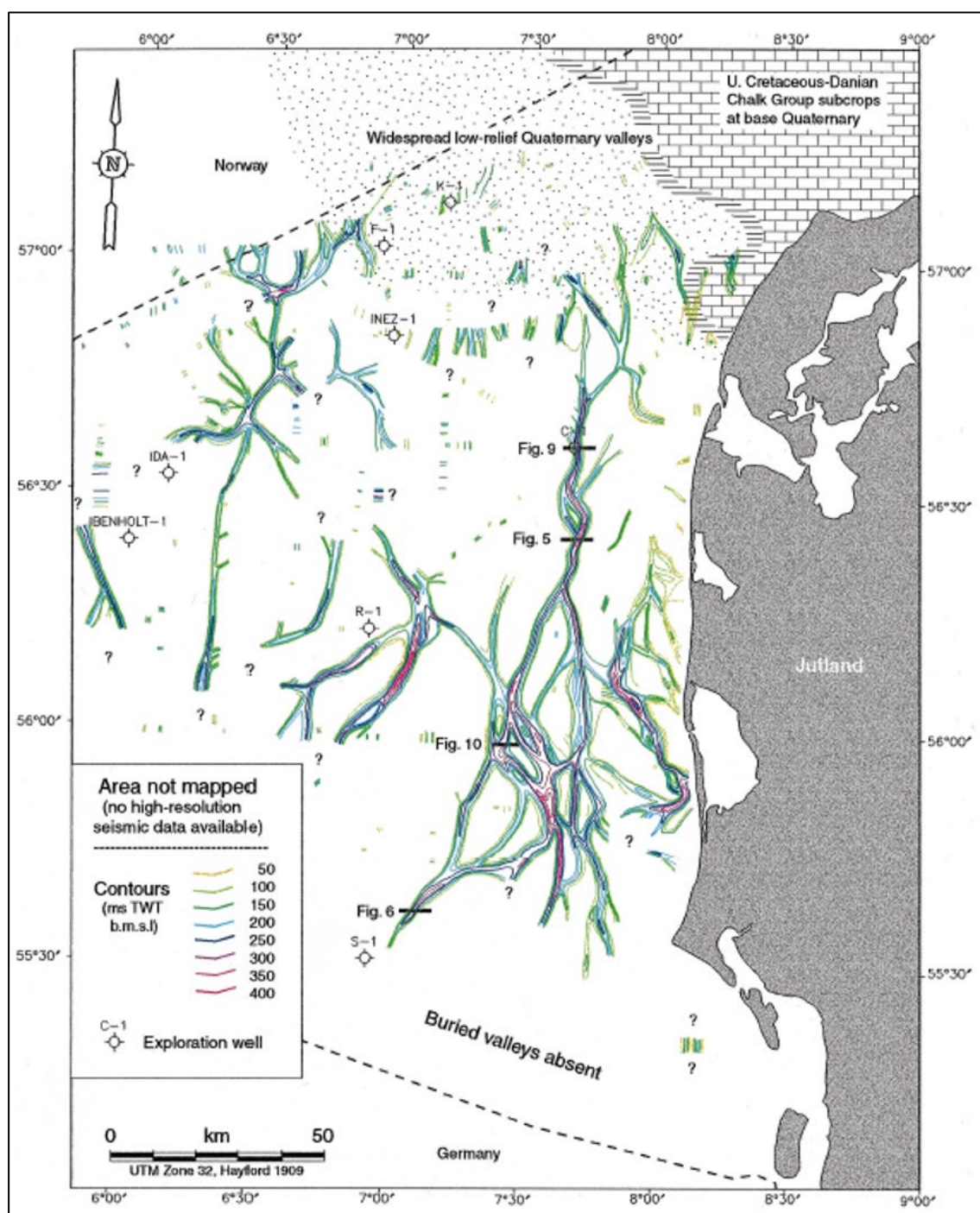


Figure 5.8. Mapped buried valleys in the eastern Danish North Sea (from Huuse & Lykke-Andersen, 2000a).

Figure 5.9 from the central part of the screening area shows a high-resolution multichannel seismic profile of a buried valley truncating glaciotectionic thrust structures in the eastern part of the profile.

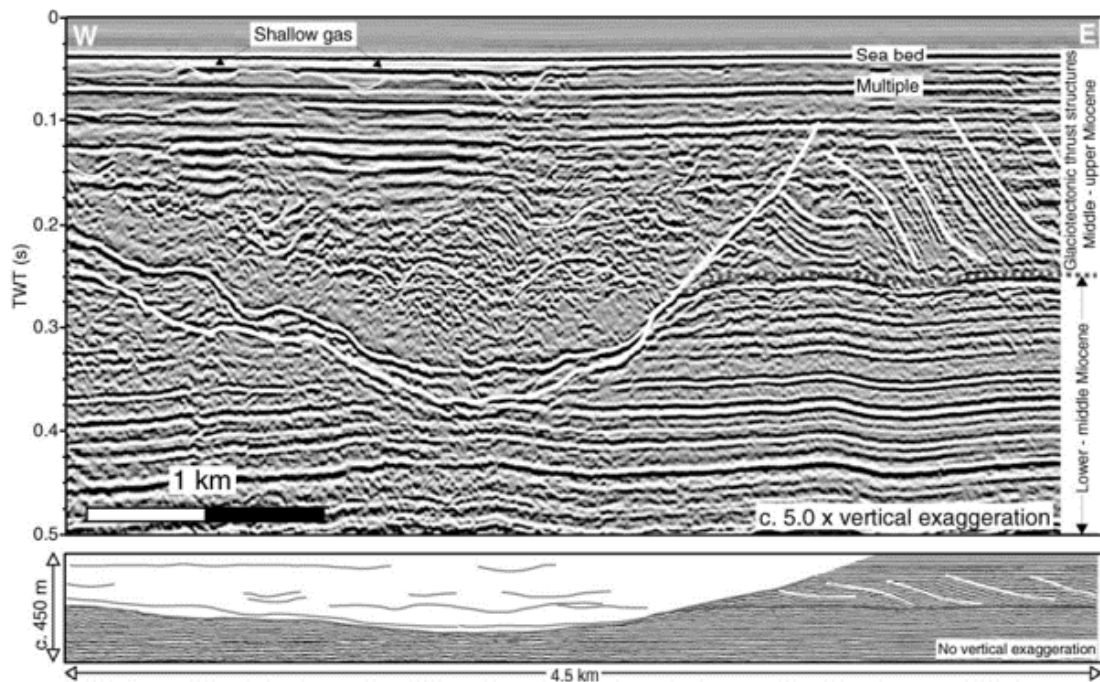


Figure 5.9. Example of multichannel seismic profile of a large buried valley eroded into pre-Quaternary layers in the central part of the screening area. The valley formation is postdating the formation of glaciotectionic thrust structures observed in the eastern part of the section (from Huuse & Lykke-Andersen, 2000).

Glaciotectionic deformations in terms of folding and thrust faults formed by glacier ice moving westwards have also been observed in e.g. Fanø Bugt, northwest of Horns Rev, and west of Ringkøbing Fjord.

During the latest glaciation (Weichselian), the relative sea level was generally low, and sandy fluvial deposits and clayey lake sediments are dominating, but glaciomarine deposits show that marine conditions occurred in the deeper part of the Danish North Sea (below c. 50 m) around 30000-50000 years BP (Knudsen, 1985; Larsen et al., 2009).

In late glacial time, the sea covered Skagerrak and the northern parts of the Danish North Sea, where the thickness of the ice sheet was at its maximum during the last glaciation and pressing down the crust. Local lakes with deposition of clay and gyttja existed in the shallower parts of the North Sea and peat deposits have been found throughout the North Sea from this period.

From about 10000 years BP the sea further transgressed into the North Sea (Figure 5.10), and during the next thousands of years, the current extent of the North Sea was formed. In the same period, the English Channel was inundated and the pattern of sea currents we know today was established and is now dominating the Norths Sea together with tide and wave energy.

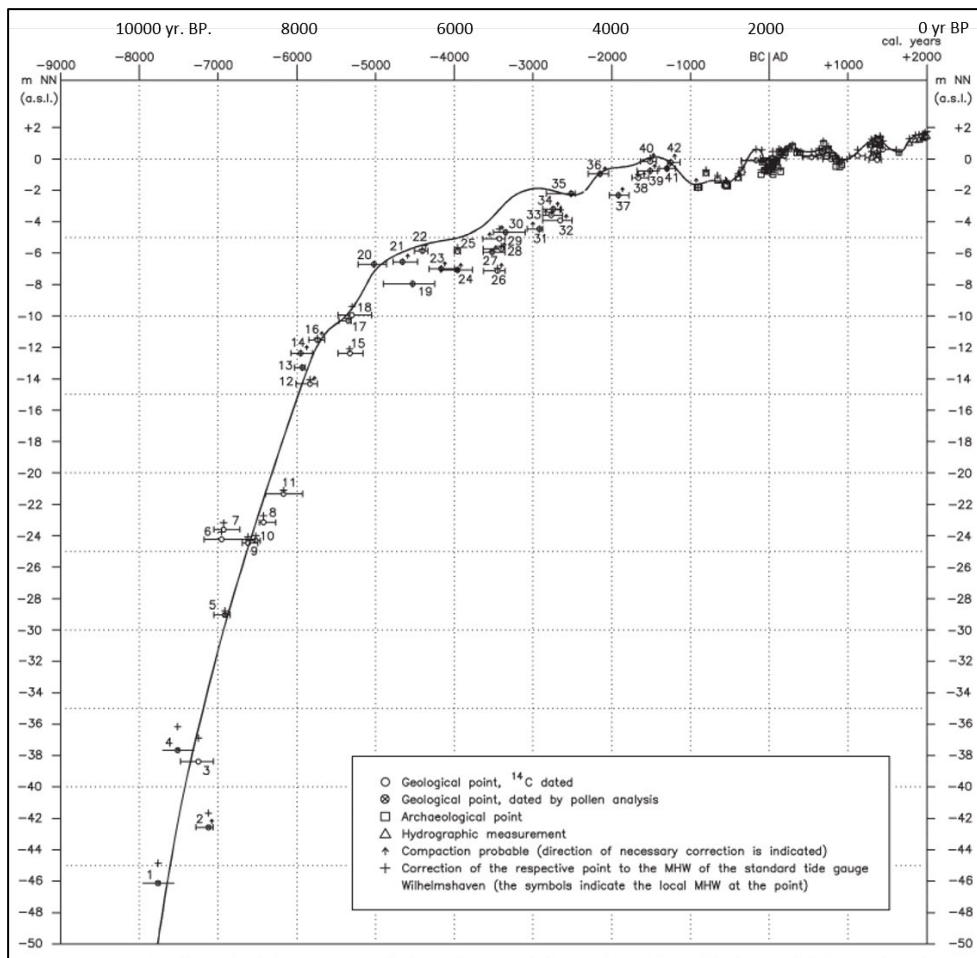


Figure 5.10. Relative sea-level curve for the southern North Sea during the last 10000 yr BP (Behre, 2007).

Deposition of sand is taking place along coastal sandbars and shallow banks with high energy level and the northbound Jutland Coastal Current is important for the deposition and transport of sediment along the west coast of Denmark (Anthony & Leth, 2002), while fine-grained material primarily is deposited in the deeper central parts of the North Sea (Bockelmann et al., 2018).

5.4 Stratigraphic model and geological evolution of screening area

Pre-Quaternary strata, most likely of Miocene age, comprise the basement of the Quaternary deposits generally located >50 m below the seabed. The Miocene deposits consist of weakly consolidated sand and clay units deposited in a fluvio-deltaic to shallow marine environment (Huuse & Lykke-Andersen, 2000b; Andersen, 2004; Rasmussen, 2017). Drainage of melt-water from Quaternary ice sheets have formed large buried channel systems eroded several hundred metres into the underlying pre-Quaternary formations (Huuse et al., 2001; Prins et al., 2020).

The Quaternary consists of glacial and interglacial deposits overlain by a variable cover of Holocene marine deposits. Above the pre-Quaternary surface is a lower glacial unit of Saalian and/or older age glacials (Larsen & Andersen (2005). The lower glacial unit forms a bank about 30 km offshore Blåvands Huk (Vovov hill island) and between the bank and the shore, the surface of the Saalian glacial landscape forms a wide depression c. 50 m below sea level, see Figure 5.11. This basin has controlled deposition in the area since the late Saalian and is filled with sediments of late Saalian (glacial), Eemian (interglacial), Weichselian (glacial) and Holocene (interglacial) age. Close to the coast northwest of Ringkøbing Fjord the seaward extension of another Saalian glacial hill island (Skovbjerg Bakkeø) occurs (Figure 5.7). Here glaciotectionised Miocene clayey deposits commonly occur right up to the seabed.

In the central parts of the basin, a 10-20 m thick layer of late Saalian meltwater sediments was deposited followed by up to 13 m of Eemian marine deposits of silty clay and sandy silt corresponding to a sea level high-stand, where the sea covered almost the entire area, except the Saalian glacial deposits at the Vovov hill island and the Skovbjerg Bakkeø. In the lowermost part of the Eemian succession freshwater deposits occasionally has been observed.

During the Weichselian, the sea level dropped again, and the area became land with rivers and lakes. The Weichselian ice sheet did not reach the southern part of the Danish North Sea, but it is generally assumed that the large alluvial outwash plains west of the ice margin in central Jutland extended into the North Sea area through valleys between hills in the old Saalian landscape (Houmark-Nielsen, 2003). Thus, Weichselian meltwater sediments partly eroding or covering the Eemian deposits in the area are probably remnants of distal alluvial fans mostly fed from north and east.

Following the final ice sheet retreat and general climate amelioration, a tundra landscape in the late glacial period was followed in the Holocene by a forest covered landscape with local rivers and streams. From about 9000-7000 years BP the area was progressively transgressed by the North Sea. During the first thousand years, the relatively shallow sea in the area may have been characterised by an isthmus and islands of higher-lying glacial deposits causing local sheltered marine- to brackish sea areas. However, as the sea rose, the entire area was inundated, and by establishment of the Jutland Coastal Current and increasing exposure to the harsh wind and wave conditions from the North Sea, the seabed was exposed to selective erosion and deposition of late Holocene mobile sand units, which are intricately related to the circulation and dynamic sediment transport pattern around Horns Rev.

Table 5-1 gives an overview of major stratigraphic units, lithology, depositional environments and estimated time ranges.

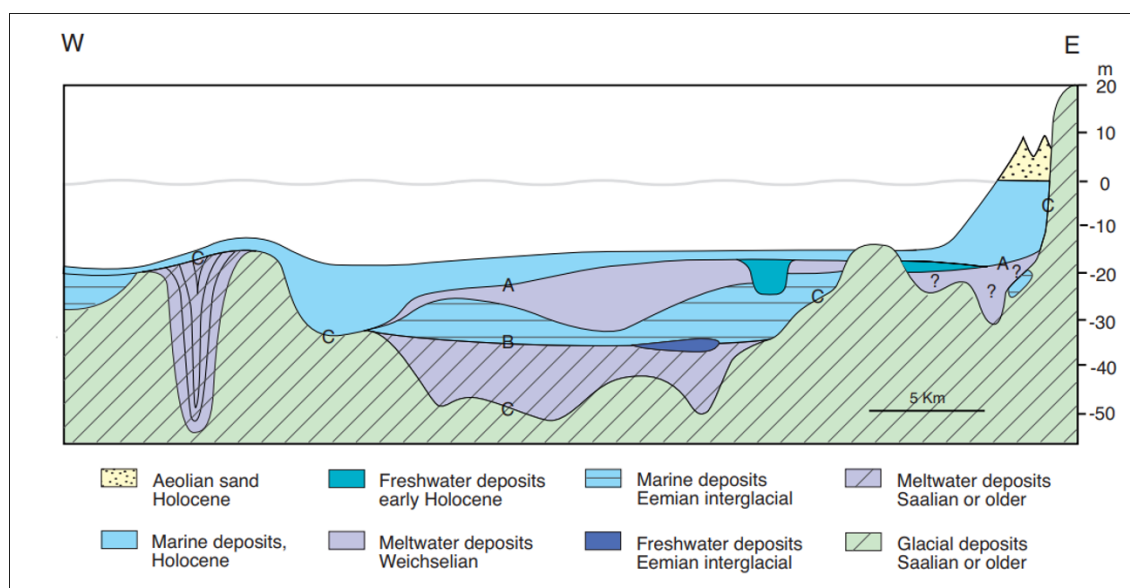


Figure 5.11. Schematic W-E profile across the wide basin in the Saalian landscape north of Horns Rev (approx. 55° 45' N). C marks the surface of the lower glacial unit of Saalian (or older) age and correlated with the Saalian hill island landscape onshore western Jutland and the Vovov hill island off Blåvands Huk. B marks the surface of a late Saalian meltwater unit. A mark the base of Holocene deposits (from Larsen & Andersen, 2005).

Table 5-1. Overview of major stratigraphic units.

Unit no.	Stratigraphic unit	Lithology	Depositional environment	Age (ka BP)
1	Holocene	Mostly well-sorted sand with shell fragments, lower part more fine-grained silty and clayey at channel/valley fill sites	Shallow marine	0-12.7
2	Weichselian	Sandy, occasionally gravelly sediment alternating with fine laminated clay-silt units	Glaciofluvatile/-lacustrine meltwater plain	12.7-120
3	Eemian	Silty clay with marine (interglacial) shells. Upper part occasionally sandier.	Shallow marine	120-130
4	Late Saalian	Sandy, occasionally gravelly sediment alternating with fine laminated clay-silt units	Glaciofluvatile/-lacustrine meltwater plain	Late Saalian
5	Saalian (or older)	Clayey-sandy till, buried valley fills and glaciotectionic units (incl. miocene deposits) with variable lithology	Sub-glacial	Saalian or older glacial period
6	Pre-Quaternary (Miocene)	Well-sorted sandy to clayey sediment. Quarts-rich and mica bearing, with plant and coal fragments	Shallow marine-fluvio-deltaic	Pre-Quaternary (Miocene)

6. Geological conditions of screening area

The shallow geology of the screening area is characterised by late Quaternary glacial and interglacial deposits overlain by a variable cover of Holocene marine deposits.

Pre-Quaternary strata, most likely of Miocene age, comprise the basement to the Quaternary deposits generally located >50 m below the seabed. In the near coastal zone cable corridor area northwest of Ringkøbing Fjord, Miocene deposits are found relatively close to the seabed and in some areas, it is directly exposed at the seabed.

Glacial deposits are presumably of Saalian or older glacial origin. A complex system of buried valleys of different magnitude characterises the glacial unit and superimposed non-marine sand units are possibly of late Saalian origin. Eemian (last interglacial) marine deposits probably covered much of the glacial landscape, but later erosion has removed larger parts of the unit. Proof of an Eemian age is based on scientific studies using micropalaeontological evidence and absolute dating (Konradi et al., 2005; Cohen et al., 2021). Superimposed Weichselian meltwater sand and silt/clay deposits represents large sandur plains and lake systems, which characterised the area during the late Weichselian period, when Scandinavian Ice Sheet front systems reached the central part of Jutland.

In Section 7 and 8, specific data and geological conditions for the North Sea I OWF area and the adjacent cable corridor area will be described separately.

6.1 Bathymetry

The bathymetry of the OWF screening area varies between c. 15 m in the shallowest southern part and about 38 m in the western part of the area (Figure 6.1). Two more or less parallel shallow sand bank areas in the south are progressively getting deeper towards the north. Depths in the cable corridor area are maximum c. 30 m.

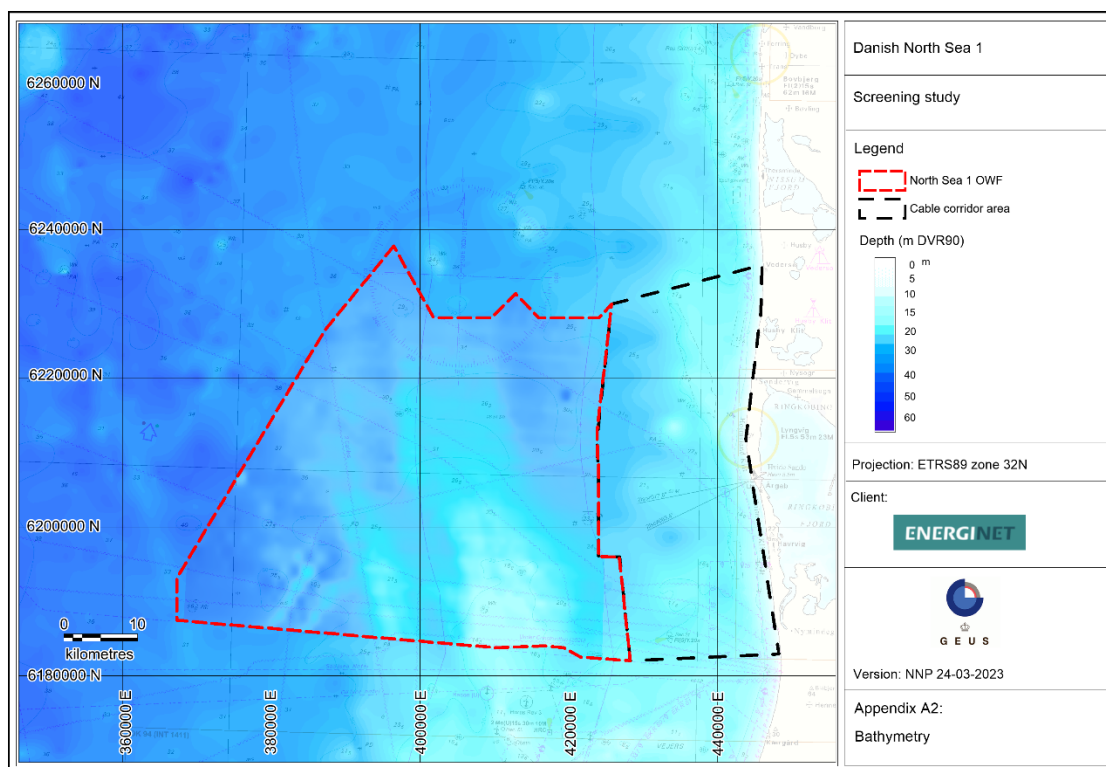


Figure 6.1. Bathymetry of screening area based on 2019 GEUS survey data overlain on background bathymetry data from the Danish Geodata Agency. Appendix A2.

6.2 Seabed surface sediments

The seabed surface sediment map shows that the screening area is dominated by a sandy seabed (Figure 6.2). Gravelly sand is second most common and occur in large irregular long stretched bands in the southwestern part of the area as well as in a zone northwest of Ringkøbing Fjord. Stone covered moraine/till seabed occurs only in relatively small areas (< 5 km²), typically associated with the gravelly sand areas. Fine-grained silty sand is observed in the southeasternmost part of the area. Quaternary clay-silt (subcropping Eemian) is observed at the seabed close to Ringkøbing Fjord.

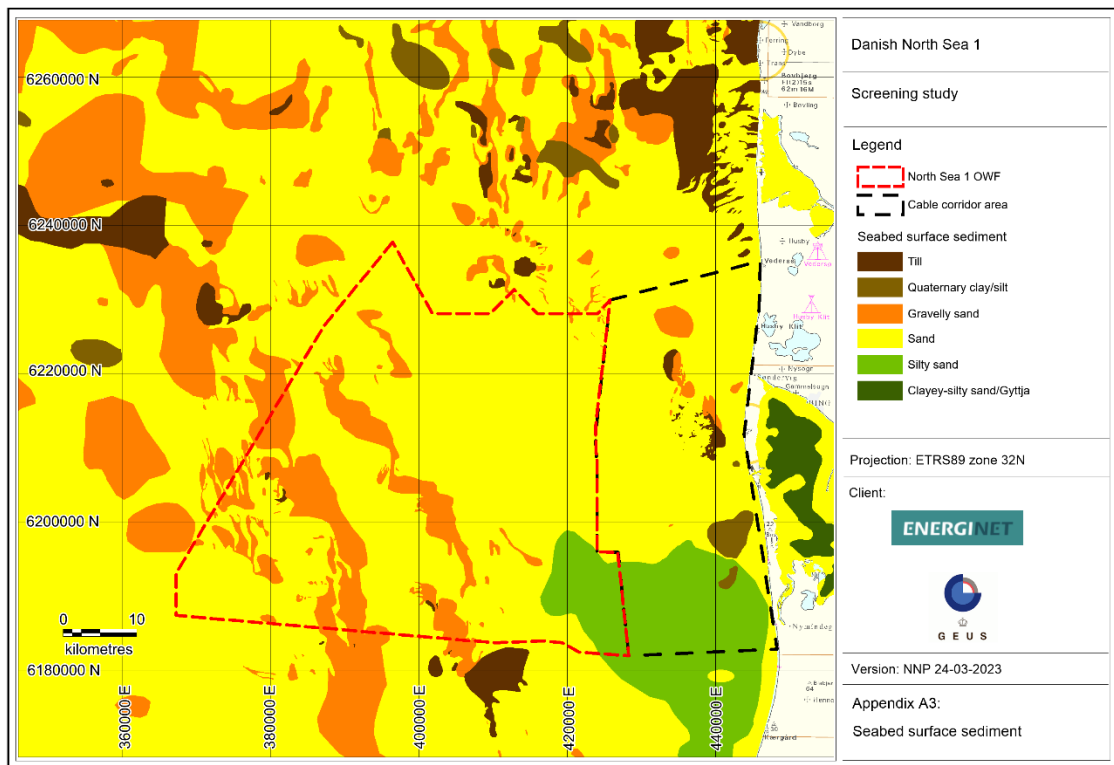


Figure 6.2. Seabed surface sediment map of the screening area (from GEUS' Marta database). Appendix A3.

6.3 Sediment cores

183 sediment cores located in and adjacent to the screening area were used for verification of seismic interpretations and general description of the near surface geology (Figure 6.3). Appendix D contains a list of all sediment cores including GEUS Marta database link to a detailed core description for each core. The cores are mostly vibrocores less than 6 m in length. However, longer cores up to c. 50 m in length from the Horns Rev 3 and Thor OWF areas also exist.

Figure 6.4 shows examples of descriptions of typical vibrocores. Cores 550706.21 and 560722.8 contain glacial and late glacial deposits overlain by early Holocene peat, marine gyttja and sand. Cores 550701.3 and 550723.5 contains glacial till (Saalian?) overlain by Eemian marine silty clay with numerous shells, Weichselian meltwater sand (termed late glacial in descriptions) and Holocene marine sand and gravel. Core 560730.4 contains meltwater sand and silt (possibly Weichselian) overlain by Holocene marine sand.

Figure 6.5 shows a description of one of the 50 m long sediment cores from the northern part of the Horns Rev 3 windfarm area, immediately to the south of the screening area. The core reveals Miocene sand and clay up to 36 m below sea floor. The Miocene sediments are overlain by a thin stony layer and sand up to 28 m below sea floor. Above this, an 18 m thick dark grey clay layer with shell fragments is found. The clay has in the core log description been assessed to be of Holocene age, but in light of scientific geological studies from the

Horns Rev area, it appears likely that the marine clay unit is of Eemian age. Above the clay layer, 10 m slightly gravelly Holocene marine sand is found.

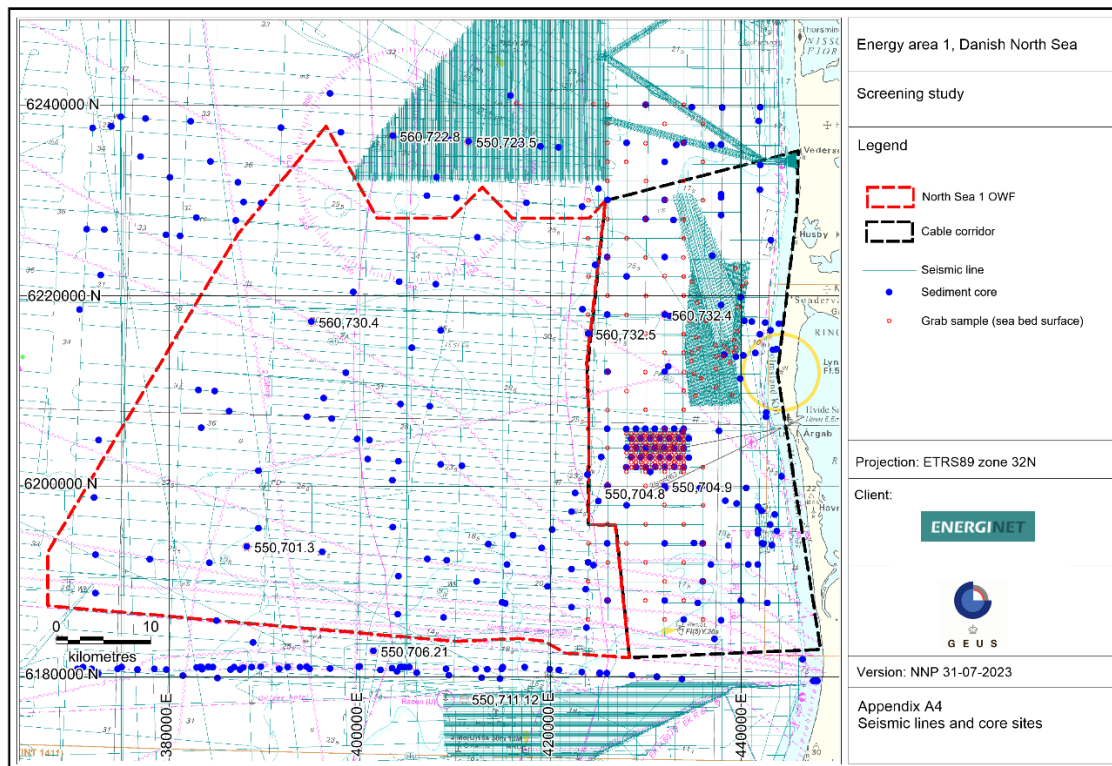


Figure 6.3. Seismic lines and sediment cores in and adjacent to the screening area. Appendix A4.

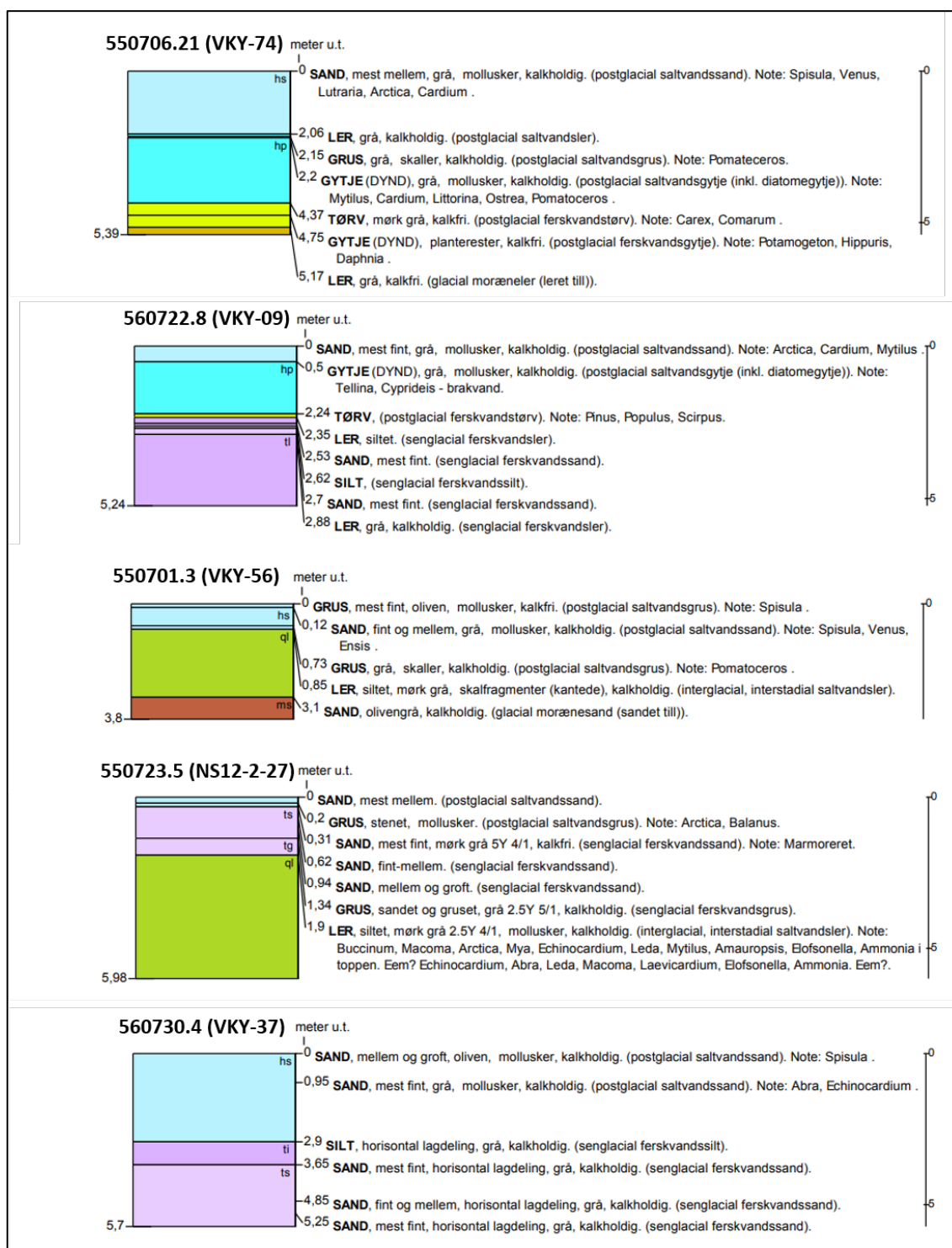


Figure 6.4. Examples of vibrocores up to 6 m long in and adjacent to the screening area (see Appendix C for further descriptions). Core locations are indicated at Figure 6.3.

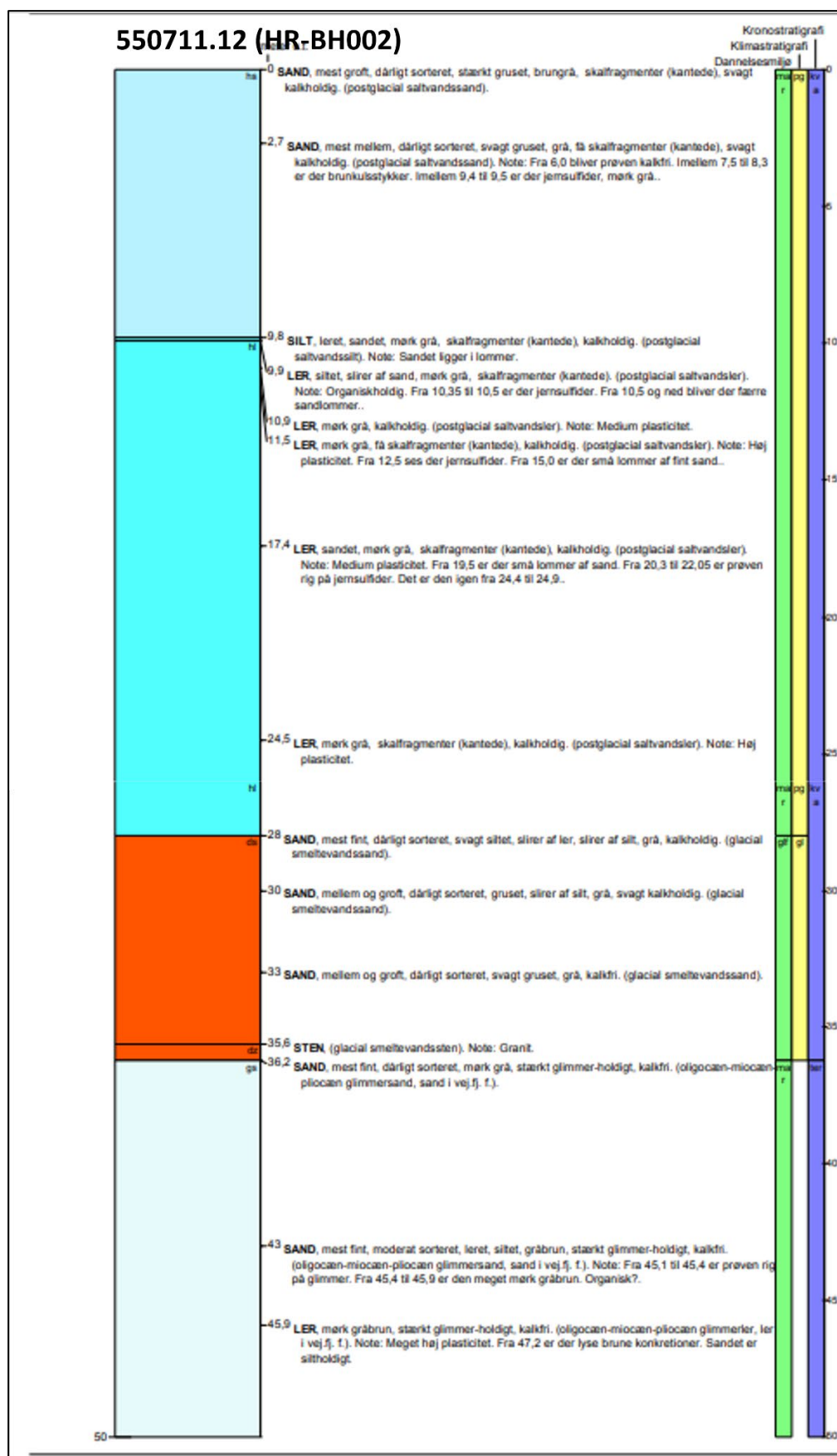


Figure 6.5. Example of 50 m long core from the northern part of the Horns Rev 3 wind farm area. Core location are indicated at Figure 6.3.

6.4 Seismic data

Seismic single channel sparker data from two regional raw material surveys for the EPA performed by GEUS in 2012 and 2019 was used for the screening study of the OWF area (Figure 6.3). In the cable corridor area, single channel sparker data was used from a mapping campaign by GEO for the Danish Coastal Authority (GEO, 2011a and 2011b), covering the coastal sector about 10-20 km from the coast. Data from the near-coastal fringe, about 1-10 km from the coast, consist mainly of older boomer seismic data performed by GEUS for the Danish Coastal Authority (GEUS Rep. 1999/75). Detailed data exist from Husby Klit dredging area northwest of Hvide Sande (GEUS Report 2021/21), where sand for coastal nourishment has been dredged for several decades. Moreover, Energinet performed an OWF investigation of the area Vesterhav Syd northwest of Hvide Sande in 2013, and in connection to this, GEUS performed data analysis in relation to potential archaeological interests (GEUS Rep. 2015/17).

Selected seismic data was reprocessed to enhance the signal/noise ratio. The GEUS 2012 dataset has a line distance of 2.5 km between east-west orientated lines, with few supplementary north-south orientated lines. The GEUS 2019 dataset which covers the central to eastern part of the OWF screening area, has lines placed between the 2012 lines, reducing the line distance in this part of the area to about 1.25 km. In the cable corridor area, the line distance is general 2x2 km, with some overlap between the near coastal older data and the outer sector newer data.

The single channel sparker data in the area generally allows detection of seismic reflectors down to about 50-60 ms TWTT (Two Way Travel Time) below seabed corresponding to about 40-50 m below seabed. However, high lying glacial till or Miocene deposits may limit the penetration considerably.

Processed seismic data in SEG-Y format was analysed in Kingdom and GeoGraphix seismic interpretation software. Seismic interpretation was performed with integration of available sediment cores.

6.5 Geological/seismic units

Seven distinct seismic units was identified and boundaries between units was traced on seismic profiles. Table 6-1 gives a general description of the seismic units as well as corresponding lithology (based on sediment core data), proposed depositional environment and stratigraphic age.

Table 6-1. Description of seismic units, corresponding lithology, depositional environment and estimated age.

Unit	Seismic reflection pattern	Lithology	Depositional environment	Age
1	Youngest unit, well defined medium amplitude parallel reflections, occasionally as sigmoidal fill of depressions	Mostly well-sorted sand with shell fragments, lower part more fine-grained at channel/valley fill sites	Shallow marine	Holocene
2	High amplitude reflection pattern, rare units in local depressions	Peat or gyttja sediment	Fen and lake	Early Holocene
3	High amplitude reflection pattern with discontinuous and undulating reflections, lower boundary distinct undulating (erosive)	Sandy, occasionally gravelly, sediment alternating with fine laminated clay-silt units	Glaciofluvial plain/glaciolacustrine lake	Weichselian
4	Transparent unit with low amplitude parallel reflections, where preserved, upper part with more distinct medium amplitude reflections	Silty clay with marine (interglacial) shells	Shallow marine	Eemian
5	High amplitude reflection pattern with discontinuous and undulating reflection, lower boundary distinct undulating (erosive)	Sandy, occasionally gravelly, sediment alternating with fine laminated clay-silt units	Glaciofluvial/-lacustrine meltwater plain	Late Saalian
6	Massive-chaotic reflections, distinct reflector marks upper boundary	Clayey-sandy till, buried valley fills and glaciotectionic units with more varied lithology: sand, silt, clay, gravel	Sub-glacial	Saalian or older glacial period
7	Parallel reflections, deformed and/or inclined layering is common	Well-sorted sandy to clayey sediment, often rich in mica minerals	Shallow marine-fluvio-deltaic	Pre-Quaternary (Miocene)

7. North Sea I OWF area

7.1 Seismic type profiles

Six long seismic sparker profiles 1-6 (Figure 7.1) were selected and presented with subdivision of main seismic units in order to demonstrate the variability of the seismic architecture in different parts of the screening area (Appendix B). The five west-east orientated profiles 1-5 are shown in Figure 7.2.

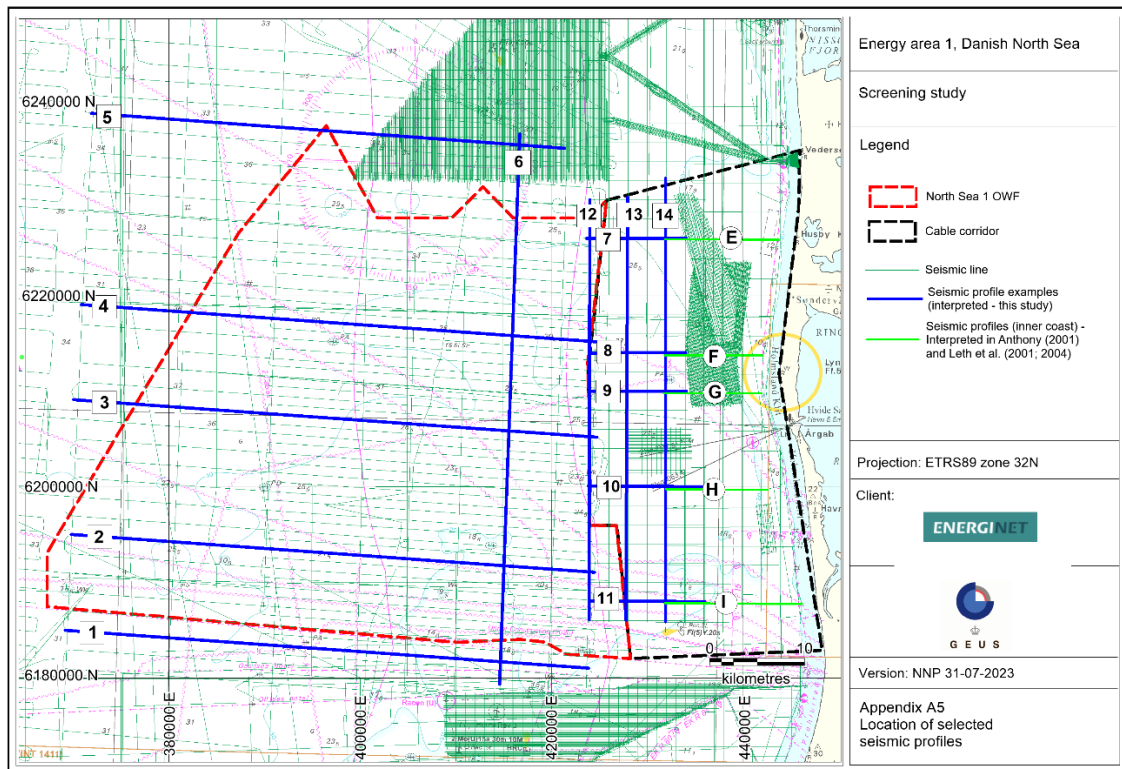


Figure 7.1. Location of selected seismic profiles. The blue marked profiles (1-14) have been interpreted in connection to the present screening project. The green marked profiles (E,F,G,H,I) from the inner coast have been interpreted in earlier studies.

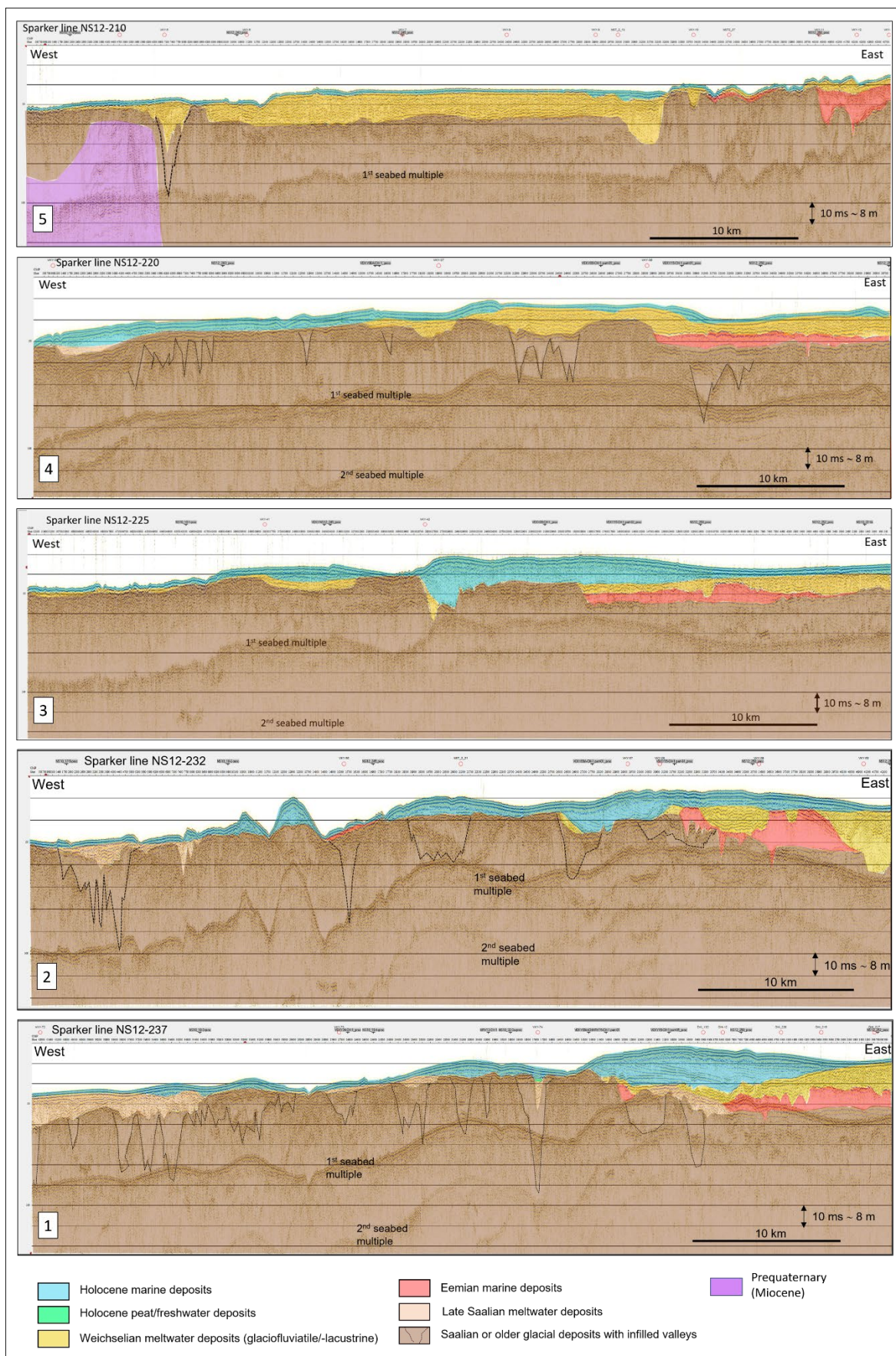


Figure 7.2. Interpreted seismic profiles (1-5) with colouration of main seismo-stratigraphic units. See Figure 7.1 for location of profiles and Appendix B for higher resolution.

7.2 Mapped seismic units

The seabed and boundaries between main seismic units were interpreted on the available seismic profiles. Gridded data files of the seismic surfaces (xyz grid files) were produced and exported for visualisation in GIS software and subsequent production of isopach maps (thickness) of specific units as well as maps of depth below seafloor and below sea level of the seismic units.

The following maps are presented in Figure 7.3 to Figure 7.10 below, and in larger scale in Appendix A:

A11 - Top of Saalian or older glacial unit (depth below sea level)

A10 - Top of Saalian or older glacial unit (depth below sea floor)

A9 - Eemian unit thickness (isopach map)

A8 - Weichselian Meltwater unit thickness (isopach map)

A7 - Base of Holocene unit (depth below sea level)

A6 - Holocene unit thickness (isopach map)

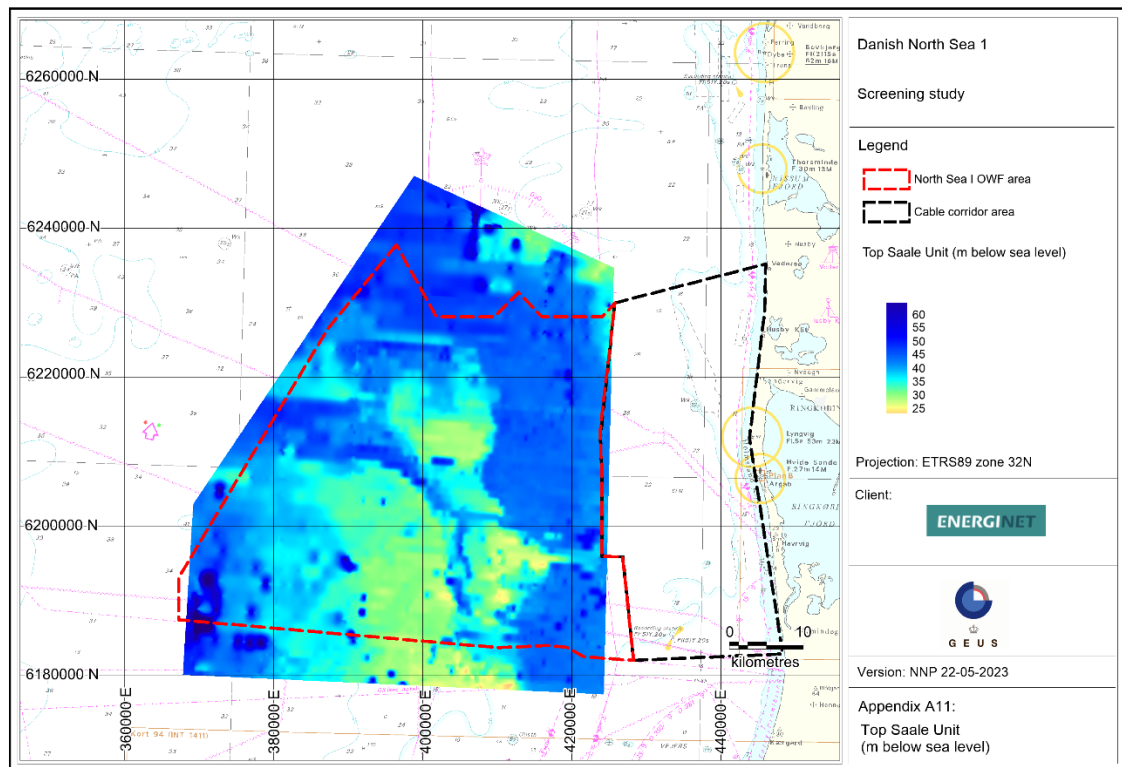


Figure 7.3. Mapped Top Saale Unit (m below sea level). Appendix A11.

The map in Figure 7.3 shows how the top of the Saalian or older unit lies deepest (c. 50 m below sea level) in the eastern, northern and westernmost part of the mapped area and more shallow in the central-southern part (c. 25-30 m below sea level).

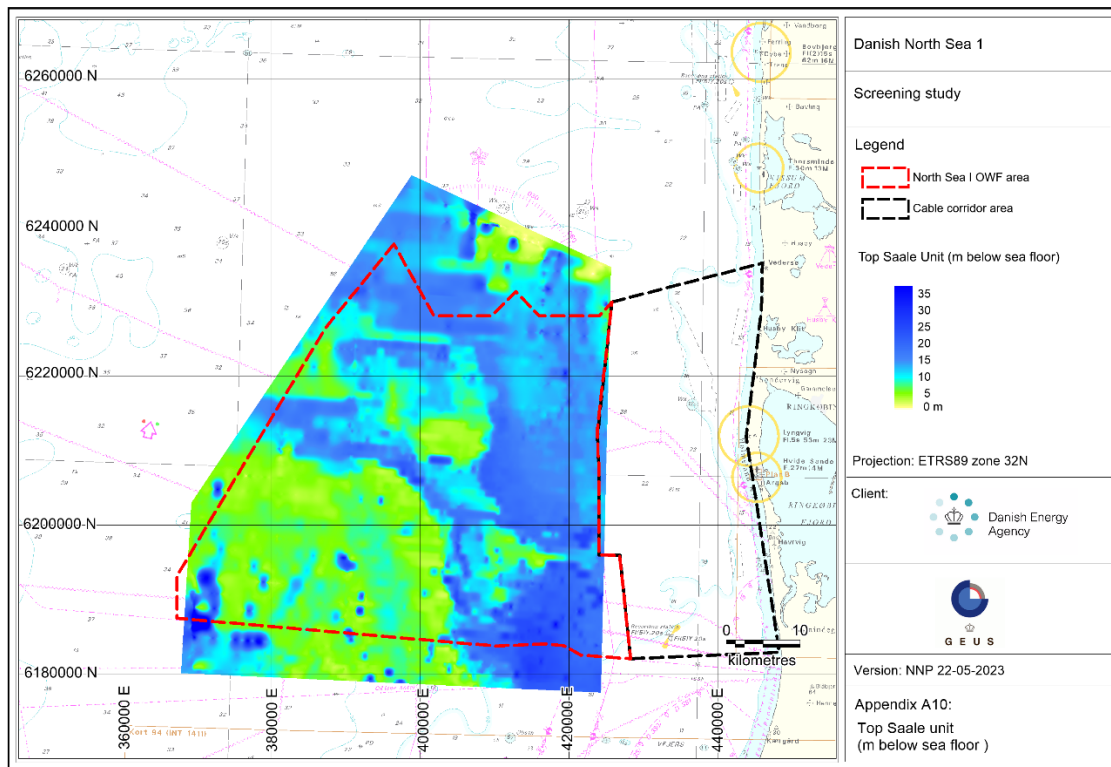


Figure 7.4. Mapped Top Saale Unit (m below sea floor). Corresponds to isopach map of superimposed deposits. Appendix A10.

The map in Figure 7.4 shows that the thickness of the deposits above the Saalian or older unit is up to 15-30 m in the eastern and northern part of the mapped area and around 5 m or less in the southwestern part. In Figure 7.5 the corresponding mapped base of non-glaciated layers in Thor OWF (COWI, 2021) is shown.

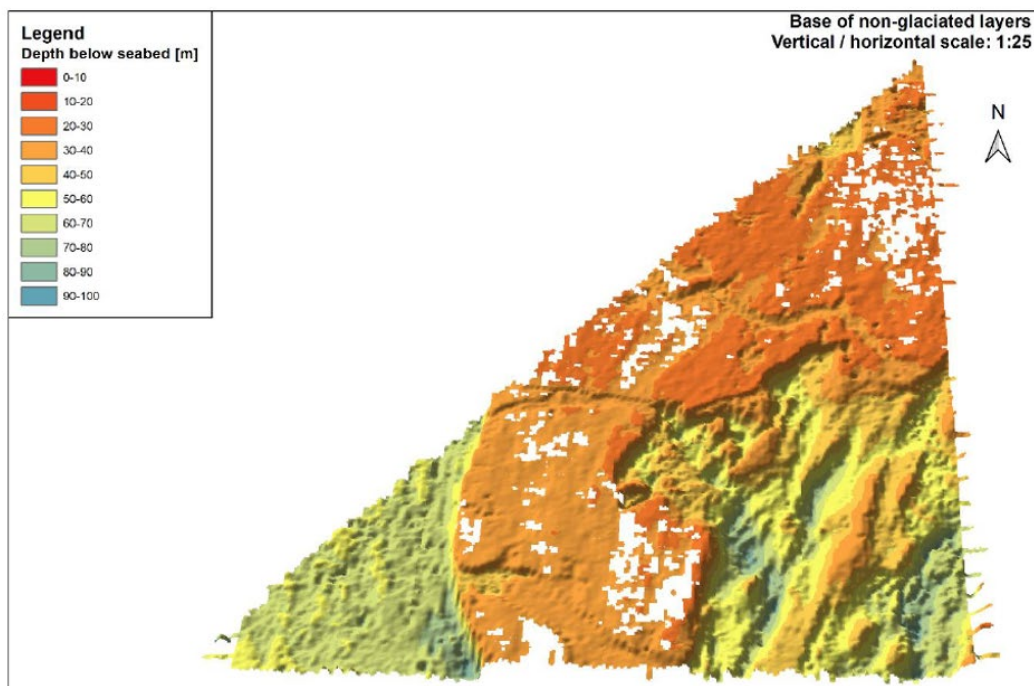


Figure 7.5. Detailed mapped base of non-glaciated layers in Thor OWF (COWI, 2021).

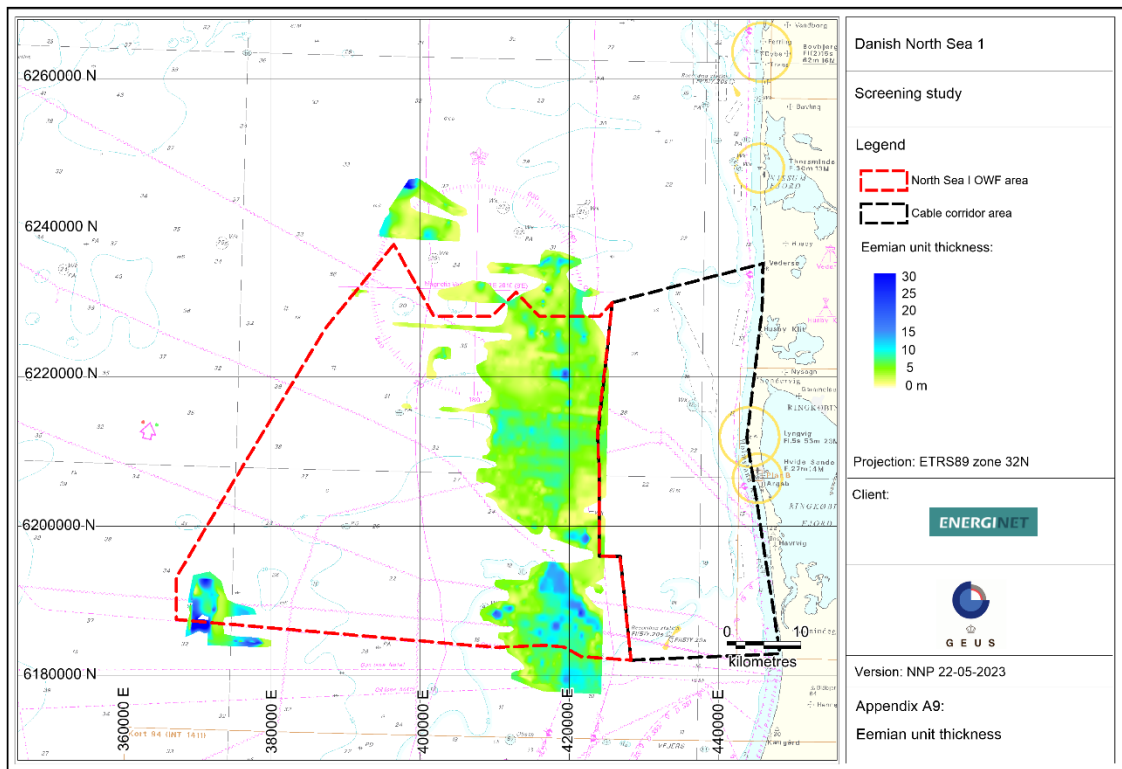


Figure 7.6. Mapped thickness (m) of Eemian Unit. Appendix A9.

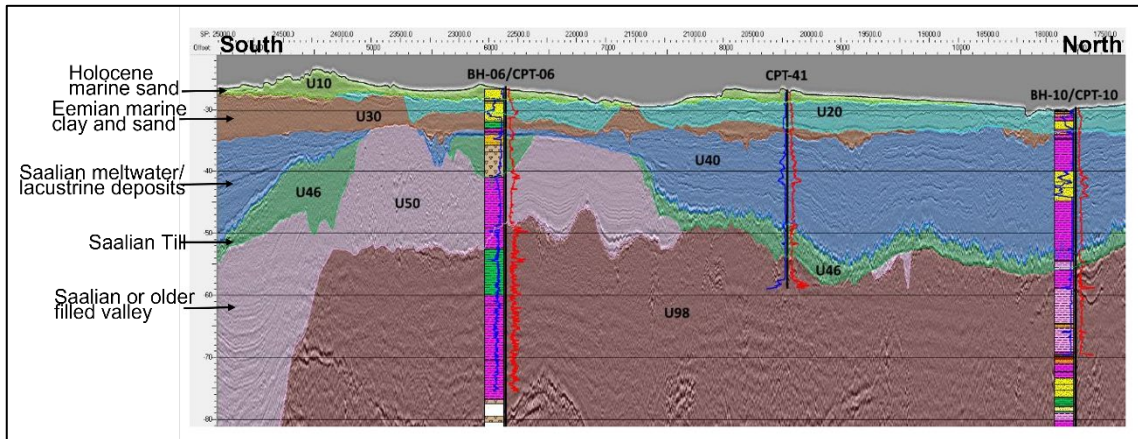


Figure 7.7. Thor OVF seismic profile from eastern part of area. Stratigraphic units have been labelled at left side of figure. Modified from COWI Report (2021.)

The map in Figure 7.6 shows that the Eemian unit is present in the eastern part of the mapped area with a thickness around 5-10 m and in places up to 15-20 m as well as in the south-western corner of the area, thus filling in the relief of the Saalian surface. Figure 7.7 shows that the Eemian unit (termed U30) identified in the eastern part of the Thor OVF area is thinning from south to north.

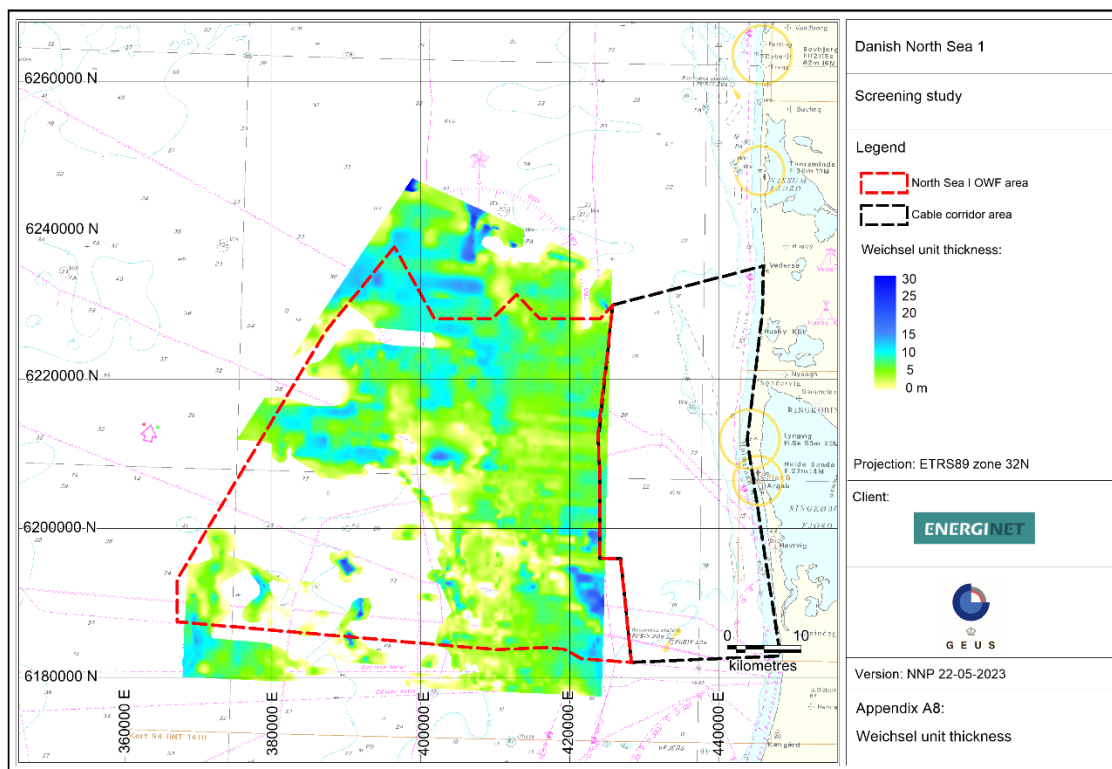


Figure 7.8. Mapped thickness (m) of Weichselian Meltwater Unit. Appendix A8.

The map in Figure 7.8 shows that the Weichselian unit is present in the eastern and northern part of the mapped area with a thickness around 5-10 m and in places up to 20 m or more as well as in the southwestern corner of the area with a thickness up to c. 10 m, thus filling in the relief of the Saalian surface.

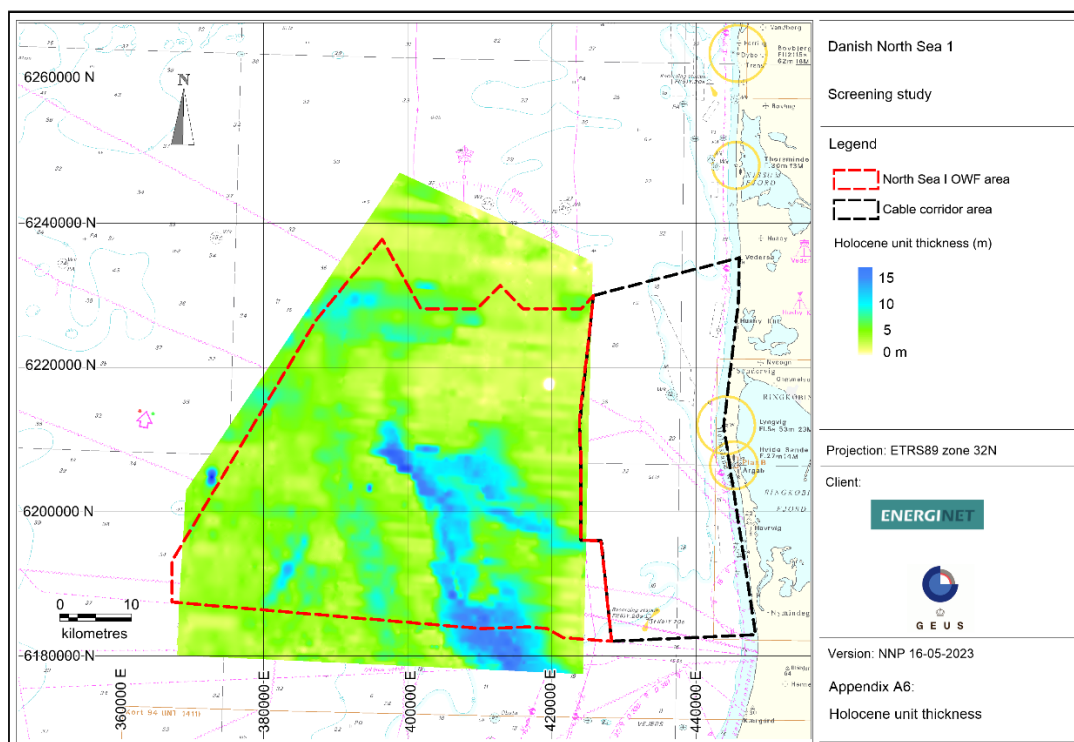


Figure 7.9. Mapped thickness (m) of Holocene Unit. Appendix A6.

The map in Figure 7.9 shows how the thickness of the Holocene unit is relatively uniform and just a few metres in most of the mapped area except in the central and southeastern part, where two longitudinal channel-like areas with a thickness of up to 15 m occur.

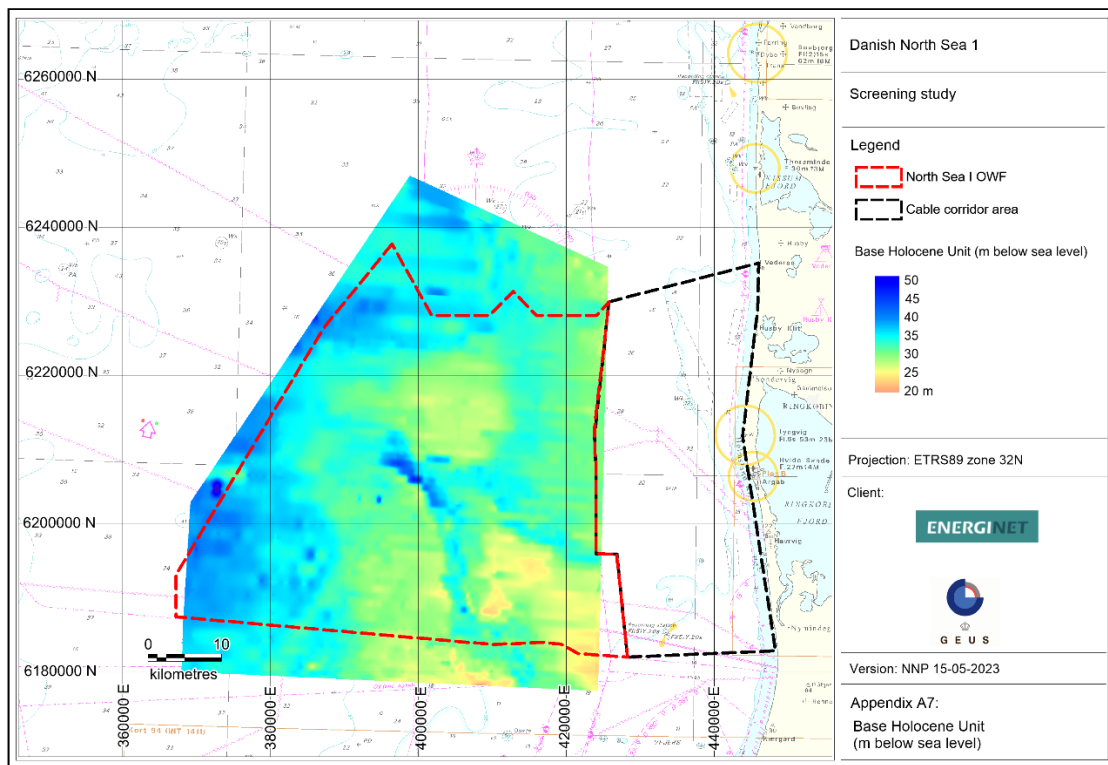


Figure 7.10. Mapped base of Holocene Unit (m below sea level). Corresponds to palaeolandscape before Holocene marine transgression. Appendix A7.

The map in Figure 7.10 shows the relief at the base of the Holocene unit with the most shallow position of the base to the southeast around 20-35 m deepening towards northwest to around 30-45 m or more along the northwestern boundary of the mapped area. The relief of the mapped surface corresponds to the palaeolandscape before the Holocene marine transgression of the area.

7.3 Conceptual geological model of OWF area

A conceptual model of the upper 50 m of the subsurface geology of the OWF area was established based on the interpretation of seismic sparker profiles verified by numerous sediment cores (Figure 7.11). The schematic geological cross section shows a high-lying Saalian glacial surface with in-filled valleys. In the eastern part, where the Saalian surface is lower, Eemian marine clayey deposits and Weichselian sandy meltwater deposits partly fill the accommodation space. On top of these, early Holocene marine, fine-grained deposits fill a channel-like feature. In late Holocene sedimentation continued with build-up of positive morphology large scale sand bars. The model appears in general to be in accordance with the stratigraphic model established for the northern Horns Rev area by Larsen & Andersen (2005) and described in section 5.4. In the western part of the screening area, erosional remnants of possibly both Saalian and Weichselian sandy meltwater deposits are found on

top of the slightly lower Saalian glacial surface. The meltwater deposits are overlain by a thin cover of sandy Holocene marine deposits. Early Holocene freshwater deposits in the form of peat and gyttja appears to be very thin and only occurs locally in former landscape depressions.

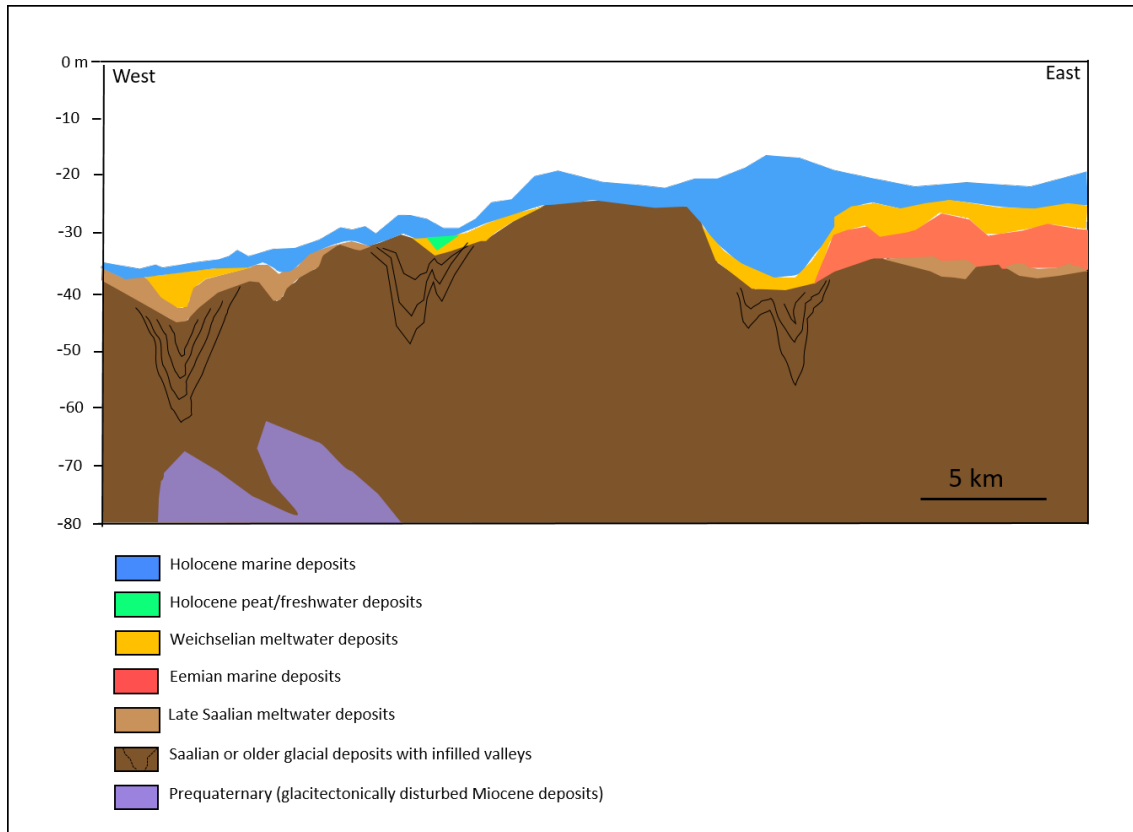


Figure 7.11. Conceptual geological model established for the screening area.

8. Cable corridor area

For investigation of the cable corridor area, a synthesis of data from earlier investigations of the coastal zone (0-12 km from coast, GEUS Rep. 1999/75) which was revised by Leth et al. (2004) has been combined with an analysis of data from a zone c. 10-20 km from the coast (GEO, 2011a and 2011b). Moreover, investigations of OWF area Vesterhav Syd (GEUS Rep. 2015-17) and Husby Klit dredging area (GEUS Rep. 2021-21) have been included.

Emphasis have been on correlation and description of the surface near geological units. Moreover, the dynamics of the mobile sand unit that partly covers the underlying seabed geology are shortly discussed.

8.1 Seismic type profiles

In connection to earlier mapping of surface near geology and sand resource distribution for the Danish Coastal Authority, a number of interpreted representative seismic type sections were produced perpendicular to the coast (Leth et al., 2001). Five of these type sections (E, F, G, H, I) cover the eastern part of the North Sea I cable corridor area (Figure 8.1). The type sections supported by vibrocore data reveal that Miocene clayey sediments are found right up to the seabed in the northeastern part of the cable corridor. The Miocene highs are dissected by units of glacial outwash deposits and minor areas with till units (profiles E-F-G). The upper part of the Miocene sediments often have a folded and thrust appearance due to glaciotectionic deformation. This can be observed in deeper penetrating multichannel sparker seismic from the Vesterhav Syd OWF survey area northwest of Hvide Sande (Figure 8.2). The complex of glacially deformed Miocene units and glacial deposits northwest of Hvide Sande has been interpreted as the seaward extension of the Skovbjerg hill island (possibly of Saalian age) found on land north of Ringkøbing Fjord.

Toward the central and southern part of the cable corridor, the top glacial surface becomes buried by a thicker cover of marine sandy and clayey deposits and sandy meltwater deposits. At places up to 20 m deep glacial valleys/troughs occur infilled with younger sediments (profile H). Originally the marine sediment units (clay, silt and sand) were all interpreted as of Holocene age. However, a later study confirmed that the older and typically clayey to silty units were part of the Eemian succession, that can be traced in many sediment cores and seismic sections from outside Ringkøbing fjord to the Inner Horns Rev and the Wadden Sea (Konradi et al., 2005). A thin young Holocene sand unit characterised by large sand bedforms covers part of the area.

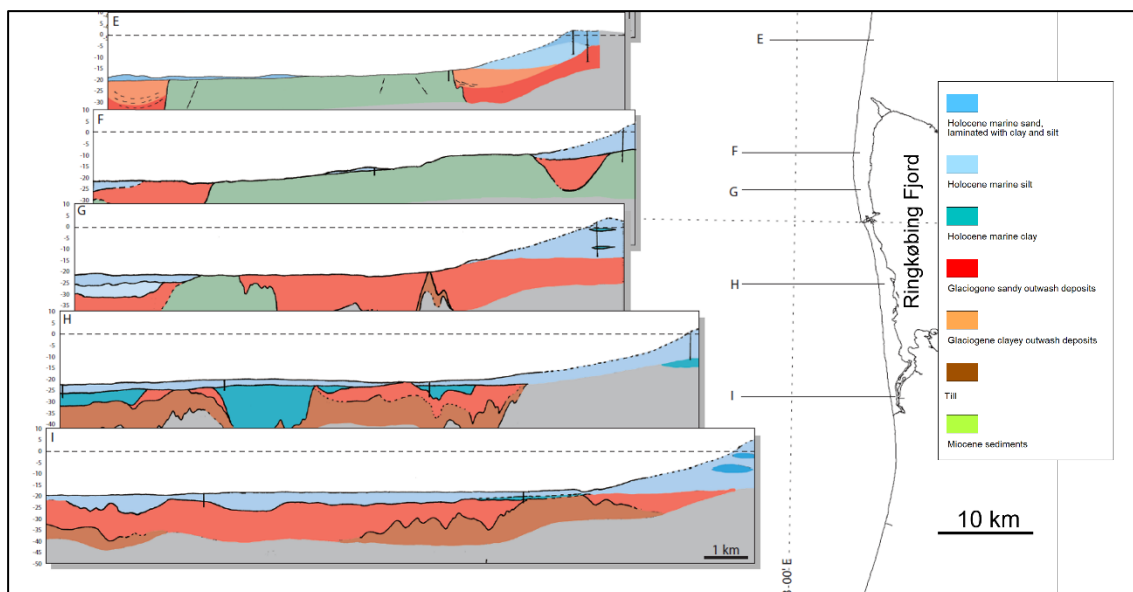


Figure 8.1. Interpreted seismic type sections west of Ringkøbing Fjord (GEUS Rep. 1999/75). Note that the 'Holocene marine clay unit' in section H has later been reinterpreted as Eemian interglacial clay (Leth et al., 2004).

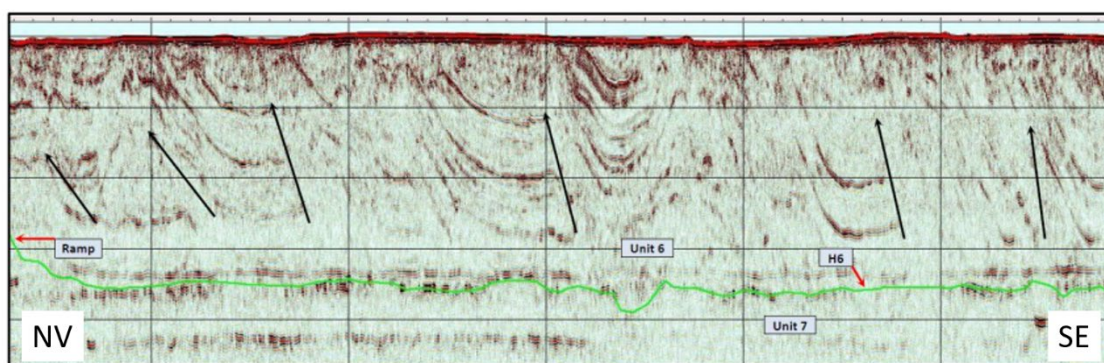


Figure 8.2. Multichannel sparker seismic profile from the southern part of Vesterhav Syd OWF survey area west of Hvide Sande (GEUS Rep 2015/17). Glaciotectonically deformed Miocene sediments (Unit 6) are found above undeformed Miocene Unit 7.

To extend the knowledge of the near surface geology of the eastern part of the cable corridor to the western part, GEO's data set from 2010 (2x2 km sparker seismic grid) and 2011 (small detail study area) including a large number of sediment cores have been investigated. West-east orientated interpreted seismic lines (sections 7-11) which partly overlap with the E-F-G-H-I sections (Figure 8.1) are presented here (Figure 8.3) together with three north-south orientated lines (sections 12-14) (Figure 8.4). The following seismic unit boundaries, also identified in the OWF area, have been traced where possible:

- Base Holocene marine deposits
- Base Weichselian meltwater deposits
- Base Eemian marine deposits
- Base Saalian meltwater deposits
- Top glacial (Saalian or older till deposits)
- Top Pre-Quaternary (Miocene)

In the northwestern part of the cable corridor area, the Miocene highs descend to several tens of metres below the seabed (e.g. seismic sections 7 and 8). Weichselian sandy meltwater deposits dominate close to the seabed, with a variably but relatively thin cover (1-2 m) of Holocene mobile sand. Eemian clayey and silty marine deposits are found below Weichselian sandy deposits, and the Eemian deposits are seen to onlap and come close to the seabed along the rim of the glacial/Miocene deposits described above. Further to the south, outside the middle to southern part of Ringkøbing Fjord, Eemian deposits are found throughout the seismic sections (e.g. seismic sections 9, 10 and 11), and where Weichselian meltwater deposits and/or early Holocene channels have not eroded the Eemian sequence, Eemian mostly clayey deposits are found close to the seabed. The Eemian deposits generally show a seaward progradation with slightly westward inclined stratification. The thickness of the preserved Eemian sequence in general appear to be about 7-10 m. However, a more than 20 m thick Eemian sequence may be preserved in an infilled deeper channel seen on the eastern part of section 10 corresponding to the channel feature seen on section H (Figure 8.1). In the southern part of the cable corridor area, infilled Holocene channel-like features with a maximum thickness of about 5-10 m are seen (e.g. seismic section 11, 12, 13, 14). Based on sediment core data, the Holocene infill is dominated by fine-grained silty sand in the upper part, whereas the lower part is more fine-grained and organic-rich or gyttja.

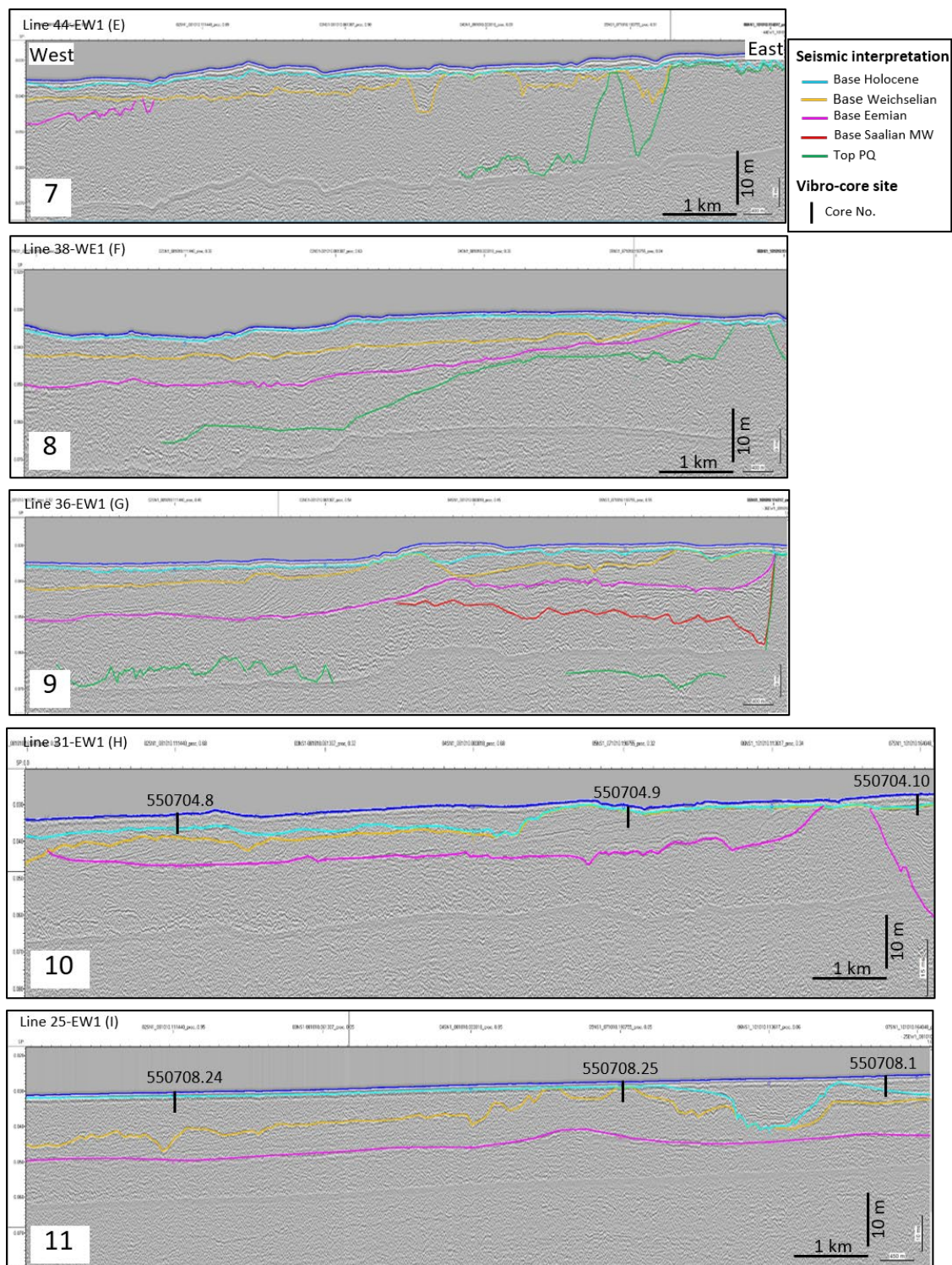


Figure 8.3. Interpreted west-east orientated seismic sections (7-11) from the western part of the cable corridor. The sections represent westward extensions of the E-F-G-H-I sections presented in Figure 8.1.

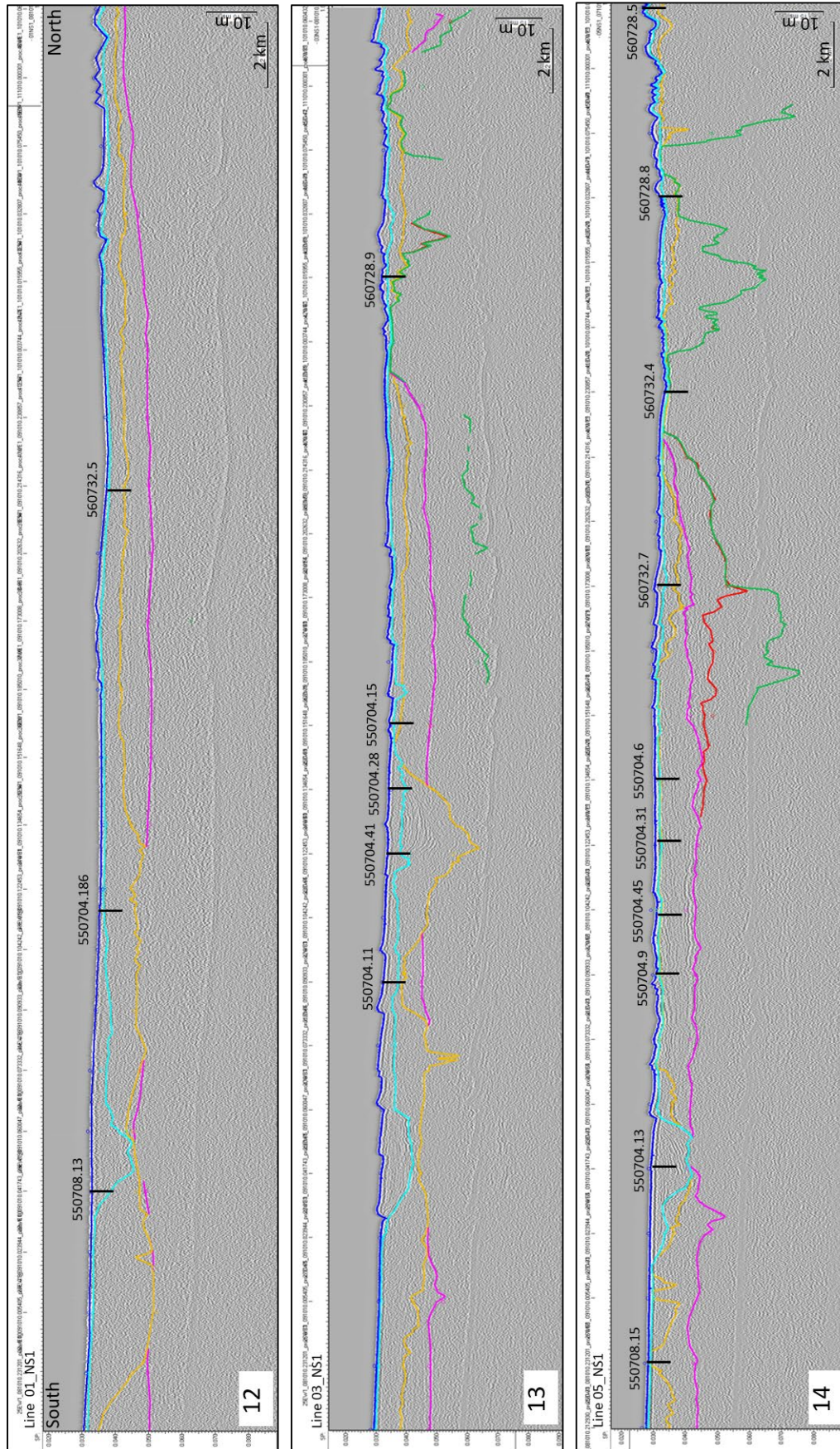


Figure 8.4. Interpreted north-south orientated seismic sections (12-14) with 4 km in between from the west-ern part of the cable corridor. For legend see Figure 8.1.

The sediment core data from the relatively large number of vibrocores (< 6m) allow a detailed interpretation of the sparker seismic data, and identification of lithological and stratigraphical units in the area (Figure 8.5). The present study indicates that some of the stratigraphical designations to units in the original vibrocore descriptions (GEO 2011a and 2011b) may be questionable. An example of this is seen in core 560732.5 (VC-57) where a 3.5 m thick unit of fine sand with some organic content but no shell fragments originally was designated an interglacial (Eemian age). The seismic stratigraphy and inter-correlation with other cores indicate however that the fine sandy unit possibly is of Weichselian age (possibly late glacial).

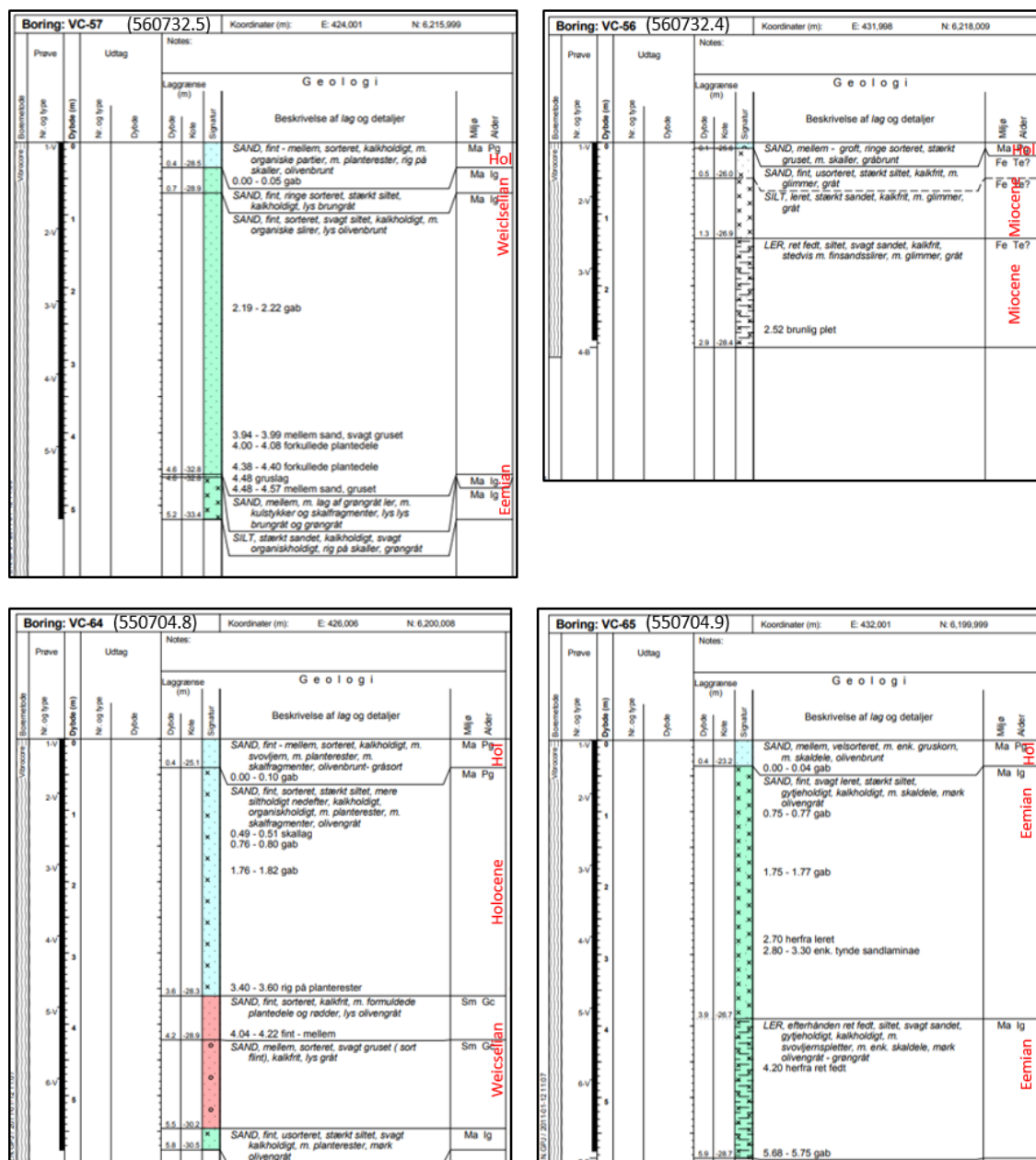


Figure 8.5. Example of vibrocore log descriptions from the cable corridor area (GEO, 2011a). DGU core nos. are indicated as well as a partly revised stratigraphic interpretation (unit age in red) based on the present study. Core locations are indicated at Figure 6.3.

8.2 Seabed geological map

For the cable corridor area, a geological map of units found at the seabed or below the relatively thin layer of mobile Holocene sand have been produced by extending the information from an earlier mapping campaign of the inner coast seabed (GEUS Rep. 1999/75 and Leth et al. (2004)) with data from the 2010-2011 mapping campaign by GEO for the Danish Coastal Authority. The new map (Figure 8.6) indicates that smaller Miocene 'highs' are also found in the north-western part of the cable corridor, which otherwise is dominated by Weichselian sandy and sometimes slightly gravelly meltwater deposits close to the seabed. In the central to southern part of the cable corridor, Eemian silty to clayey deposits are found in a large area outside Ringkøbing Fjord. To the west and south of the Eemian subcrop area, Holocene channelised deposits are found. The Holocene deposits are generally fine-grained silty sand, with gyttja layers in the lower part.

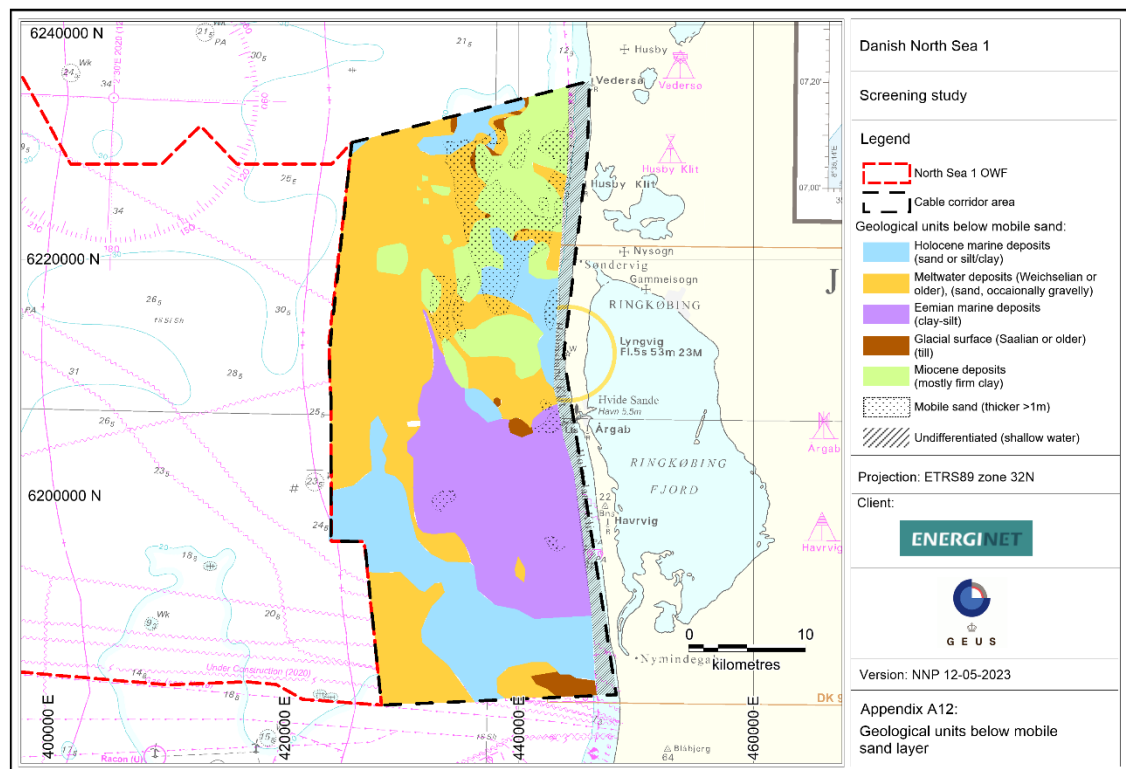


Figure 8.6. Seabed geology map for the cable corridor area, representing geological units occurring below a thin top layer of mobile sand.

8.3 Mobile sand layer

Earlier studies of focus areas along the Jutland west coast have verified the existence of major dynamic sandy bedforms of different scales (Anthony & Leth, 2002) on areas characterised by thicker accumulation of Holocene mobile sand (Figure 8.7) (Leth et al., 2004). Very large bedforms have a mean wavelength of c. 500 m and heights of 1-3 m. Large dunes with

wave lengths in the range 10-100 m and smaller bedforms have also been recorded, as well as large shoreface-connected ridges with several km spacing. These bedforms indicate in general a north-going net sediment transport. The areas with thicker layers of mobile sand appear to be stable on time scales of several decades, and the occurrence appears to be connected to sand-rich substrata.

Thicker units of mobile sand (2-4 m) are found in the north-eastern part of the cable corridor area (Figure 8.7), where Husby Klit dredging area (bygherreområde) for local coastal nourishment of sand by the Danish Coastal Authority has been situated for several decades. The last detailed mapping of surface-near features including large bedforms and sand thickness in the dredging area took place in 2020 (Figure 8.8). In the western part of the cable corridor, large assymetric bedforms or ridges with heights of a few m and wave lengths of several hundred to about 2 km are clearly visible on S-N orientated seismic sections (Figure 8.4). Noteworthy, the bedform asymmetry there, indicates a southward sediment transport direction.

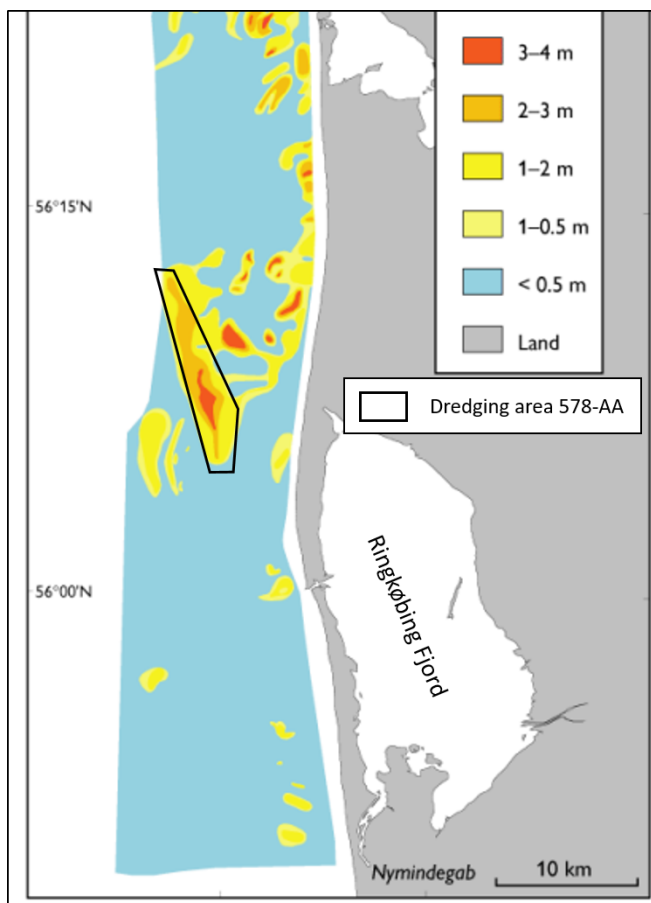


Figure 8.7. Mobile sand layer thickness in the near coastal area west and north of Ringkøbing Fjord (Leth et al., 2004).

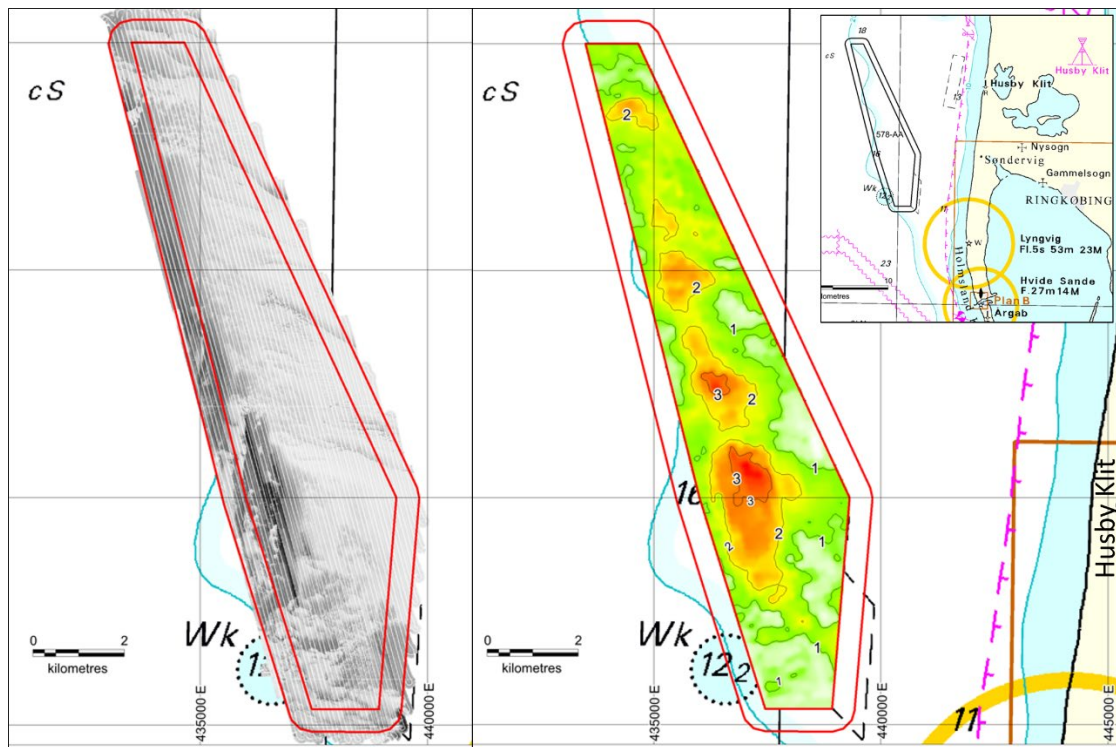


Figure 8.8. Side-scan sonar mapped seabed surface (left) and mobile sand layer thickness in metres (right) in Husby Klit dredging area northwest of Ringkøbing Fjord. GEUS Rep. 2021-21).

9. Key geological conditions

The screening has revealed geological conditions and sediment characteristics that may have implications for the assessment of wind farm foundation conditions and cable laying. The following key geological characteristics are shortly discussed here:

- High-lying over-consolidated glacial sediments (incl. glaciotectionised Miocene)
- Glaciotectionic deformations
- Buried Quaternary valleys/palaeo-channels
- Marine dynamic sand deposits
- Soft silty marine clays and gyttja
- Peat layers

With reference to Velenturf et al. (2021), some of the possible implications of these geological conditions are described below:

Soft sediments can imply a risk for low geotechnical strength and be a challenge for the foundation design. At the seabed, soft sediments can potentially be unable to bear large loads from e.g. a jack-up rig during construction.

Marine dynamic sand deposits may imply migrating erosional and depositional bedforms that can change the seabed topography over the operational lifetime of an OWF site in terms of scouring or burial of e.g. piles or cables.

The glacial deposits which have formed under ice sheet load may represent over-consolidated and strong sediments, which generally can provide a difficulty during construction e.g. for driving piles. They may also comprise more specific hard, potentially heterogeneous, coarse lag deposits (gravel to boulders) that can be difficult to penetrate and may lead to refusal of foundation infrastructure or damage of equipment. Near the seabed, a hard, heterogeneous surface can make it more difficult to predict scour behavior.

Furthermore, the sediment thickness and lithology may vary abruptly over short distances especially in the glacial deposits, and the Quaternary deposits in general, complicating turbine siting and cable routing as well as foundation design(s). In glaciotectionically deformed areas, steeply dipping and alternating layering may occur with dislocated floes of soft sediments and abrupt changes in geotechnical properties.

The occurrence of palaeochannels or buried valleys with steep sides may also imply large-variations in sediment composition in either side and within the channel fill, potentially complicating foundation design.

No signs of gas or over-pressured pore fluids have been observed in the shallow subsurface, but if present, it may lead to blow outs when drilling for sediment sampling and infrastructure construction. The presence of shallow gas/pressured fluids may be indicated by pockmarks in the seabed and can also be indicated by acoustic blanking of seismic reflection data,

preventing interpretation of units below. Pockmark areas can be unstable and should be avoided for turbine locations and cable routing.

In Table 9-1 an overview of sediment types identified in the screening area, related potentially critical geotechnical conditions and general foundation suitability is given.

Table 9-1. Sediment types identified in the screening area, related potentially critical geotechnical conditions and general foundation suitability.

Sediment type	Critical geotechnical conditions/challenges	Foundation suitability
Marine sand	n.a.	Well suited
Marine clay/soft mud	Low geotechnical strength	Not well suited if thick
Peat	High compressibility, low geotechnical strength	Not well suited
Meltwater sand	n.a.	Well suited
Meltwater clay	Low geotechnical strength if not overconsolidated	Not well suited if thick
Moraine clay/till	Overconsolidated and potentially heterogeneous, can contain coarse lag deposits, boulder stones and dislocated floes of older sediments	Potentially problematic
Buried valley sediments	Potentially heterogeneous with variable glacial/non glacial deposits, sharp variations in sediment composition across flanks	Potentially problematic
Miocene sand	n.a.	Well suited
Miocene clay	Low geotechnical strength if not overconsolidated	Not well suited if thick

An overview map has been compiled of the areal extent of key geological units that might have considerable influence on the variability of sediment characteristics and planning of turbine locations, foundation design and preferred cable corridor location. The extension of the following units was delineated: High lying Miocene deposits, high-lying Saalian glacial surface, buried Quaternary valleys, Eemian silty clays, Holocene marine silty clays and gyttja, and Holocene mobile sand unit (Figure 9.1, Appendix A13).

The OWF screening area is generally characterised by high-lying glacial sediments from Saalian or older glacial periods. The glacial sediments are especially close to seabed in the southwestern part of the screening area. The glacial sediments can be expected to be of heterogeneous composition and over-consolidated, due to prior ice-loading, subaerial exposure and desiccation. The sediments consist of clayey or sandy tills with variable stone content, deformed meltwater sediment layers (sand, gravel and clay) and locally glaciotectionically disturbed floes of Miocene sediments (sands and clays). From deeper seismic sections, the area is also well-known for glaciotectionic thrust structure complexes (Huuse & Lykke-Andersen, 2000; Nielsen et al., 2008). Thrust structure complexes can locally bring floes of pre-Quaternary sediments (clay or sand) close to the surface and in general create a complicated stratigraphy with low lateral predictability.

The area is dissected by a dense network of buried Quaternary valleys, several hundred metres in depth and cutting into the pre-Quaternary unit. Buried valleys are especially common in the eastern to central part of the screening area. As described above, the buried valleys can show sharp variations in sediment composition across the flanks and within the

channel fill. Little is known about the lithology of the complex sediment in-fill of the valleys, but a few drilled sections through similar structures in other parts of the North Sea, suggest a variable composition with both sandy, clayey and gravelly sediment fill (Cotterill et al., 2017).

Thicker units of soft clayey sediments are related to interglacial deposits from the Eemian period as well as early Holocene deposits. Moreover, older interglacial or late glacial lacustrine clays may also occur as interbedded subunits in Saalian and Weichselian meltwater units, respectively. Eemian silty clays is present in the central to southeastern part of the screening area, as well as in two minor areas in the western part. The thickness of the unit is mostly in the range of 5-10 m, but locally it may reach 15 m. Early Holocene marine clays and gyttja appear is located in palaeo-landscape depressions in the central and southeastern part of the screening area, where the thickness of the Holocene unit may reach about 15 m. However, only the lower 5-10 m of the Holocene unit appears to be fine-grained material.

Peat layers observed in sediment cores appear to be very thin (few decimetres) and likewise located in Holocene palaeo-landscape depressions, that later was drowned during the Littorina transgression in early Holocene. The peat findings appear to be quite randomly localised outside the main Holocene palaeo-channel system. This may rather reflect the limited length of the vibrocores retrieved (typically <6 m), i.e. peat has only been verified in shallower landscape depressions, where the corer was able to penetrate down to the peat-covered lower part of the depression.

Based on the overview map of key geological units in Figure 9.1, it may be concluded that most parts of the screening area are characterised by specific geological conditions that will have to be considered in the planning of the most optimal location of wind farm sites and cable corridor.

It shall be noted that the Horns Rev 2, Horns Rev 3 and Thor wind farm parks are characterised by similar geological settings. In this sense, specific considerations and lessons learned from these projects may be highly relevant for further site evaluation of North Sea I OWF area.

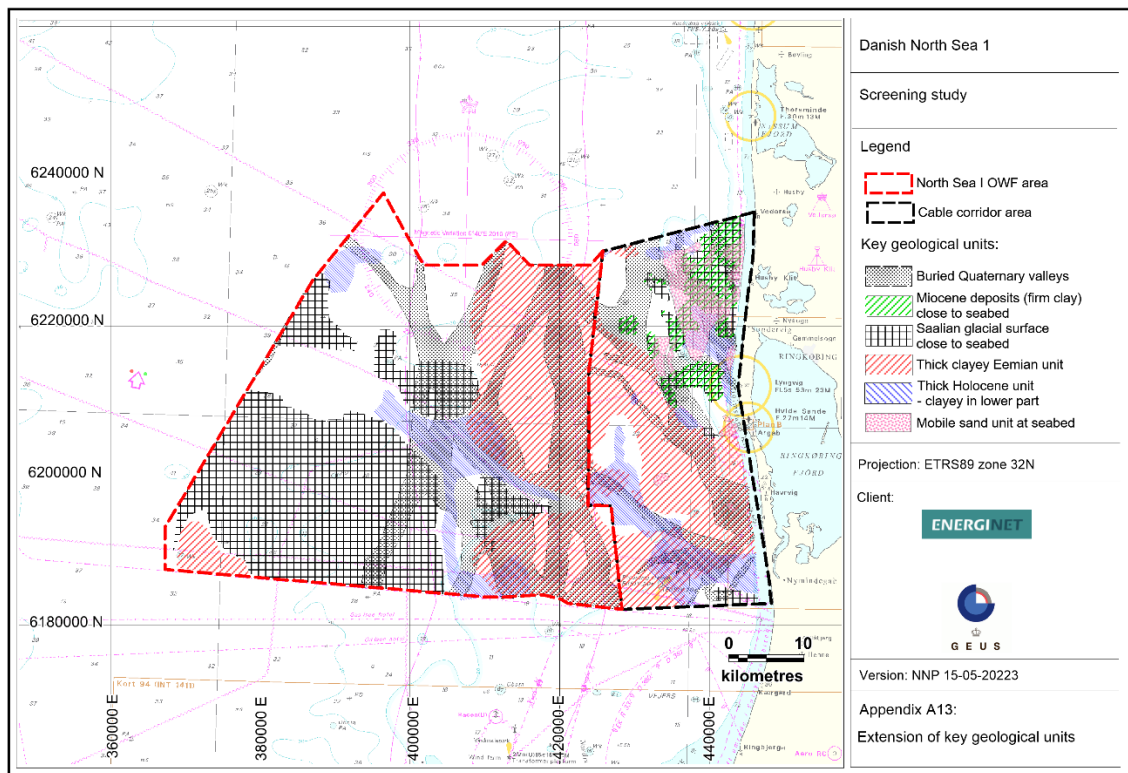


Figure 9.1. Key geological unit distribution in the screening area. Appendix A13.

10. Relative sea level changes and archaeological interests

10.1 Relative sea level changes

Due to the combined effect of eustatic sea level rise and glacio-isostatic rebound during the postglacial period, relative sea level (RSL) led to transgression of the screening area and to drowning of potential Stone Age settlements. The glacio-isostatic uplift pattern following the demise of the Scandinavian Ice Sheet shows a concentric pattern with a maximum over the northern Botnian Bay and northern Sweden and near zero values along a margin crossing the southern North Sea. From the early last deglaciation till today, the isostatic uplift rates have diminished. Since about 10000 years BP, where a very rapid deglaciation took place during the final ice retreat in central Fennoscandia, uplift in northernmost Jutland have been about 50 m, decreasing to about 10 m at 5000 years BP. Present day isostatic uplift are about 1 mm/year in northernmost Jutland decreasing to about zero at the central Danish west coast. The eustatic global sea level curve based on a very large dataset from tropical areas with minimal tectonic influence shows a marked rise in sea level from about 15000 years BP (below -100 m) to about 8000 years BP (-15 m) (Lambeck et al., 2014). Hereafter the eustatic sea level rise gradually diminished till today's value.

Site-specific RSL curves (coastline displacement curves) can be constructed using relative sea level indicators such as radiocarbon-dated peat and other terrestrial items combined with carefully selected radiocarbon-dated marine shells believed to represent the transgression horizon. By combining the dated shore level information with an empirical digital elevation model, RSL curves have been calculated for many sites in Scandinavia including the German North Sea coast (Påsse & Anderson, 2005). For the Danish North Sea, apart from the southern part adjacent to northern Germany, no well-constrained local RSL curves exist. In order to overcome this, studies in relation to offshore windfarm investigations in the Danish North Sea have used RSL curves for sites in eastern Denmark placed more or less on the same uplift isolines as the investigation area (e.g. Storebælt RSL curve). In order to verify if this 'along isoline method' can be considered valid, projects aiming at establishing local RSL curves attempt to radiocarbon date terrestrial and marine material taken at different depths in the investigation area and combining this with any existing radiocarbon dates from the surrounding area. The general experience from projects which have included a large number of terrestrial and marine dates from a limited geographical area is that a relative large number of the age/depth data falls relatively far from the suggested RSL curve, which in theory have to be placed with terrestrial age/depth fix points situated on one side of the curve and marine age/depth fix points situated on the other side of the curve. In order to constrain the attempt to draw a best-fit line between data points, it must be assumed that the slope of the line in general cannot be steeper than the slope of the eustatic sea level curve. Due to the larger glacio-isostatic uplift in northern Denmark, RSL curves from northern Denmark show a less steep rise in RSL for the last 10000 years compared with RSL curves from southern Denmark/northern Germany.

In order to evaluate the timing of the postglacial transgression in the screening area five relevant RSL curves have been considered: the global eustatic curve (Lambeck et al., 2014), two North Germany curves (Påsse & Anderson, 2005; Behre, 2007), Storebælt curve (Påsse & Anderson, 2005) and the curve recently established for the Thor OWF area (Jonsson and Astrup, 2020), Figure 10.1. Terrestrial and marine radiocarbon dates within and relatively close to the screening area have been selected by Ole Bennike (GEUS) (Table 10-1; Figure 10.2), and the dates have been plotted versus depth below present sea level (Figure 10.3). Comparing the distribution of terrestrial and marine shoreline indicators, it appears that the best fit segregation line of the five RSL curves shown in Figure 10.1, is the global eustatic curve which, in the 10000-8000 years BP span, is not lying far from the North Germany curves. It shall be emphasised that the limited number of dates does not allow to reconstruct an independent RSL curve for the area.

A major challenge in connection to establishing an RSL curve for Thor OWF was that many new radiocarbon dates gave ages close to non-finite (>40000 years), possibly because a large part of the dated shell samples is of Eemian and not Holocene age. In order to acquire enough data for constructing a RSL curve, the study, in addition to a limited number of new radiocarbon data from the area, included a number of published data from far north of the Danish North Sea coast (including Jyske Rev and the western Limfjord). The resulting curve was provided with arrows on most data points, indicating the direction of supposed correction due to the very large geographical extent of data points. The slope of the curve presented from 10000-9000 years BP is considerably steeper than the eustatic sea level curve, the North German curve and the general trend of the curves from south to north in Denmark. Based on this, the present study considers it problematical to use the Thor RSL curve for evaluation of the Holocene palaeo-landscape evolution of the screening area.

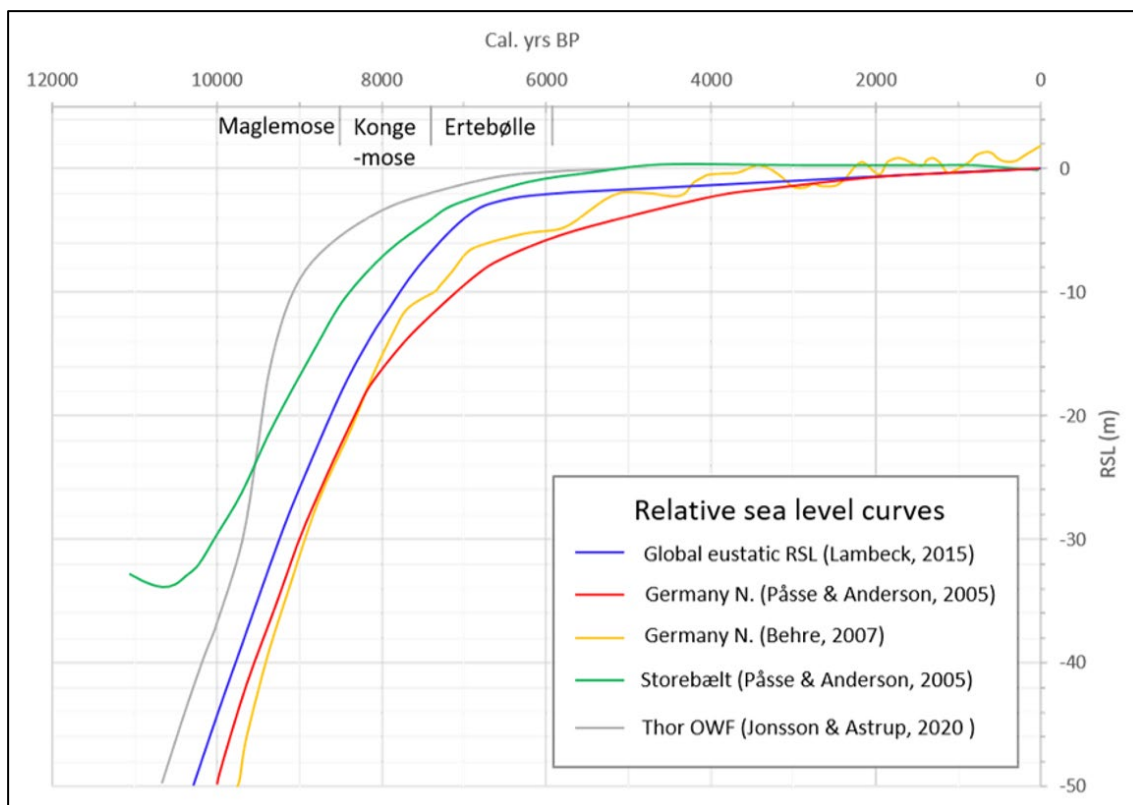


Figure 10.1. RSL curves for the global eustatic signal and relevant published curves for the Danish west coast area.

Table 10-1. Selected terrestrial (yellow marked) and marine (blue marked) material radiocarbon dates shown in Figure 10.2 and Figure 10.3.

Lab. No.	Core site	X (UTM 32N)	Y (UTM32N)	Material	Species	Sample elevation (m)	Cal. Yrs BP
Beta-573641	550715.37 (HR-30)	411633	6153152	Peat	<i>Phragmites</i>	-13.3	8506
Beta-573626	550719.25 (HR-19)	416615	6149686	Peat	Radicells	-22.4	9057
Beta-573637	560726.1 (VKY-34)	404169	6221448	Peat	Wood fragment	-26.9	9586
Beta-573639	550706.21 (VKY-74)	401464	6182721	Peat	Wood fragment	-28.3	9386
Beta-573634	550717.3 (HRV-32)	374542	6144490	Peat	<i>Alnus</i>	-31.8	9150
AAR-31711	282-VC-OWF-B1- 004	410789	6244688	Peat	Twig	-29.5	10968
AAR-31713	282-VC-OWF-B1- ARC-004	405491	6238662	Mud/Peat	Wood fragment	-20.0	10089
Beta-573635	550717.3 (HRV-32)	374542	6144490	Peat	<i>Populus</i>	-32.7	10900
KIA-51170	DOG 2	321417	6248391	Peat	Bulk smpl.	-47.2	10558
Beta-479843	Beta-479843, Baltic Pipe	368159	6186112	marine shell	<i>Macoma baltica</i>	-37.3	9285
Beta-573642	560722.8 (VKY-09)	403487	6236723	marine shell	<i>Schoenoplectus</i>	-34.3	9942
UBA-32860	B0203VC, VIKING LINK	443802	6181000	marine shell	<i>Scrobicularia</i>	-17.8	8912
Beta-573630	550708.33 (VKY-60)	422247	6191282	marine shell	<i>Littorina</i>	-27.0	9037
Beta-573631	550708.33 (VKY-60)	422247	6191282	marine shell	<i>Menyanthes</i>	-27.0	9150
AAR-31702	282-VC-OWF-B2- 005	416055	6243509	marine shell	<i>Cerastoderma edule</i>	-27.9	10075
AAR-31679	282-VC-OWF-B1-007	404742	6233577	marine shell	<i>Cerastoderma edule</i>	-32.6	9816
Beta-403137	VHS_CR1_VC+007	440373	6217326	marine shell	<i>Ostrea edulis</i>	-19.8	7649

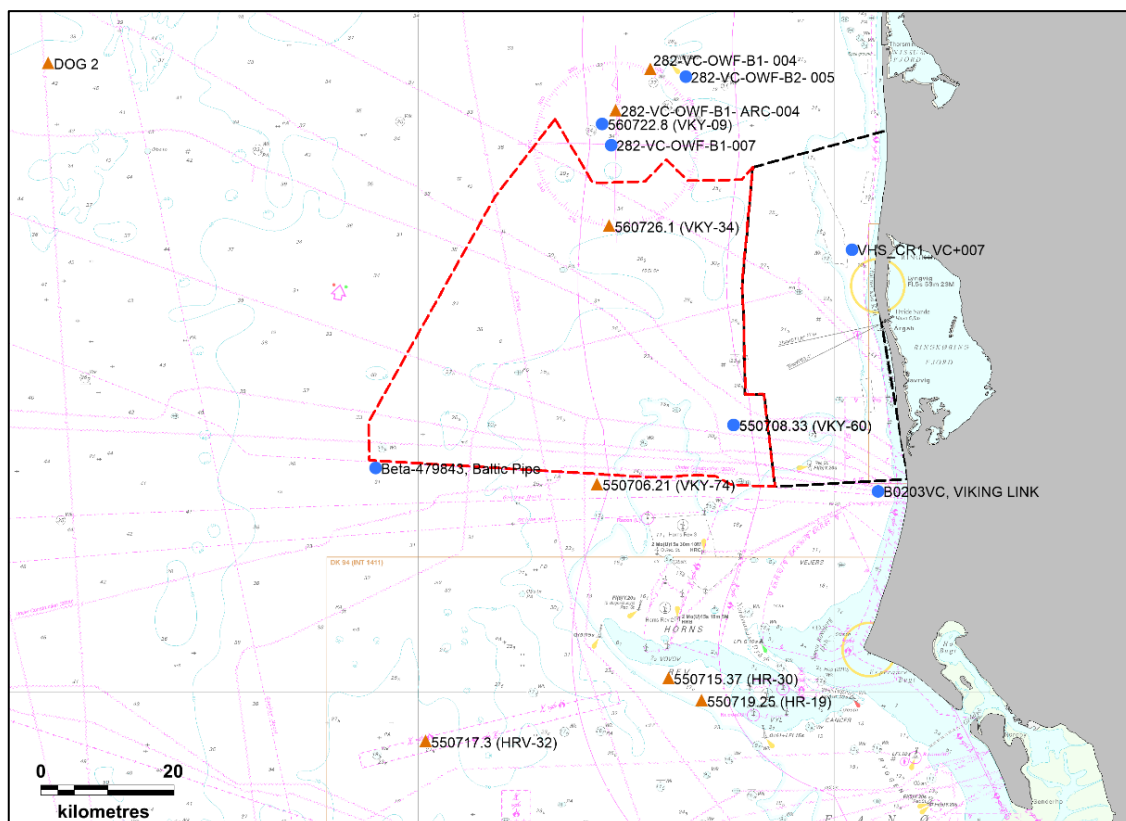


Figure 10.2. Location of selected radiocarbon dates adjacent to the screening area. Marine material samples are indicated by blue dots and terrestrial material samples are indicated by orange triangles.

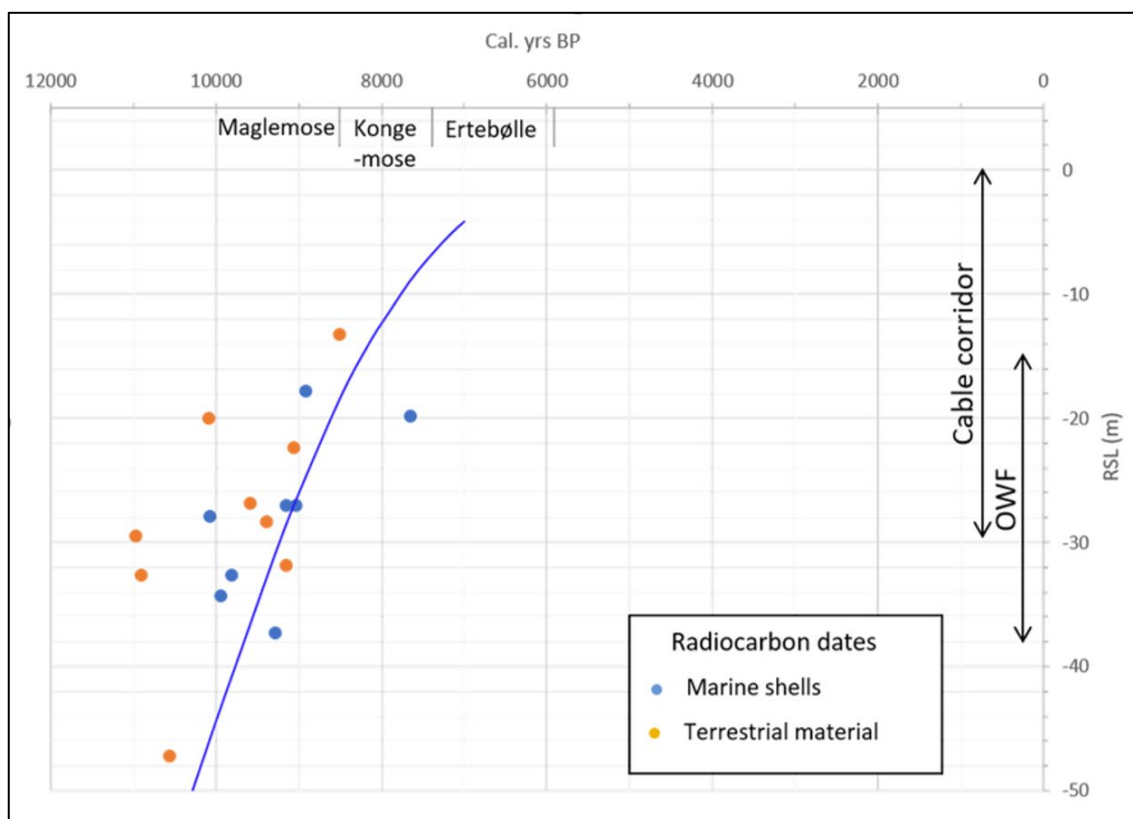


Figure 10.3. Local radiocarbon-dated marine and terrestrial material versus RSL curve from Lambeck et al. (2014) and indicated depth ranges of the North Sea I OWF and cable corridor areas.

10.2 Archaeological implications

Most studies infer that most parts of the Danish North Sea were dry land at about 10000 years BP. The present-day coastline configuration was reached at about 7000 years BP (Figure 10.4). This is supported by data from close to the screening area, as shown in the previous section.

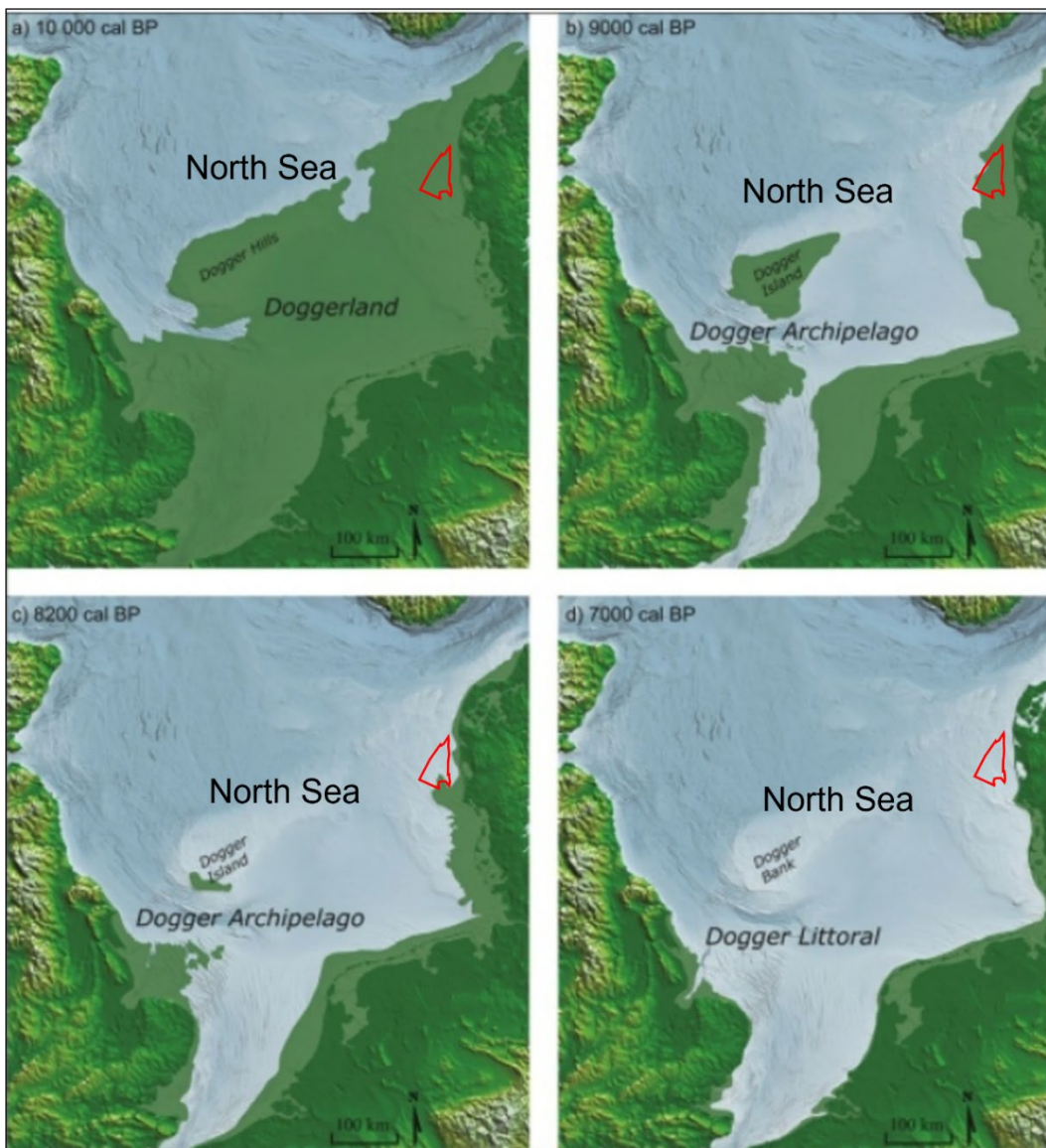


Figure 10.4. Reconstructed coastline evolution and palaeolandscapes of the North Sea for the Holocene time slices: 10000 yrs BP, 9000 yrs BP, 8200 Years BP and 7000 yrs BP. Modified from Walker et al. (2020).

According to the relative sea level curve shown in Figure 10.3, the North Sea I OWF area may have been transgressed and inundated by the North Sea in the period from c. 9500 to 8200 years BP (Figure 10.3, Figure 10.4), and hence it can be expected that only early

Mesolithic Maglemose culture remains can be found in the area. The shallower cable corridor area may have been transgressed during the period from c. 9200 to 7000 years BP. Accordingly, it is possible that both Maglemose, Kongemose and oldest Ertebølle culture remains may be found in the cable corridor area. The possibility that finds from younger cultures can be made in shallow water in the coastal zone must, due to the generally high energy level of waves and currents, be considered as very low. Taken into consideration that infilled early Holocene throughs or channels have been observed in the south-eastern part of the screening area (OWF and cable corridor), it is likely that the earliest transgression locally went closer to the present shoreline there. Depending on the magnitude of palaeotidal conditions, such waterways may have had a profound influence on coastal conditions and possibilities for human settlement and subsistence. Archaeological analyses of Horns Rev 2, Horns Rev 3 and Thor OWF areas have also shown a theoretical possibility for settlements of the Maglemose culture. However, no archaeological objects have been found in these areas, not even during specific dedicated studies.

11. Conclusions

Screening of existing shallow seismic data, sediment cores and published literature of the North Sea I area and the adjacent cable corridor has given an overview of the geological development and the distribution and composition of Miocene to Quaternary units in the area. Thickness and levels of main Quaternary stratigraphic/genetic units have been compiled by mapping of key seismic surfaces and verification with sediment core data.

The following observations are emphasised:

- Most parts of the screening area are characterised by specific geological conditions that will have to be considered in the planning of the most optimal location of wind farm sites.
- The screening area is dominated by a high lying glacial surface of Saalian or older glacial age and the glacial unit is cut by major buried valley systems. It can be anticipated that parts of the glacial unit have been glaciotectonically deformed, causing laterally heterogenous soil conditions including both very hard and soft beds.
- Miocene mostly firm clayey deposits occur as highs, locally subcropping at the seabed in the north-eastern part of the cable corridor area. The Miocene sediments appear to be glaciotectonically deformed as an integral part of the glacial Skovbjerg Bakkeø hill island complex, continuing inland.
- Meltwater sediments from both the late Saalian glacial period as well as the Weichselian glacial period occur as channel elements and as major sheets which have partly levelled the older glacial landscape. The unconsolidated sediments are mostly less than 15 m thick and are varying between sandy and softer silty-clayey subunits.
- Eemian (last interglacial) soft marine clayey sediments are mainly confined to the eastern part of the area where the unit reaches a thickness of about 5-10 m. The unit is typically overlain by c. 5-15 m of Weichselian glaciofluvial sand and/or Holocene marine sediments, but in the cable corridor area adjacent to Ringkøbing Fjord, Eemian deposits are found at the seabed.
- The uppermost marine Holocene unit is mostly composed of fine-medium grained sand but soft silty and clayey or even gyttja like sediments, possibly early Holocene, appear in confined/channelised areas where the Holocene unit reaches up to 15 m in thickness.
- Peat layers have only been observed in a limited number of sediment cores, and typically only few decimetres in thickness. Dating of twigs in the peat layers gave ages of c. 11000-9000 years BP. It is possible, that thicker peat layers are found in larger infilled landscape depressions, which it has not been able to reach with a standard 6 m vibrocorer.

Based on the mapping results of the screening area and settings of nearby OWF's, it is concluded that most parts of North Sea I area appear to be suitable for foundation of wind turbines. However, the area exhibits different character with respect to the level of the glacial surface, the occurrence of several hundred-meter-deep buried valleys and composition and thickness of surficial sediment units composed mostly of sandy or clayey deposits. The occurrence of soft marine Eemian clays with up to 10-20 m in total

thickness in the eastern part of the area, is a point of attention. The same clay unit was identified by Thor and Horns Rev 3 OWF integrated geological model studies and geotechnical parameters from these projects may thus serve as a guide for potential challenges and foundation solutions.

The cable corridor shows from north to south quite different sediment units close to the sea floor. The northeastern part contains a glacial complex with high-lying glaciotechnically deformed Miocene clay deposits, whereas the southern part is dominated by more fine-grained Eemian clayey deposits and channelised Holocene deposits. In the western part of the area, Weichselian sandy meltwater deposits dominate. Late Holocene mobile sand areas with large bedforms on top are predominantly found in the northern part of the cable corridor area.

The Holocene transgression of the OWF area took place c. 9500-8200 years BP indicating that only Maglemose culture remains can be found. The shallower cable corridor area on the other hand was transgressed c. 9200-7000 years BP indicating the possibility to find Maglemose, Kongemose and older Ertebølle culture remains. However, due to the common high energy environment of the West Jutland North Sea coast, the probability of making archaeological finds in the screening area, is expected to be relatively low.

12. References

- Anthony, D. & Leth, J.O. 2002. Large-scale bedforms, sediment distribution and sand mobility in the eastern North Sea off the Danish west coast. *Marine Geology* 182, 247-263.
- Cohen, K.M., Westley, K., Erkens, G., Hijma, M.P. & Weerts, H.J.T. 2017. Chatter 7, The North Sea. In: *Submerged landscapes of the European continental shelf: Quaternary Palaeoenvironments*, First Edition. Ed. By N.C. Flemming, J. Harff, D. Moura, A. Burgess and G.N. Baily. J.
- Cotterill, Carol J.; Phillips, Emrys; James, Leo; Forsberg, Carl Fredrik; Tjelta, Tor Inge; Carter, Gareth; Dove, Dayton. 2017 The evolution of the Dogger Bank, North Sea: a complex history of terrestrial, glacial and marine environmental change. *Quaternary Science Reviews*, 171. 136-153. <https://doi.org/10.1016/j.quascirev.2017.07.006>
- Gaffney, V., Gaffney, V., Thomson, K., Fitch, S., Briggs, K., Bunch, M., & Holford, S. (2007). An Atlas of the Palaeolandscapes of the Southern North Sea. In *Mapping Doggerland: the Mesolithic Landscapes of the Southern North Sea*.
- Huuse, M. & Lykke-Andersen, H. 2000a. Overdeepened Quaternary valleys in the eastern Danish North Sea: morphology and origin. *Quat. Sci. Rev.* 19, 1233-1253.
- Lambeck, K., Rouby, H, Purcell, A, Sun, Y., & Sandbridge, M. 2014. Sea level and global ice volumes from the Last Glacial Maximum to the Holocene. *Proceedings of the National Academy of Sciences* 111(43). DOI: 10.1073/pnas.1411762111.
- Leth, J.O., Larsen, B. & Anthony, D. 2004, Sediment distribution and transport in the shallow coastal waters along the west coast of Denmark. *Geological Survey of Denmark and Greenland Bulletin* 4, 41–44.
- Konradi, P.B., Larsen, B. & Sørensen, Aa.B. 2005. Marine Eemian in the Danish eastern North Sea. *Quaternary International* 133, 21–31.
- Larsen, B. & Andersen, L.T. 2005. Late Quaternary stratigraphy and morphogenesis in the Danish eastern North Sea and its relation to onshore geology. *Netherlands Journal of Geosciences, Geologie en Mijnbouw*, 84, 2.
- Larsen, N.K., Knudsen, K.L., Krohn C.F., Kronborg, C., Murray, A.S. & Nielsen, O.B. 2009. Late Quaternary ice sheet, lake and sea history of southwest Scandinavia – a synthesis. *Boreas*, Vol. 38, pp. 732–761.
- Nielsen, T., Mathiesen, A. & Bryde-Auken, M. 2008. Base Quaternary in the Danish parts of the North Sea and Skagerrak. *Geological Survey of Denmark and Greenland Bulletin*, 15, 37-40.
- Velenturf, A.P.M., Emery, A.R., Hodgson, D.M., Barlow, N.L.M., Mohtaj Khorasani, A.M., Van Alstine, J., Peterson, E.L., Piazzolo, S. & Thorp, M. 2021. Geoscience Solutions for Sustainable Offshore Wind Development. *Earth Science, Systems and Society*. The Geological Society of London. 2 November 2021. Volume 1. Article 10042.
- Walker, J., Gaffney, V., Fitch, S., Muru, M., Fraser, A., Bates, M., & Bates, R. (2020). A great wave: The Storegga tsunami and the end of Doggerland? *Antiquity*, 94(378), 1409-1425. doi:10.15184/aqy.2020.49

12.1 Background reports

COWI for Energinet.DK. 2014. OWF Horns Rev 3 – Integrated Geological Model (Final Report).

COWI for Energinet Eltransmission A/S, 2021. Thor offshore windfarm - integrated geological model. Report.

Johnson, M. & Astrup P.M., 2020. Thor Offshore wind farm – Geoarchaeological analysis. De kulturhistoriske Museer, Holstebro Kommune, 55 pp.

GEO, 2011a. Nordsøen – Efterforskning og kortlægning af sandressourcer, Fase 1A, GEO projekt nr. 33776, Rapport 1. Udført for Kystdirektoratet.

GEO, 2011b. Nordsøen – Efterforskning og kortlægning af sandressourcer, Fase 1B, detaljområde 1-1. GEO projekt nr. 33776, Rapport 2. Udført for Kystdirektoratet.

GEUS Rep. 1999/75. Leth, J.O., Anthony, D., Andersen and L.T, Jensen, J.B. (1999): Geologisk kortlægning af Vestkysten. Regionalgeologisk tolkning af kystzonen mellem Lodbjerg og Nymindégab., Geological Survey of Denmark and Greenland.

GEUS Rep. 2001/96. Larsen, B. & Leth, J.O., 2001. Geologisk kortlægning af Vestkysten. Regionalgeologisk tolkning og en samlet vurdering af aflejringsforholdene i området mellem Nymindégab og Horns Rev. Udført for Kystdirektoratet 2000 og 2001. Vol. 1 og 2. Geological Survey of Denmark and Greenland.

GEUS Rep. 2006/4. Jensen, J.B. & Lomholt, S. 2006: Råstoffer ved HR2 Vindmølleparken. Vurdering af mulige sand- og grusforekomster på Horns Rev. Udarbejdet for ENERGI E2., 15 pp. Geological Survey of Denmark and Greenland.

GEUS Rep. 2009/48. Gravesen, P., Leth, J.O. & Jensen, J.B., 2009. Nordsøen - Havbundsdata og kortlægning. Status for data, kortlægning, ressourcer, Kvartær stratigrafi og fremtidsperspektiver., 48 pp. Geological Survey of Denmark and Greenland.

GEUS Rep. 2013/5. Lomholt, S., Leth, J.O., Skar, S. Marin råstofkortlægning i Nordsøen 2012. Detaljeret undersøgelse af 3 delområder. Udført for Naturstyrelsen. Geological Survey of Denmark and Greenland.

GEUS Rep. 2015/17. Al-Hamdany, Z. & Jensen, J.B. Vesterhavet Syd Havvindmøllepark – Geologiske modeller som basis for udpegning af arkæologiske hotspots. Geological Survey of Denmark and Greenland.

GEUS Rep. 2021-21. Nørgaard-Pedersen, N., Winther, L.H., and Rödel, L.G, 2021. Efterforskning og kortlægning af resterende sandressourcer i bygherreområde 578-AA Husby Klit, Nordsøen for Kystdirektoratet. Geological Survey of Denmark and Greenland.

GEUS Rep. 2022-7. Nørgaard-Pedersen, N., Vangkilde-Pedersen, T.G & Lomholt, S. 2022. Screening of seabed geological conditions for the offshore wind farm (OFW) area Nordsøen 1, Område E – Desk study for the Danish Energy Agency. Geological Survey of Denmark and Greenland.

12.2 Supplementary papers

- Andersen, L.T. 2004. The Fanø Bugt Glaciotectonic Thrust Fault Complex, Southeastern Danish North Sea. Ph.D.Thesis. 2004. Danmarks og Grønlands Geologiske Undersøgelse Rapport 2004/30, 35-68.
- Bockelmann, F.-D., Puls, W., Kleeberg, U., Müller, D. & Emeis, K.-C. 2018. Mapping mud content and median grain-size of North Sea sediments – A geostatistical approach. *Marine Geology* 397, 60-71.
- Coughlan, M., Fleischer, M., Wheeler, A.J., Hepp, D.A., Hebbeln, D. & Mörz, T., 2018. A revised stratigraphical framework for the Quaternary deposits of the German North Sea sector: a geological-geotechnical approach. *Boreas* 47, 80-105.
- Gibling, M.R. 2006. Width and Thickness of Fluvial Channel Bodies and Valley Fills in the Geological Record: A Literature Compilation and Classification. *Journal of Sedimentary Research* 76, 731-770.
- Gravesen, P., Pedersen, S.A.S. & Midtgaard, H.H. 2021. Studies of geological properties and conditions for deep disposal of radioactive waste, Denmark. Phase 1, report no. 2. Geological setting and structural framework of Danish onshore areas.
- Hepp, D.A., Warnke, U., Hebbeln, D. & Mörz, T. 2017. Tributaries of the Elbe Palaeovalley: Features of a Hidden Palaeolandscape in the German Bight, North Sea, Under the Sea: *Archaeology and Palaeolandscapes of the Continental Shelf*, pp. 211-222.
- Houmark-Nielsen, M. 2003. The Pleistocene of Denmark: a review of stratigraphy and glaciation history. In: Ehlers, J. & Gibbard, P. (eds): *Quaternary Glaciation-extend and chronology*. Vol. 1 Europe. Elsevier (Amsterdam): 321-336.
- Huuse, M. & Lykke-Andersen, H. 2000. Large-scale glaciotectonic thrust structures in the eastern Danish North Sea. In: Maltman, A., Hambrey, M. & Hubbard, B. (eds): *Deformation of Glacial Materials*. Geological Society, London, Special Publications 176, 293-305.
- Huuse, M., Lykke Andersen, H. & Michelson, O. 2001. Cenozoic evolution of the eastern Danish North Sea. *Marine Geology* 177, 243-269.
- Jensen, J.B., Gravesen, P. & Lomholt, S. 2008. Geology of outer Horns Rev, Danish North Sea. *Geological Survey of Denmark and Greenland Bulletin*, 15, 41-44.
- Knudsen, K.L. 1985. Foraminiferal stratigraphy of Quaternary deposits in the Roar, Skjold and Dan fields, central North Sea. *Boreas* 14, 311–324.
- Larsen, B. & Leth, J.O. 2001. Geologisk kortlægning af Vestkysten. Regionalgeologisk tolkning og en samlet vurdering af aflejringsforholdene i området mellem Nymindesø og Horns Rev. Udført for Kystdirektoratet 2000 og 2001. Vol. 1 og 2.
- O Cofaigh, C. 1996. Tunnel valley genesis. *Progress in Physical Geography* 20, 1-19.
- Ottesen, D., Batchelor, C.L., Dowdeswell, J.A. & Løseth, H. 2018. Morphology and pattern of Quaternary sedimentation in the North Sea Basin (52–62°N). *Marine and Petroleum Geology* 98, 836-859.

Overeem, I., Weltje, G.J., Bishop-Kay, C. & Kroonenberg, S.B. 2001. The Late Cenozoic Eridanos delta system in the Southern North Sea Basin: a climate signal in sediment supply? *BasinResearch* 13, 293-312.

Peryt, T.M., Geluk, M.C., Mathiesen, A., Paul, J. & Smith, K. 2010. Zechstein. In: Doornenbal, J.C., Stevenson, A.G., (Eds.), *Petroleum Geological Atlas of the Southern Permian Basin Area*, EAGE Publications, pp. 123-147.

Prins, L.T., Andresen, K.J., Clausen, O.R. & Piotrowski, J.A. 2020. Formation and widening of a North Sea tunnel valley - The impact of slope processes on valley morphology. *Geomorphology* 368.

Rasmussen, E.S. 2017. Sedimentology and sequence stratigraphy of the uppermost upper Oligocene -Miocene fluvio-deltaic system in the eastern North Sea Basin: the influence of tectonism, eustacy and climate. Doctoral Thesis, 440 pp..

Rasmussen, E.S., Vejbæk, O.V., Bidstrup, T., Piasecki, S. & Dybkjær, K. 2005. Late Cenozoic petroleum systems. In: Doré, A.G. & Vinning, B.A. (Eds). *Petroleum Geology: North-West Europe and Global Perspectives*. Proceedings of the 6th Petroleum Geology Conference, 1347–1358. Geological Society, London.

Rasmussen, E.S., Dybkjær, K. & Piasecki, S. 2010. Lithostratigraphy of the Upper Oligocene – Miocene succession of Denmark. *Geological Survey of Denmark and Greenland Bulletin* 22, 1–92.

Appendices

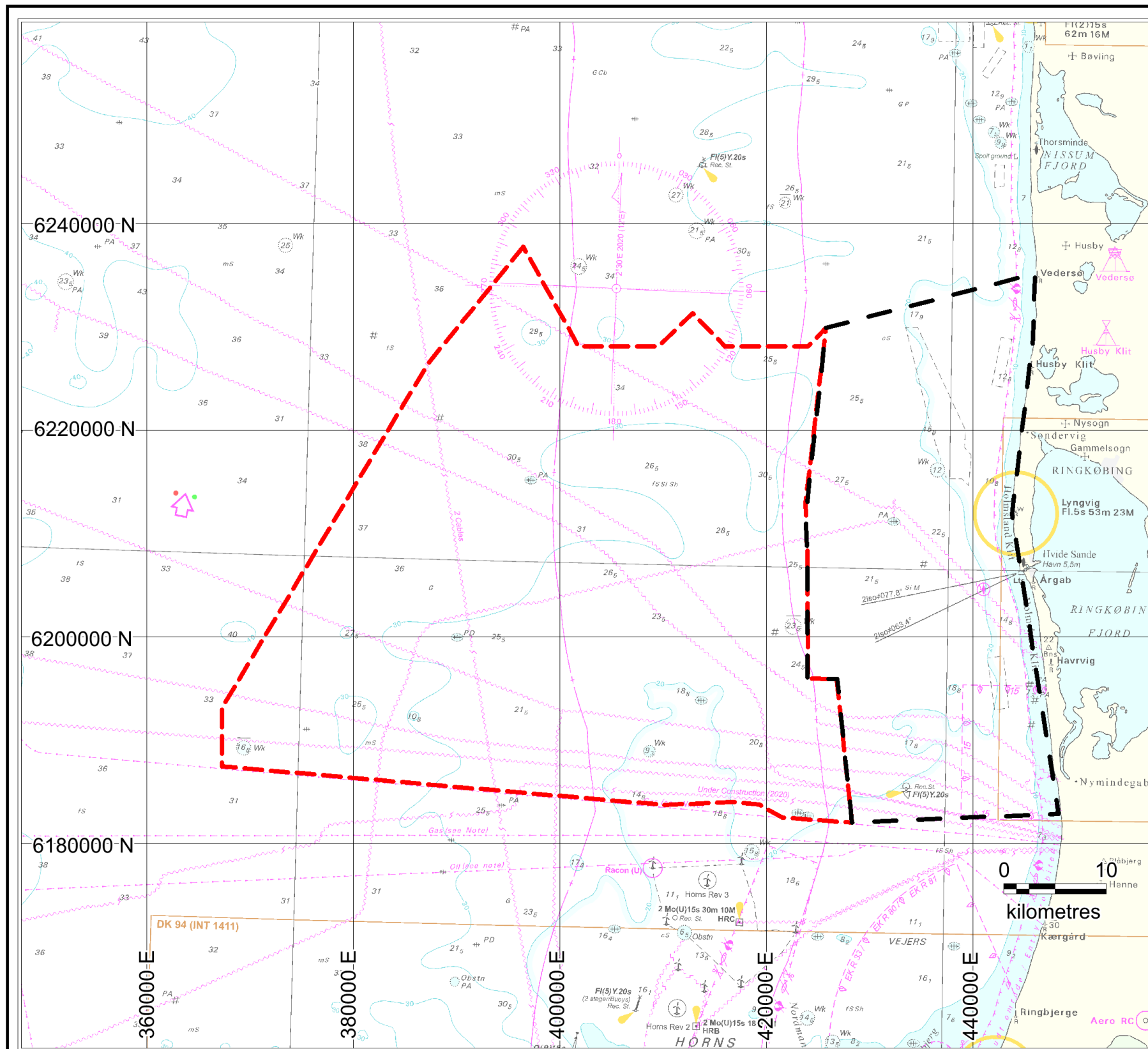
A. Maps

- A1: Screening area
- A2: Bathymetry
- A3: Seafloor sediment
- A4: Seismic lines and sediment core sites
- A5: Location of selected seismic profiles
- A6: OWF area - Holocene unit (isopach)
- A7: OWF area - Base Holocene unit (m below sea level)
- A8: OWF area - Weichsel Meltwater Unit (isopach)
- A9: OWF area - Eemian unit (isopach)
- A10: OWF area - Top Saale unit (m below sea floor)
- A11: OWF area - Top Saale unit (m below sea level)
- A12. Cable corridor – Geologic units below mobile sand
- A13: OWF and cable corridor key geological units

B. OWF area: Selected long seismic sections (1-6) with interpretation

C. Cable corridor area: Selected long seismic sections (7-14) with interpretation



D. Table with available sediment cores (with link to description)



Danish North Sea 1

Screening study

Legend

-  North Sea 1 OWF
-  Cable corridor area

Projection: ETRS89 zone 32N

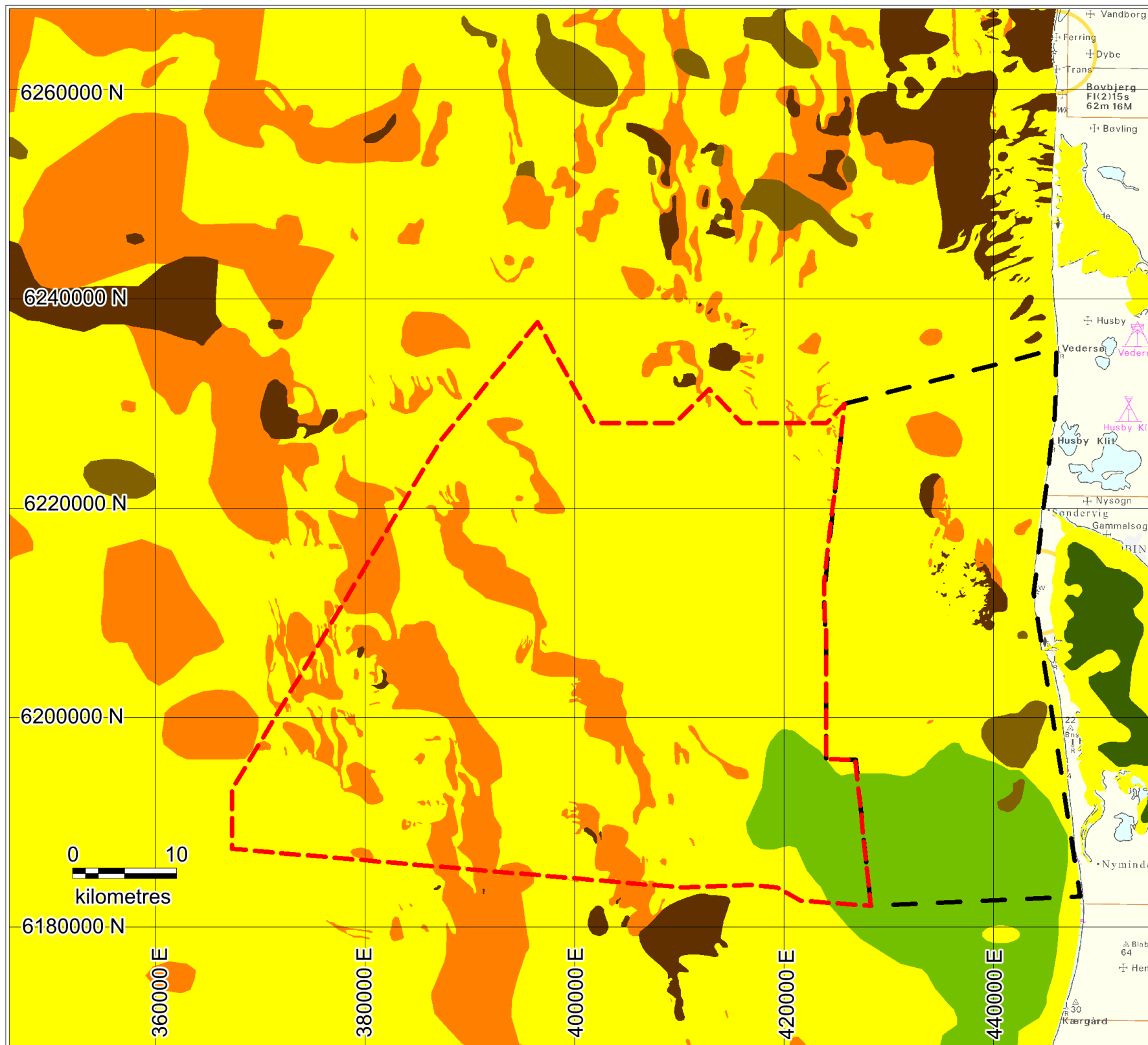
Client:



Version: NNP 24-03-2023

Appendix A1:





Screening area



Danish North Sea 1

Screening study

Legend

-  North Sea 1 OWF
-  Cable corridor area
- Seabed surface sediment**
 -  Till
 -  Quaternary clay/silt
 -  Gravelly sand
 -  Sand
 -  Silty sand
 -  Clayey-silty sand/Gyttja

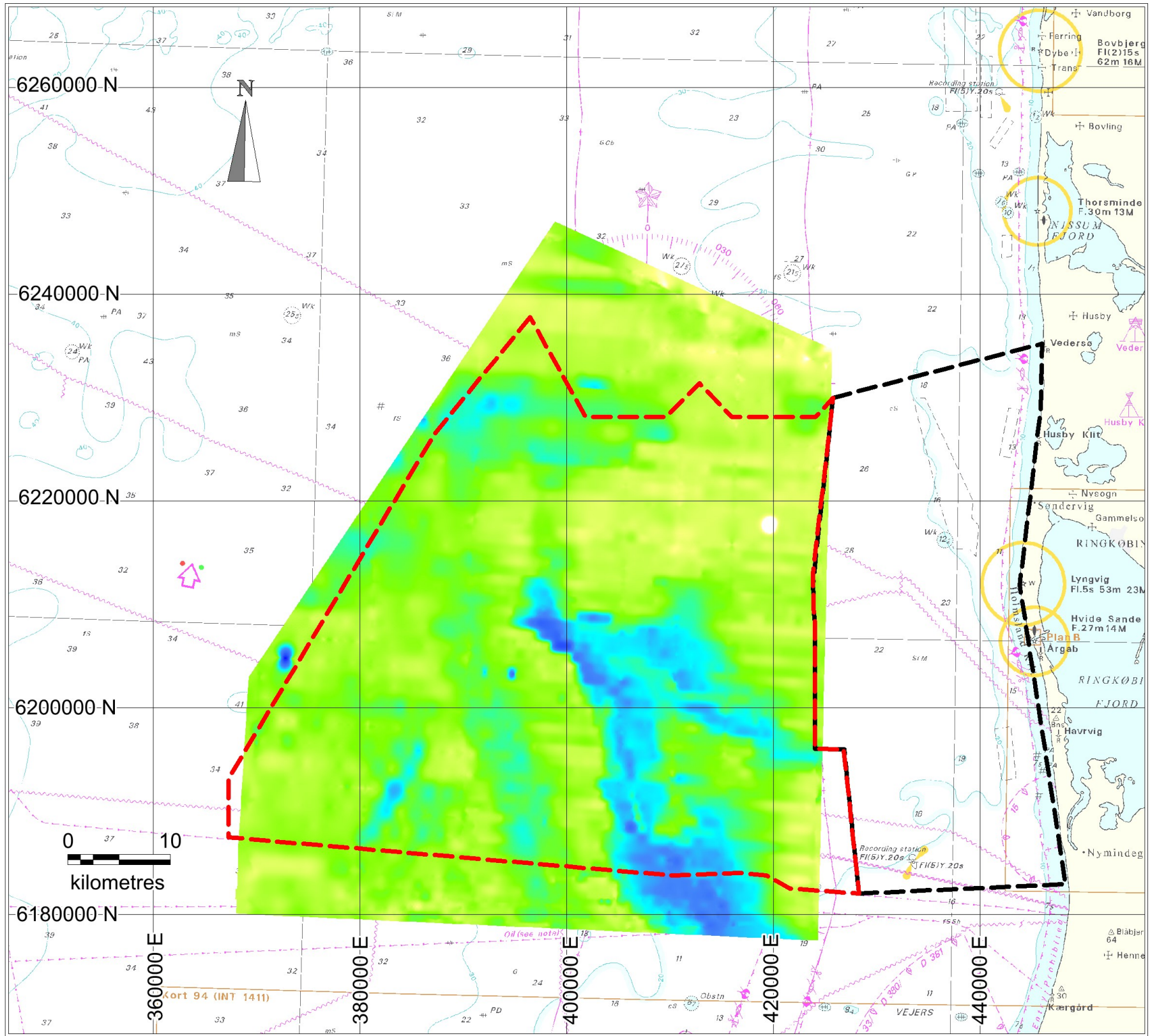
Projection: ETRS89 zone 32N

Client:



Version: NNP 24-03-2023

Appendix A3:
Seabed surface sediment



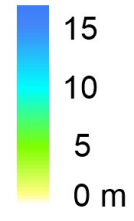
Danish North Sea 1

Screening study

Legend

- North Sea I OLF area
- Cable corridor area

Holocene unit thickness (m)



Projection: ETRS89 zone 32N

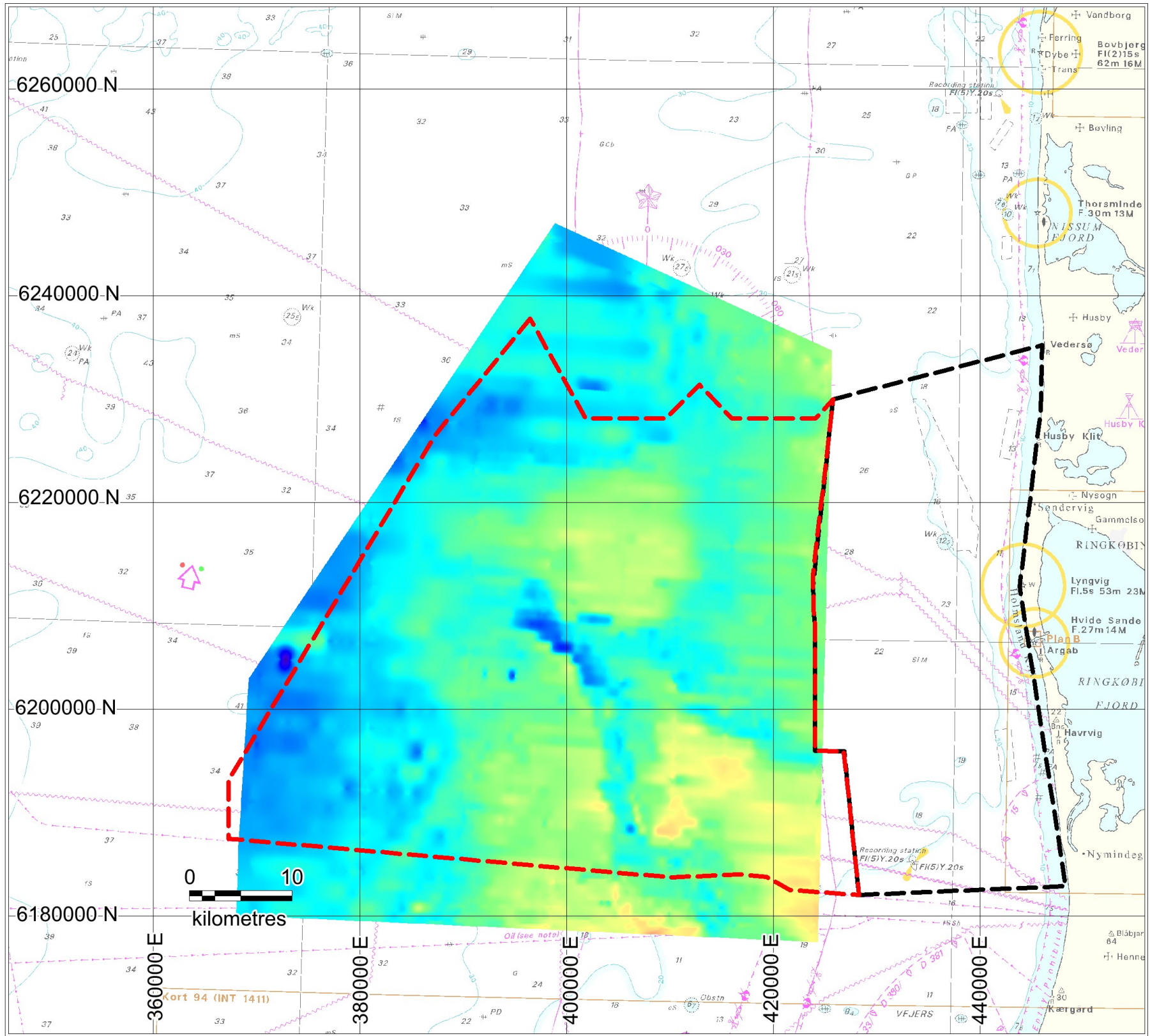
Client:



Version: NNP 16-05-2023

Appendix A6:

Holocene unit thickness



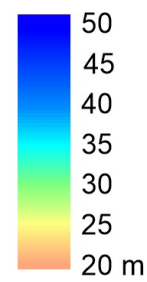
Danish North Sea 1

Screening study

Legend

- North Sea I OLF
- Cable corridor area

Base Holocene Unit (m below sea level)



Projection: ETRS89 zone 32N

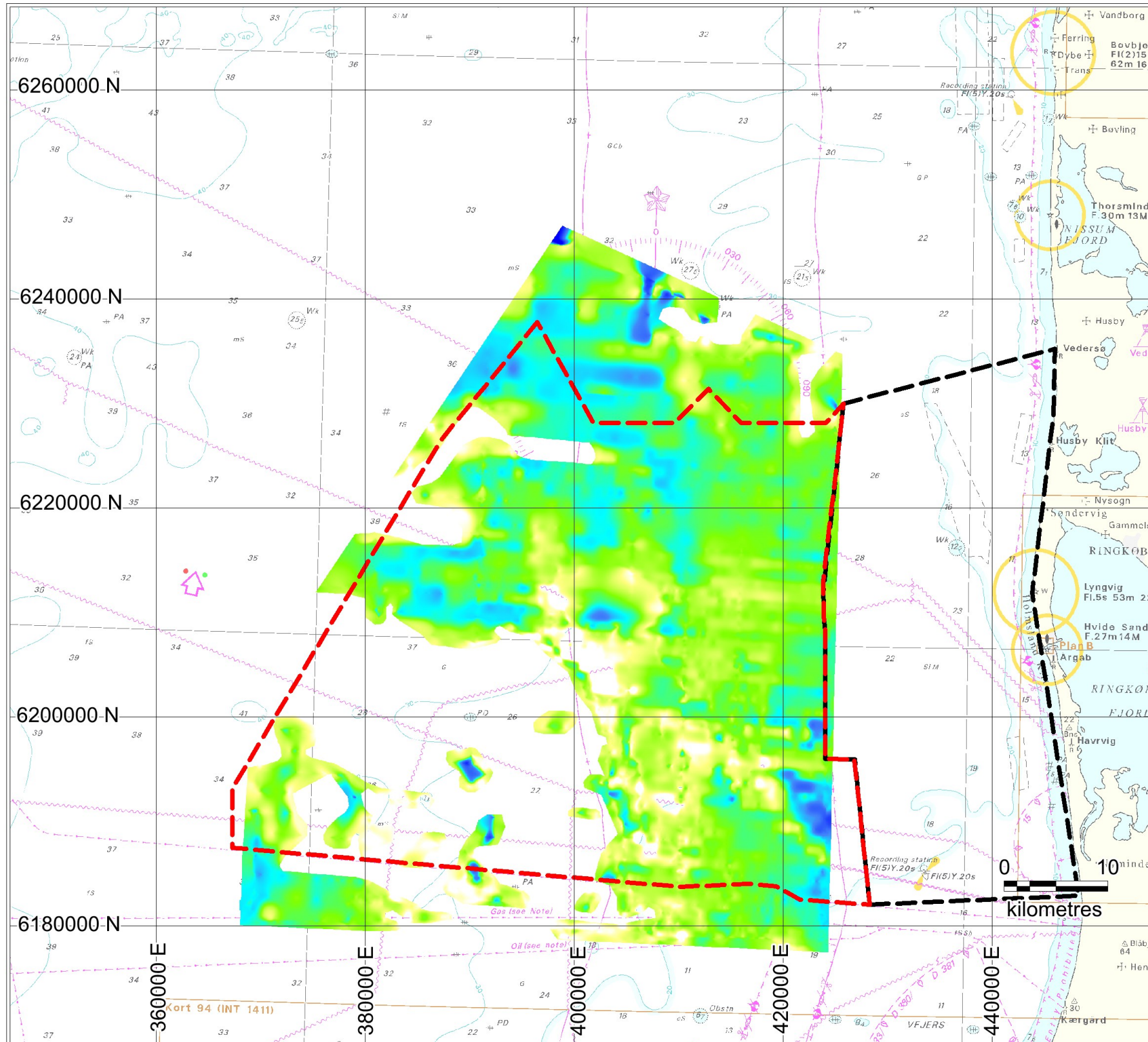
Client:



Version: NNP 15-05-2023

Appendix A7:

Base Holocene Unit
(m below sea level)




Danish North Sea 1

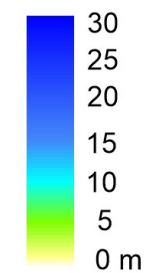
Screening study

Legend

 North Sea I OWF area

 Cable corridor area

Weichsel unit thickness:



Projection: ETRS89 zone 32N

Client:

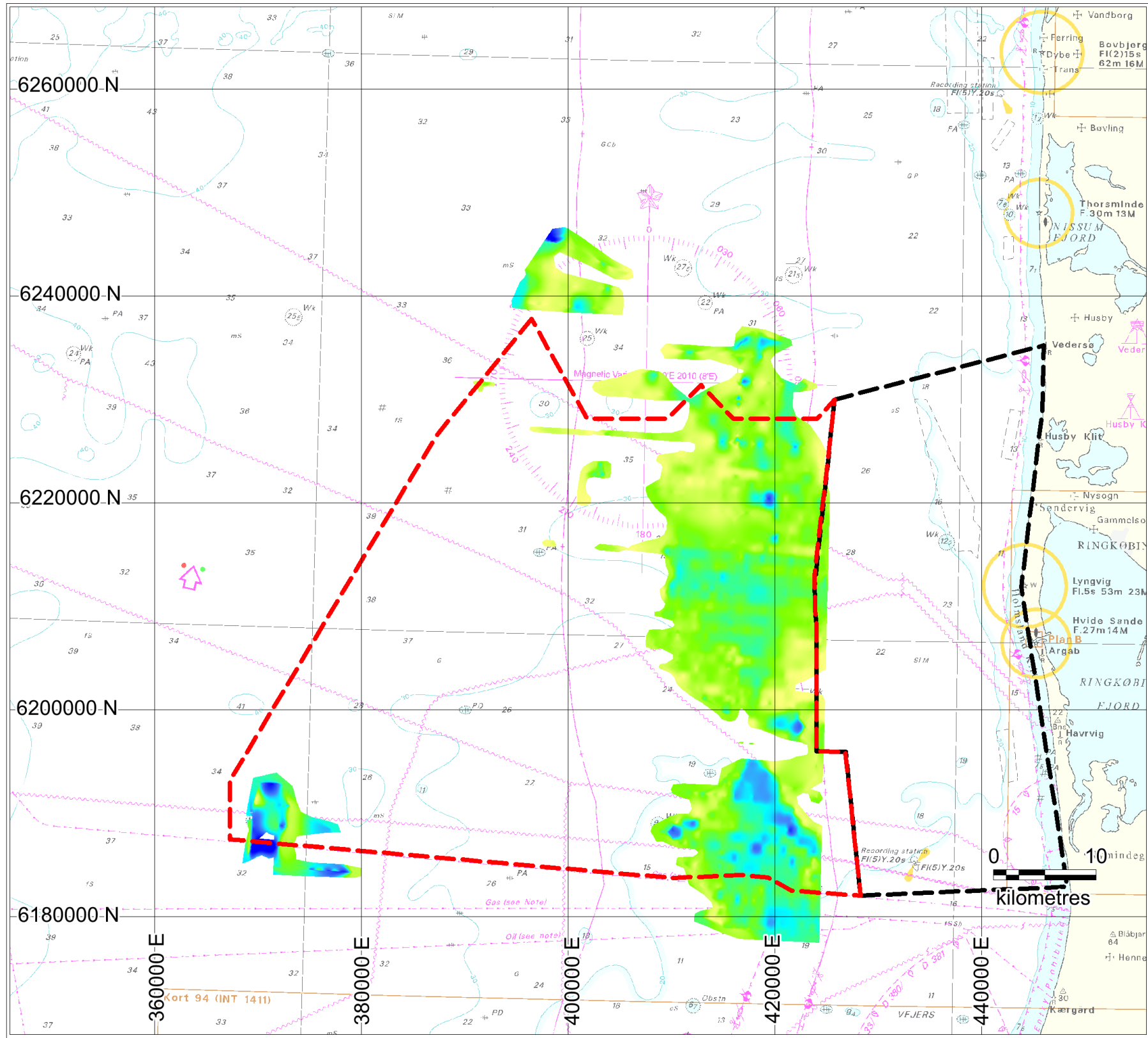
ENERGINET



Version: NNP 22-05-2023

Appendix A8:


Weichsel unit thickness




Danish North Sea 1

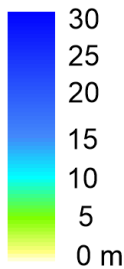
Screening study

Legend

 North Sea I OWF area

 Cable corridor area

Eemian unit thickness:



Projection: ETRS89 zone 32N

Client:

ENERGINET

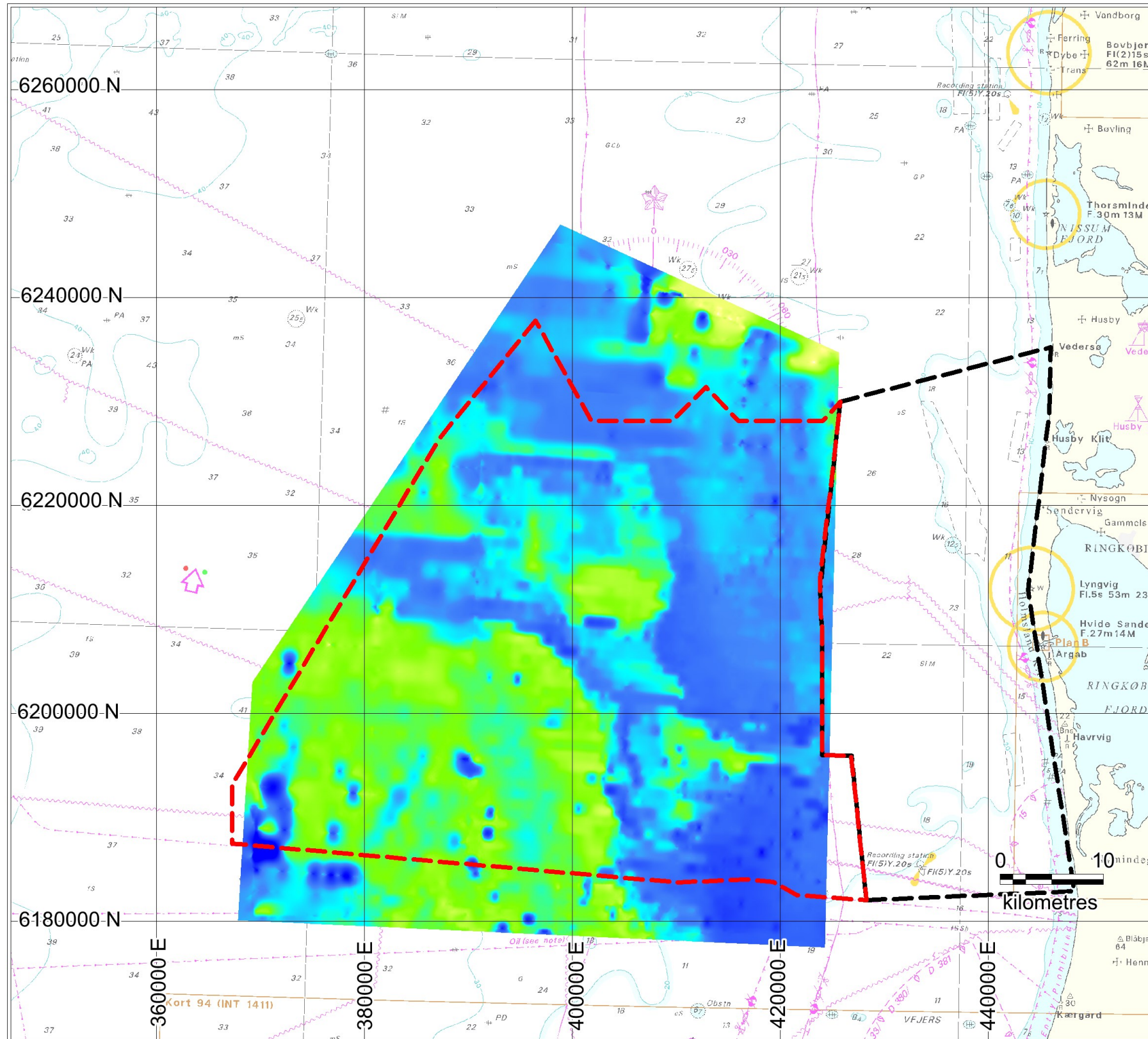


GEUS

Version: NNP 22-05-2023

Appendix A9:

Eemian unit thickness



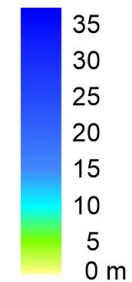
Danish North Sea 1

Screening study

Legend

- North Sea I OLF area
- Cable corridor area

Top Saale Unit (m below sea floor)



Projection: ETRS89 zone 32N

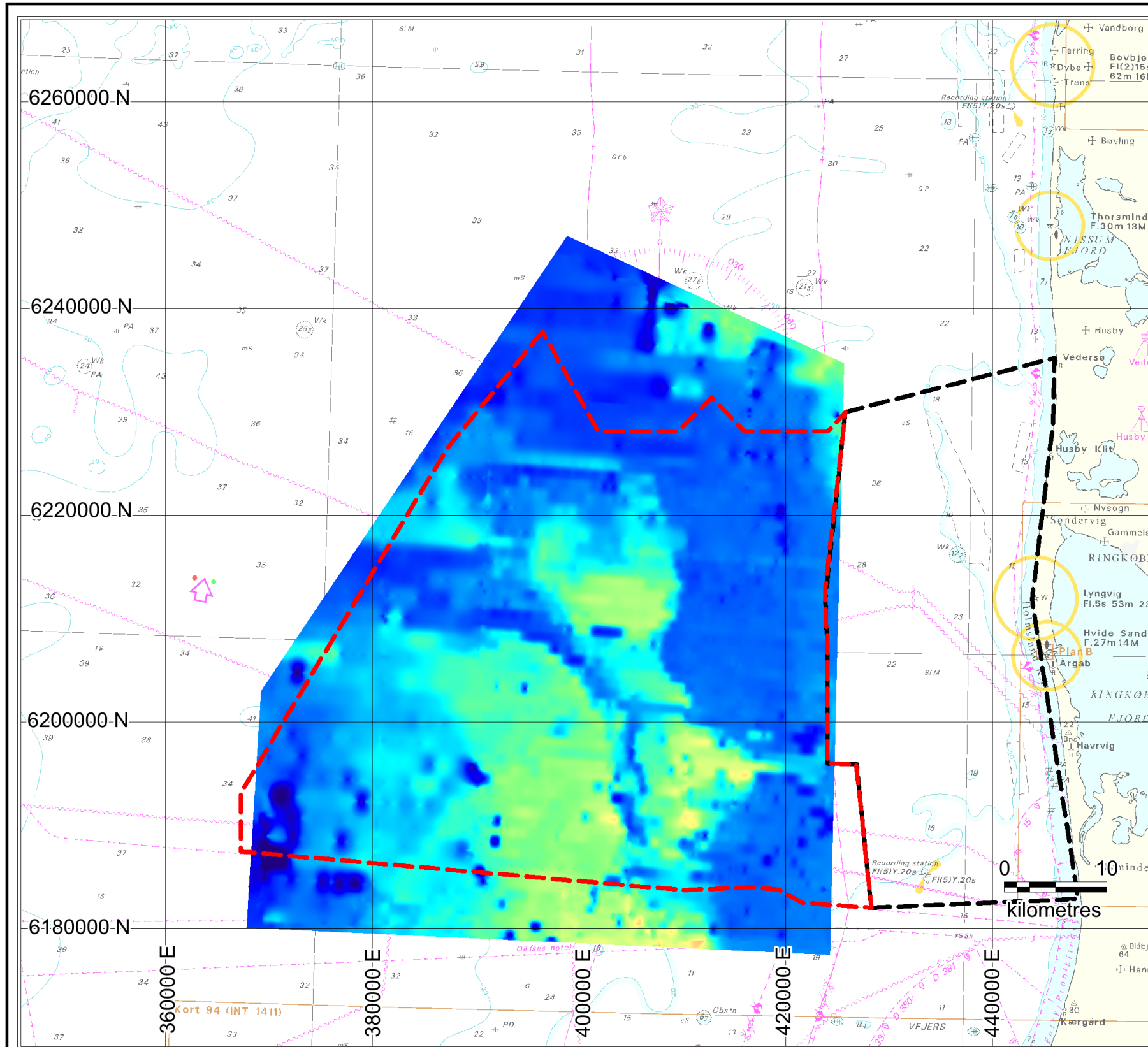
Client:



Version: NNP 22-05-2023

Appendix A10:



Top Saale unit
(m below sea floor)



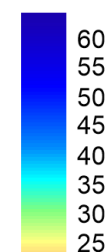
Danish North Sea 1

Screening study

Legend

-  North Sea I OLF area
-  Cable corridor area

Top Saale Unit (m below sea level)



Projection: ETRS89 zone 32N

Client:

ENERGINET

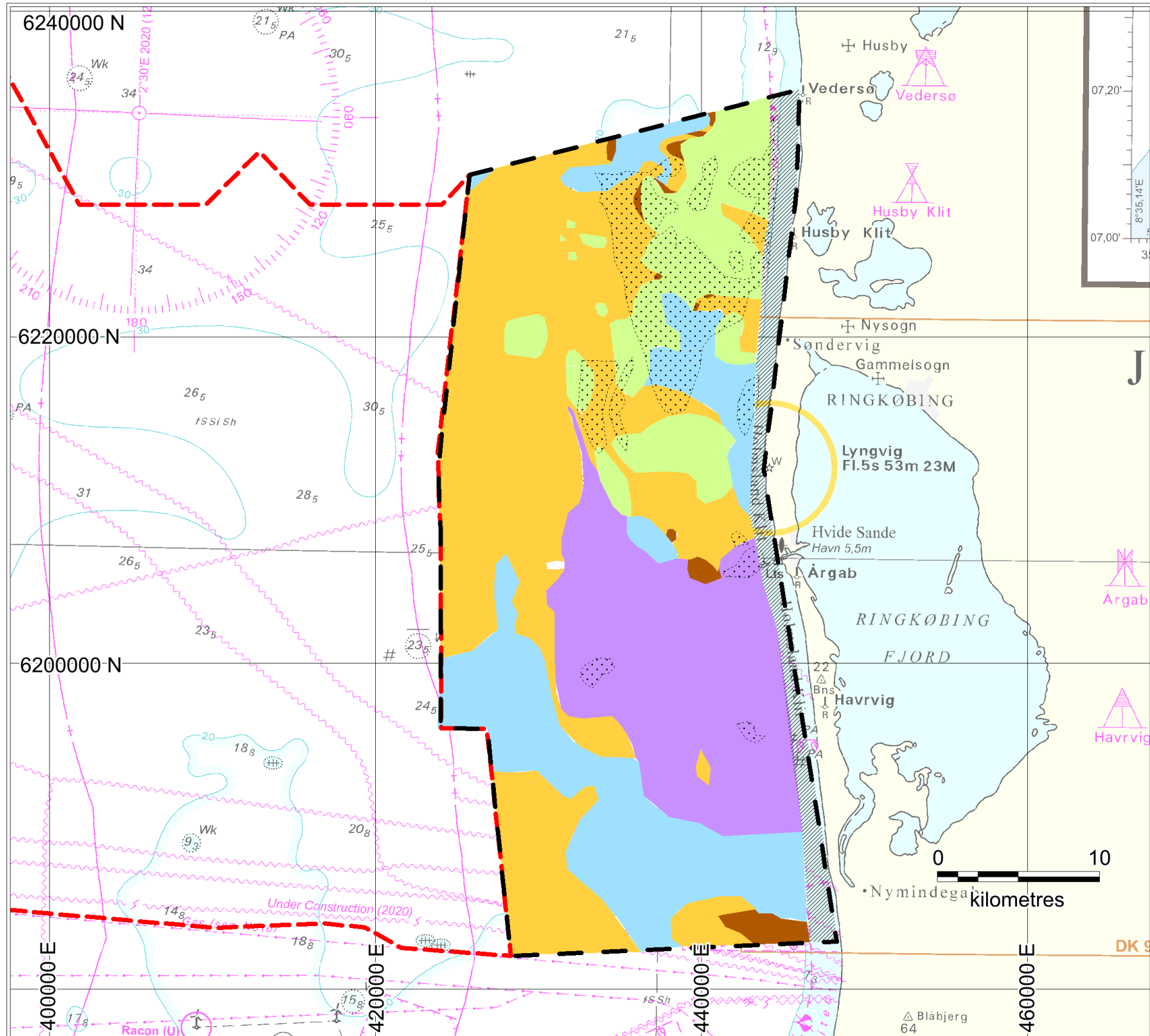


GEUS

Version: NNP 22-05-2023

Appendix A11:

Top Saale Unit
(m below sea level)




Danish North Sea 1






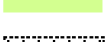
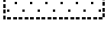
Screening study

Legend

 North Sea 1 OWF

 Cable corridor area

Geological units below mobile sand:

-  Holocene marine deposits (sand or silt/clay)
-  Meltwater deposits (Weichselian or older), (sand, occasionally gravelly)
-  Eemian marine deposits (clay-silt)
-  Glacial surface (Saalian or older) (till)
-  Miocene deposits (mostly firm clay)
-  Mobile sand (thicker >1m)
-  Undifferentiated (shallow water)

Projection: ETRS89 zone 32N

Client:

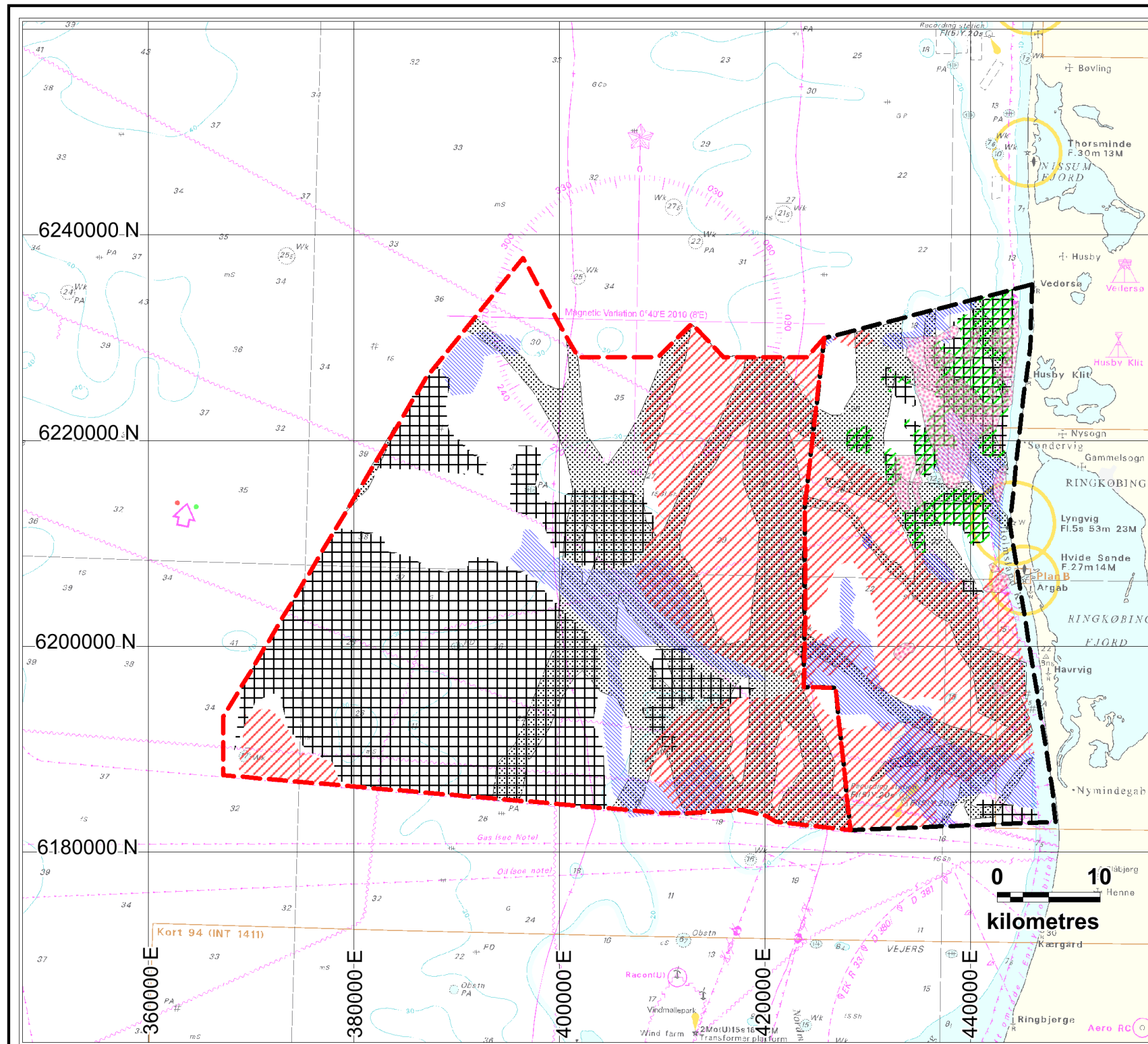
ENERGINET



GEUS

Version: NNP 12-05-2023

Appendix A12:
Geological units below mobile
sand layer



Danish North Sea 1

Screening study

Legend

- North Sea I OWF area
- Cable corridor area

Key geological units:

- Buried Quaternary valleys
- Miocene deposits (firm clay) close to seabed
- Saalian glacial surface close to seabed
- Thick clayey Eemian unit
- Thick Holocene unit - clayey in lower part
- Mobile sand unit at seabed

Projection: ETRS89 zone 32N

Client:

ENERGINET



GEUS

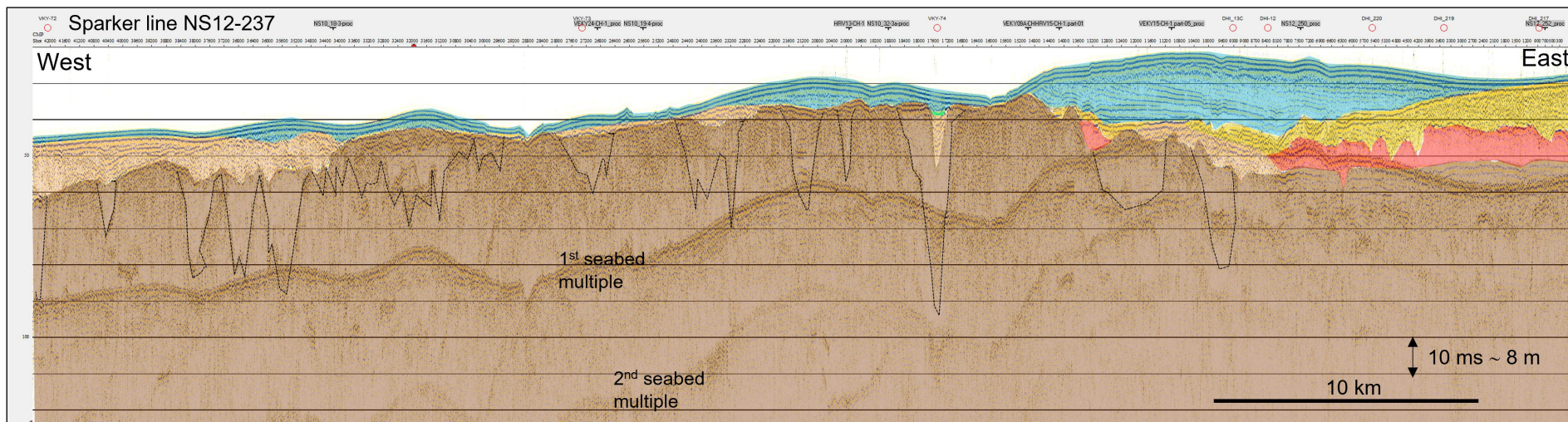
Version: NNP 15-05-20223



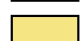
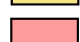
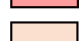

Appendix A13:

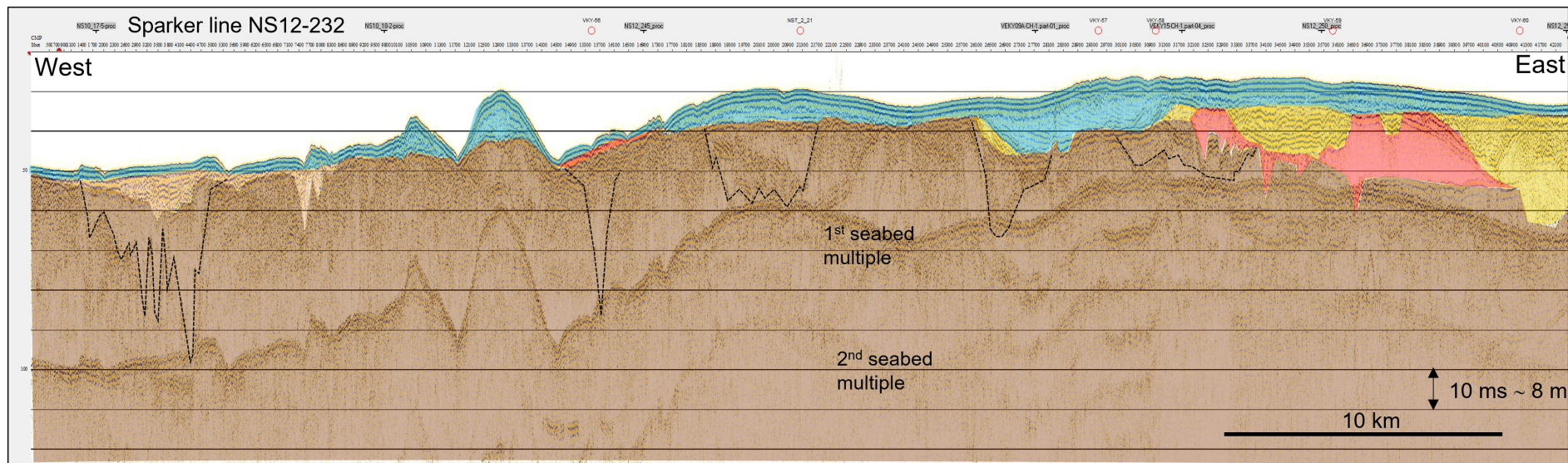
Extension of key geological units



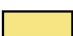



Appendix B

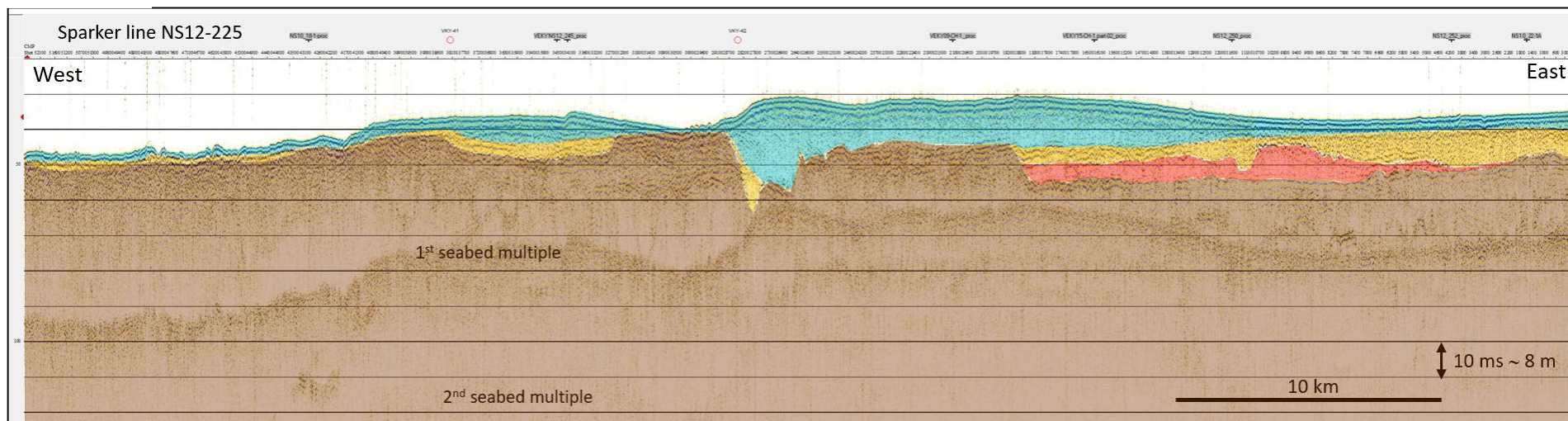
OWF area – Selected long seismic sections (1-6) with interpretation









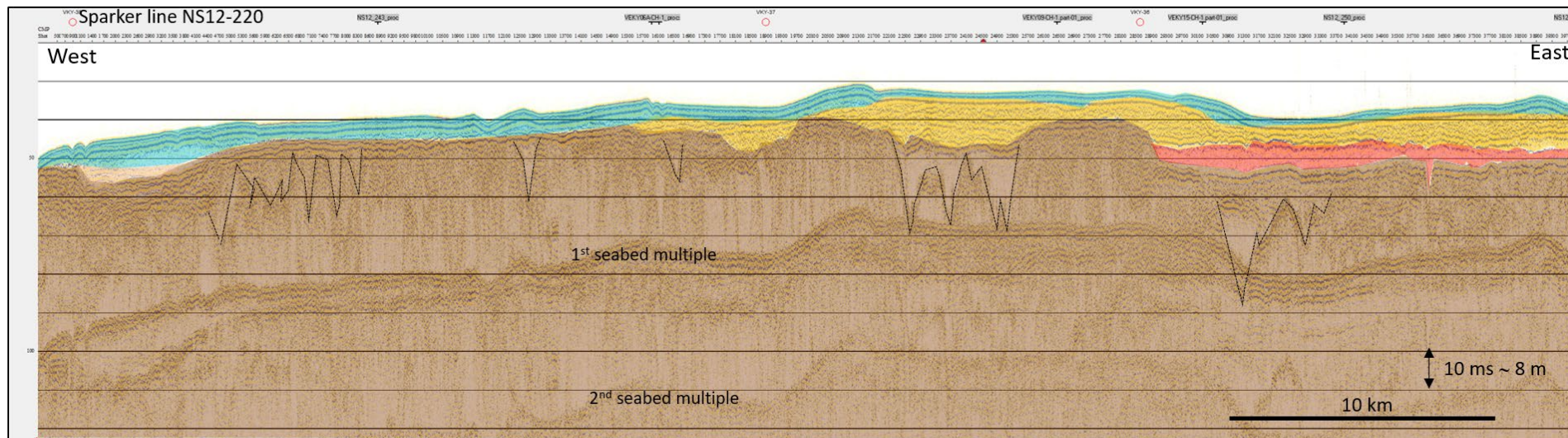
-  Holocene marine deposits
-  Holocene peat/freshwater deposits
-  Weichselian meltwater deposits (glaciofluvatile/-lacustrine)
-  Eemian marine deposits
-  Late Saalian meltwater deposits
-  Saalian or older glacial deposits with infilled valleys









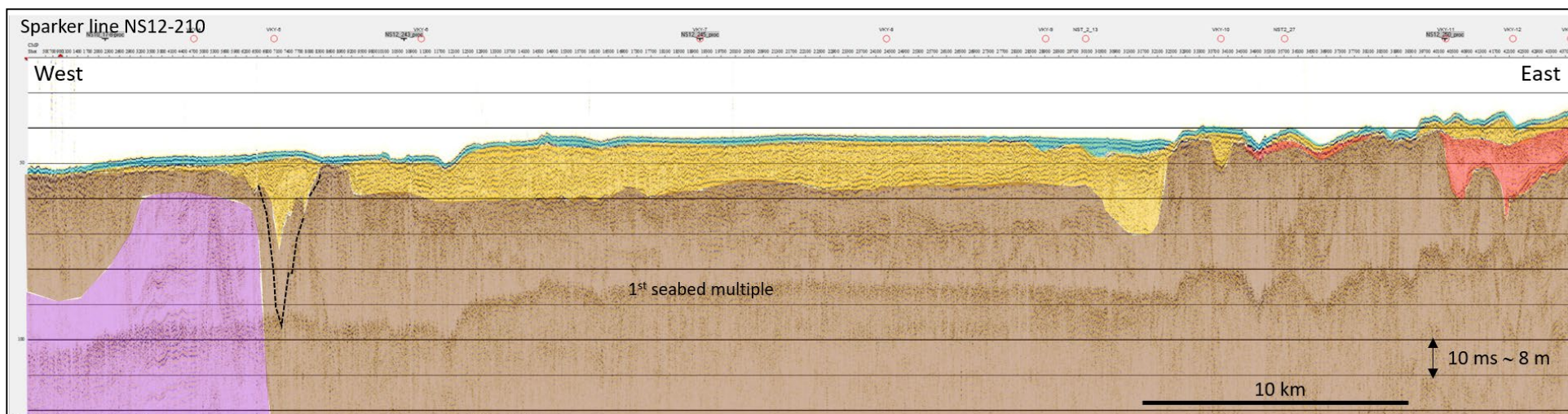
-  Holocene marine deposits
-  Holocene peat/freshwater deposits
-  Weichselian meltwater deposits (glaciofluvial/-lacustrine)
-  Eemian marine deposits
-  Late Saalian meltwater deposits
-  Saalian or older glacial deposits with infilled valleys



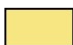
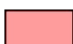


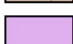


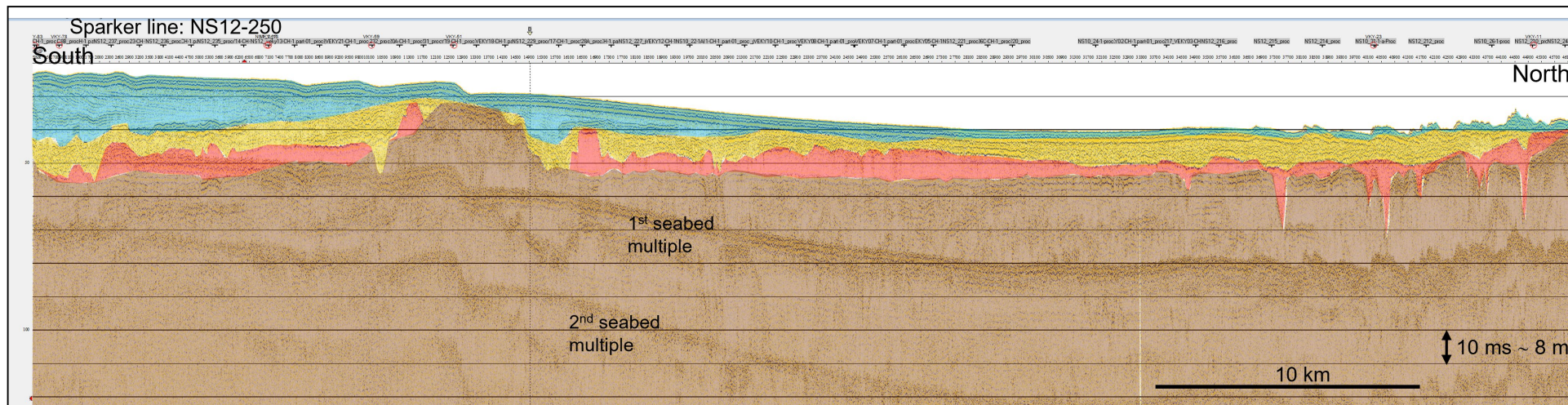
-  Holocene marine deposits
-  Holocene peat/freshwater deposits
-  Weichselian meltwater deposits (glaciofluvial/-lacustrine)
-  Eemian marine deposits
-  Late Saalian meltwater deposits
-  Saalian or older glacial deposits with infilled valleys

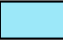







-  Holocene marine deposits
-  Holocene peat/freshwater deposits
-  Weichselian meltwater deposits (glaciofluvatile/-lacustrine)
-  Eemian marine deposits
-  Late Saalian meltwater deposits
-  Saalian or older glacial deposits with infilled valleys



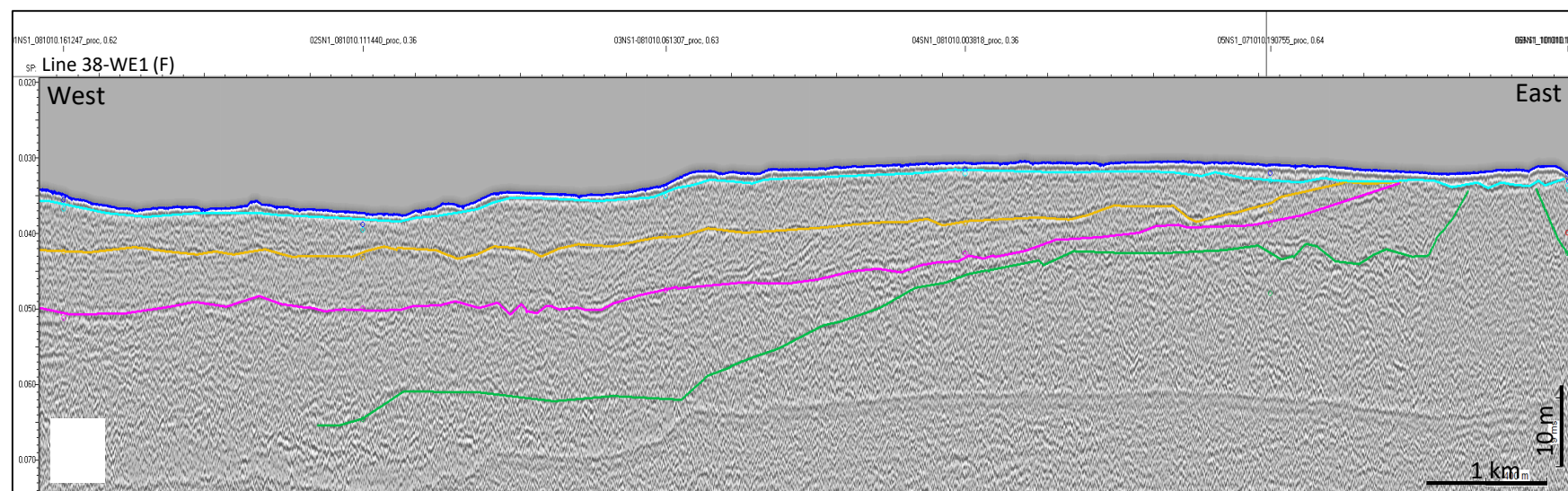
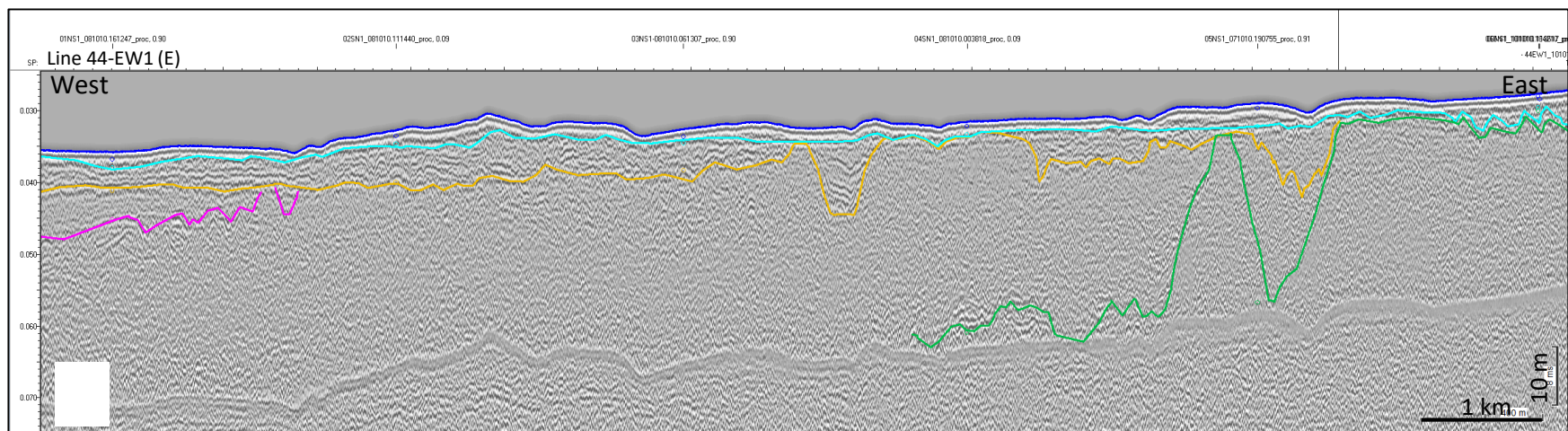
-  Holocene marine deposits
-  Holocene peat/freshwater deposits
-  Weichselian meltwater deposits (glaciofluvial/-lacustrine)
-  Eemian marine deposits
-  Late Saalian meltwater deposits
-  Saalian or older glacial deposits with infilled valleys
-  Prequaternary deposits (Miocene, glaciotectonically deformed)



-  Holocene marine deposits
-  Holocene peat/freshwater deposits
-  Weichselian meltwater deposits (glaciofluviale/-lacustrine)
-  Eemian marine deposits
-  Late Saalian meltwater deposits
-  Saalian or older glacial deposits with infilled valleys

Appendix C

Cable corridor area – Selected long seismic sections (7-14) with interpretation

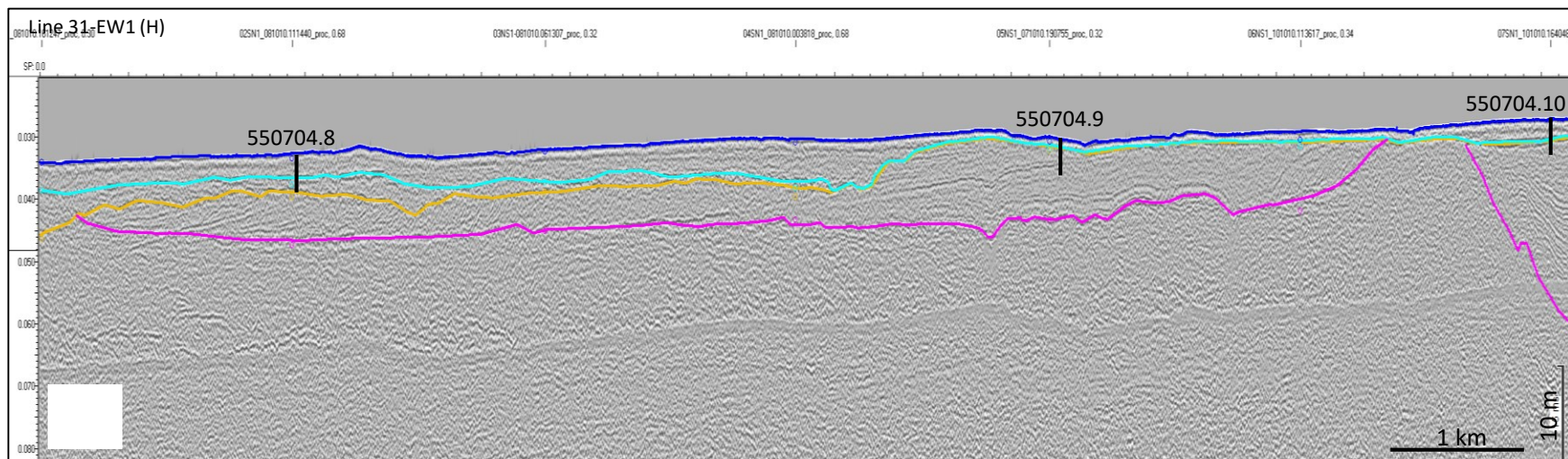
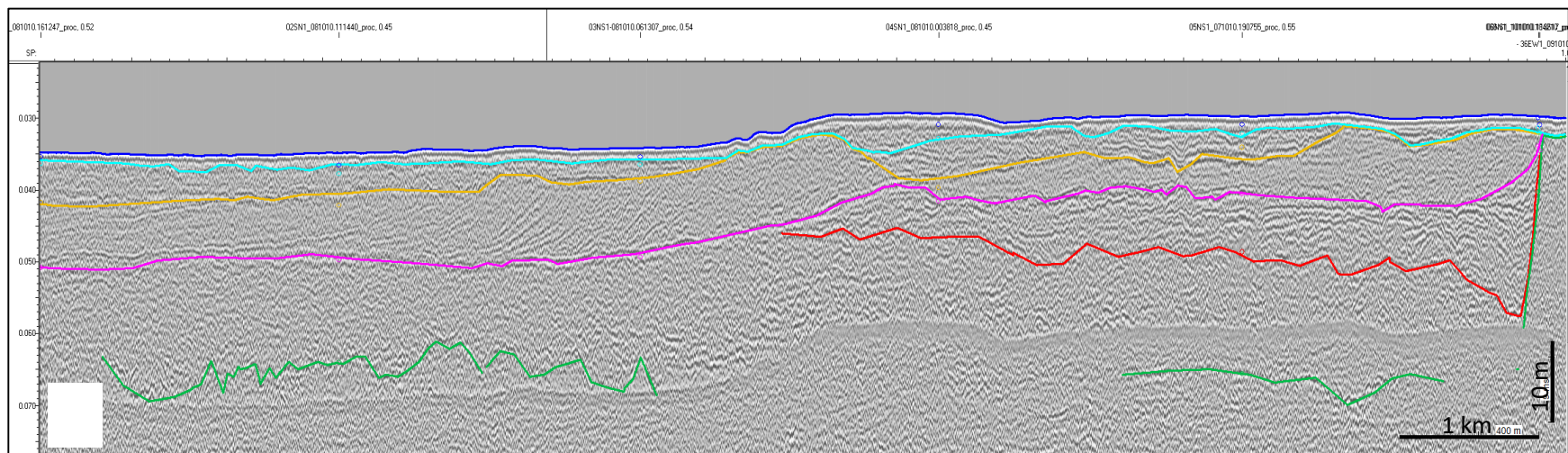


Seismic interpretation

- Base Holocene
- Base Weichselian
- Base Eemian
- Base Saalian MW
- Top PQ

Vibro-core site

| Core No.

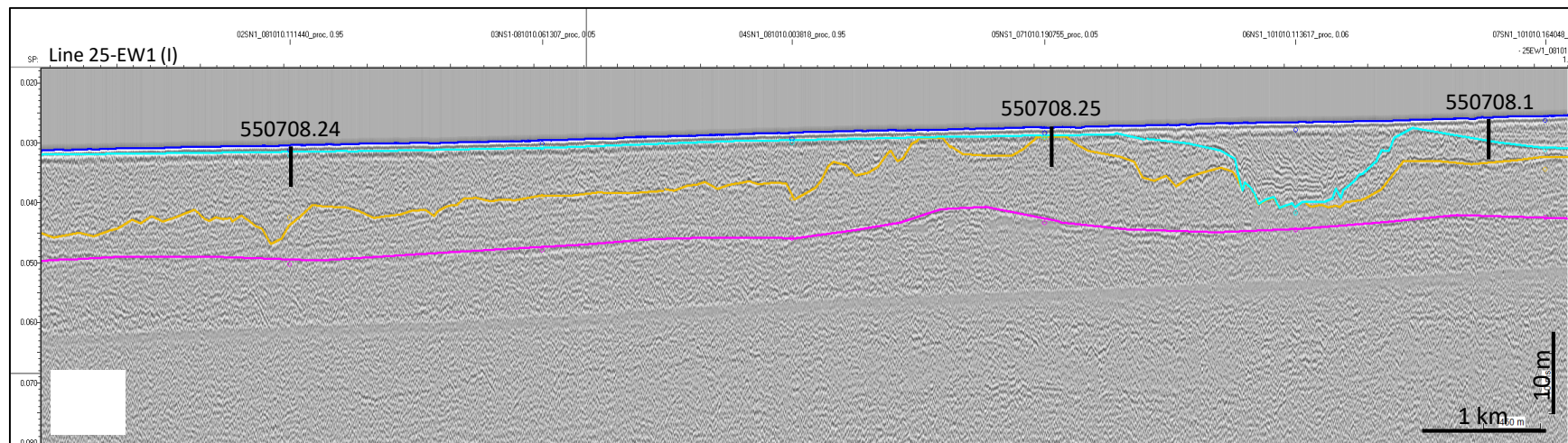


Seismic interpretation

- Base Holocene
- Base Weichselian
- Base Eemian
- Base Saalian MW
- Top PQ

Vibro-core site

| Core No.

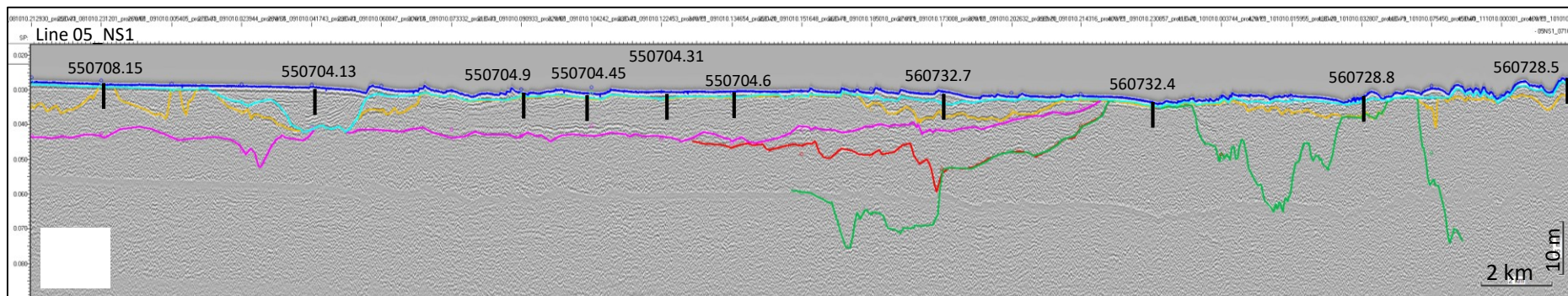
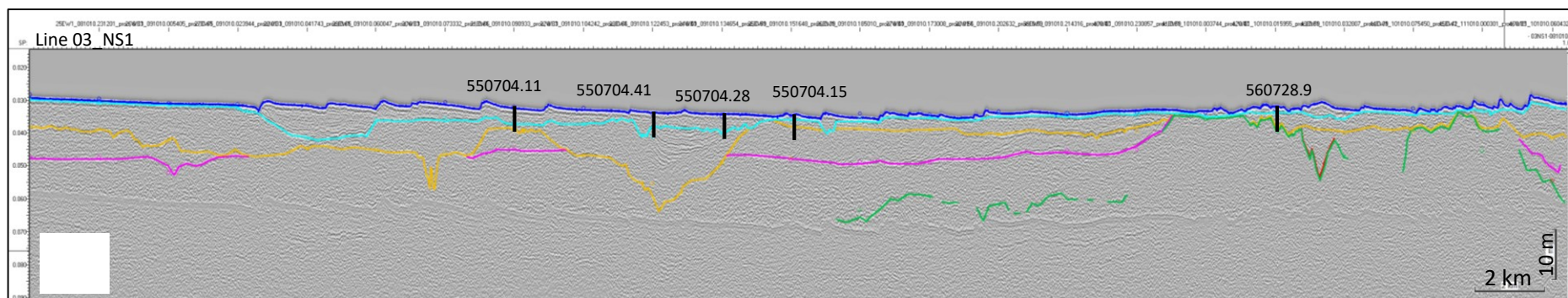
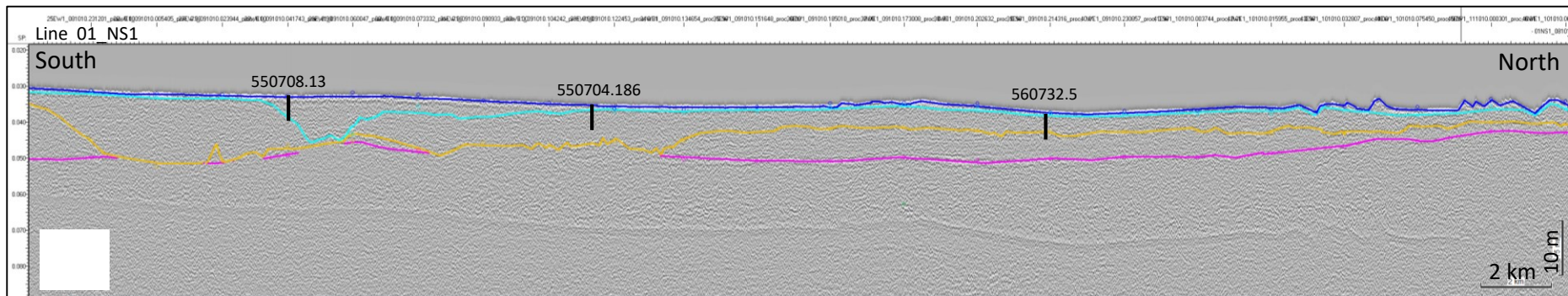


Seismic interpretation

- Base Holocene
- Base Weichselian
- Base Eemian
- Base Saalian MW
- Top PQ

Vibro-core site

Core No.



Seismic interpretation

- Base Holocene
- Base Weichselian
- Base Eemian
- Base Saalian MW
- Top PQ

Vibro-core site

Core No.

Appendix D

Table with available sediment cores (with link to core log description)

Id	Dgu No. (GEUS)	Method	Year	X utm32eur	Y utm32eur	Grade (DVR90)	Lithology	Orig. Core ID	Link to core log description
217914	560829.3	Vibrocore		443101	6216322	-9	[0.00m:hs],[1.58m:hl],[1.62m:hl],[2.40m:hl],[2.90m:hs],[3.70m:hl]	131-31-578027	Link
217915	560829.4	Vibrocore		437924	6219008	-15.3	[0.00m:hs],[2.58m:hl]	131-31-578003	Link
217916	560825.1	Vibrocore		437927	6230280	-19.4	[0.00m:hs],[1.15m:hs],[1.30m:hs],[1.35m:hs],[1.50m:gi],[1.56m:gi],[1.80m:gi]	131-31-578004	Link
217917	560825.2	Vibrocore		437917	6230594	-19.4	[0.00m:hs],[1.50m:hs],[2.70m:hl],[3.50m:hl]	131-31-578005	Link
217920	560825.3	Vibrocore		437925	6228411	-19.2	[0.00m:hs],[0.20m:ig],[0.90m:ig]	131-31-578008	Link
252491	560829.458	Vibrocore	1999	442630	6207253	-13.5	[0.00m:hl],[2.73m:hs],[4.29m:ds],[5.15m:ds],[5.69m:di]	578028	Link
252492	560829.459	Vibrocore	1999	442654	6207730	-12.5	[0.00m:hs],[1.10m:hs],[1.28m:ds],[1.89m:dl],[2.63m:dl],[3.65m:dl],[5.75m:ms]	578029	Link
252493	550801.86	Vibrocore	1999	437692	6205806	-23.4	[0.00m:hs],[1.20m:hg],[1.30m:hl]	578030	Link
252494	550704.1	Vibrocore	1999	433905	6205762	-23	[0.00m:hs],[0.18m:hs],[1.75m:hs],[1.90m:hs],[3.55m:hs],[3.65m:s],[4.60m:ds]	578031	Link
252495	551304.1	Vibrocore	1999	432029	6199760	-24.6	[0.00m:hs],[0.42m:v],[1.15m:hl],[2.22m:hl]	578032	Link
252496	550704.2	Vibrocore	1999	435696	6199786	-21.8	[0.00m:hs],[0.05m:hs],[0.12m:hs],[1.81m:hl],[2.12m:hg],[2.21m:hl]	578033	Link
252498	550801.87	Vibrocore	1999	440541	6199793	-22.4	[0.00m:v],[4.60m:hs]	578034	Link
252508	550801.88	Vibrocore	1999	444239	6201010	-11	[0.00m:hs],[0.09m:hl],[0.21m:hs],[0.35m:hl],[0.95m:hs],[2.35m:hl],[3.09m:hs]	578035	Link
252510	550704.3	Vibrocore	1999	435090	6194020	-21.7	[0.00m:hs],[0.47m:hg],[0.59m:hs],[1.24m:hs],[4.50m:hg],[4.54m:hs],[4.83m:d]	578036	Link
252511	550801.89	Vibrocore	1999	438667	6193762	-21.8	[0.00m:hs],[2.08m:ds],[3.15m:ds]	578037	Link
252512	550801.90	Vibrocore	1999	442345	6193963	-21.5	[0.00m:hs],[0.15m:hl],[2.40m:hs],[4.80m:ds],[5.60m:ms]	578038	Link
252514	550708.1	Vibrocore	1999	435497	6187762	-20.5	[0.00m:hs],[4.30m:hs],[4.55m:dl],[5.15m:t]	578039	Link
252515	550805.314	Vibrocore	1999	442759	6187742	-19.9	[0.00m:hs],[0.30m:hl],[1.40m:hs],[3.17m:ds],[3.38m:ml],[4.22m:ds],[4.88m:m]	578040	Link
252517	550805.315	Vibrocore	1999	441754	6191777	-21.3	[0.00m:hg],[0.06m:hl],[3.05m:hs],[4.70m:ds],[5.15m:ds],[5.75m:ds]	578041	Link
252518	560829.460	Vibrocore	1999	438239	6213785	-20.9	[0.00m:hs],[0.07m:hs],[0.35m:gl]	578042	Link
252520	560829.461	Vibrocore	1999	441974	6215938	-13.5	[0.00m:hs],[0.30m:hs],[0.64m:hl],[5.30m:hs],[5.39m:ts],[5.47m:ts]	578050	Link
252522	560829.462	Vibrocore	1999	440010	6219801	-17	[0.00m:hs],[0.36m:hs],[0.43m:hs],[1.24m:hs],[4.49m:hs],[4.61m:hs]	578051	Link
252523	560728.1	Vibrocore	1999	437012	6224177	-19.5	[0.00m:hs],[0.85m:hs],[0.95m:hs],[1.11m:dl],[1.40m:gl]	578052	Link
252524	560825.706	Vibrocore	1999	443132	6225794	-16.6	[0.00m:hs],[0.64m:gl]	578053	Link
252525	560825.707	Vibrocore	1999	441998	6231099	-20	[0.00m:hs],[0.05m:gl]	578054	Link
256492	550801.91	Vibrocore	1999	442207	6193977	-20.4	[0.00m:s],[1.00m:g],[1.20m:l]	578043	Link
256494	550801.92	Vibrocore	1999	441765	6195022	-21.6	[0.00m:s],[0.85m:l],[4.65m:v]	578044	Link
256496	550801.93	Vibrocore	1999	443771	6195276	-16.2	[0.00m:l],[0.80m:s],[3.05m:s],[3.65m:v],[5.30m:l]	578045	Link
256512	550801.94	Vibrocore	1999	441821	6195398	-21.5	[0.00m:v],[1.00m:l]	578046	Link
256513	550801.95	Vibrocore	1999	443047	6195950	-18	[0.00m:s],[0.20m:l],[3.19m:s],[4.20m:v],[5.15m:s]	578047	Link
256514	550801.96	Vibrocore	1999	441818	6197833	-20.7	[0.00m:s],[3.70m:l],[4.90m:ms]	578048	Link

256515	550801.97	Vibrocore	1999	443255	6193796	-13.8	[0.00m:s],[0.40m:l]	578049	Link
287042	550801.98	Vibrocore	1993	443562	6197037	-16	[0.00m:s],[0.95m:s]	VC-1a	Link
287062	550801.99	Vibrocore	1993	439539	6198185	-21.8	[0.00m:l],[2.00m:l]	VC-2	Link
287063	550704.4	Vibrocore	1993	433106	6200004	-23	[0.00m:s],[1.55m:l]	VC-3	Link
287162	560732.1	Vibrocore	1993	432362	6212567	-24.5	[0.00m:i]	VC-4	Link
287163	560732.2	Vibrocore	1993	432566	6217845	-26	[0.00m:i],[0.50m:l]	VC-5	Link
287164	560728.2	Vibrocore	1992	432943	6227920	-23.4	[0.00m:s],[0.20m:s],[0.50m:l]	VC-6	Link
300763	550708.2	Vibrocore	2001	437223	6183964	-18.2	[0.00m:hs],[1.00m:hs],[3.19m:ms],[3.36m:ds],[4.00m:ds],[5.10m:ds]	578.165	Link
300764	550805.316	Vibrocore	2001	437907	6185947	-18	[0.00m:hs],[0.35m:hs],[0.52m:hs],[0.70m:hs],[2.12m:hs],[2.14m:hs],[2.83m:h	578.166	Link
300774	550805.317	Vibrocore	2001	440000	6187992	-18.5	[0.00m:hs],[0.15m:hs],[0.35m:hs],[0.72m:hs],[0.79m:hs],[1.85m:hs],[2.85m:ts	578.167	Link
300776	550708.3	Vibrocore	2001	436837	6191782	-19.5	[0.00m:hs],[0.06m:hs],[1.00m:hg],[1.10m:hl],[1.16m:hs],[1.93m:hl],[3.05m:ts	578.168	Link
300813	550805.318	Vibrocore	2001	440787	6191790	-20	[0.00m:hl],[0.28m:hs],[1.30m:hg],[1.35m:ql]	578.169	Link
471676	560727.1	Vibrocore	2012	412386	6226078	-31.5	[0.00m:hs],[0.35m:hs],[0.95m:hs],[1.03m:fs],[1.28m:fs],[1.55m:ts],[2.66m:ti]	NS12-2-15	Link
471678	550703.1	Vibrocore	2012	420205	6195432	-26.4	[0.00m:hs],[4.85m:hi]	NS12-2-25	Link
471679	550707.10	Vibrocore	2012	419721	6189470	-23.5	[0.00m:hs]	NS12-2-07	Link
471680	550707.11	Vibrocore	2012	415281	6187697	-21.8	[0.00m:hs],[2.40m:hs],[3.00m:hs],[3.71m:hg]	NS12-2-18	Link
471682	550706.18	Vibrocore	2012	403997	6186552	-23	[0.00m:hs],[0.80m:hg],[1.00m:hs]	NS12-2-01	Link
471685	550705.21	Vibrocore	2012	385010	6185913	-26	[0.00m:hs],[1.66m:hg],[2.23m:hs],[4.50m:hg],[4.59m:hs],[5.85m:ft]	NS12-2-19	Link
471686	550706.19	Vibrocore	2012	396090	6193108	-21.5	[0.00m:hs]	NS12-2-21	Link
471711	560722.4	Vibrocore	2012	404841	6236565	-32	[0.00m:hs],[1.00m:hp],[2.78m:tv],[4.58m:ti],[4.73m:tv]	NS12-2-13	Link
472569	560728.4	Vibrocore	2010	426003	6229999	-26	[0.00m:hg],[0.10m:hs],[2.40m:hs],[4.30m:ds],[4.60m:ds],[5.00m:ds]	VC-49	Link
472570	560728.5	Vibrocore	2010	431992	6230005	-21.3	[0.00m:hs],[1.30m:hp],[1.31m:hs],[1.80m:hs],[1.90m:hs],[4.60m:hs],[5.00m:h	VC-50	Link
472571	560728.6	Vibrocore	2010	429997	6227997	-23.5	[0.00m:hs],[0.50m:hp],[0.90m:ds]	VC-51	Link
472572	560728.7	Vibrocore	2010	425991	6224003	-26.1	[0.00m:hs],[1.40m:ds]	VC-52	Link
472573	560728.8	Vibrocore	2010	431996	6224003	-24.1	[0.00m:hs],[0.40m:hg],[0.60m:hs],[3.60m:hg],[5.20m:gl],[5.50m:gs]	VC-53	Link
472574	560728.9	Vibrocore	2010	428005	6221993	-24.2	[0.00m:hs],[0.40m:hs],[0.80m:hs],[1.00m:hp],[1.10m:hs],[1.30m:hp],[1.40m:h	VC-54	Link
472575	560732.3	Vibrocore	2010	425993	6217998	-27.3	[0.00m:hs],[1.20m:hs],[4.10m:qi]	VC-55	Link
472576	560732.4	Vibrocore	2010	431998	6218009	-25.5	[0.00m:hs],[0.10m:gs],[0.50m:gi],[1.30m:gl]	VC-56	Link
472577	560732.5	Vibrocore	2010	424001	6215999	-28.2	[0.00m:hs],[0.40m:qs],[0.70m:qs],[4.60m:qs],[4.61m:qi]	VC-57	Link
472578	560732.6	Vibrocore	2010	426003	6211997	-27.5	[0.00m:hs],[0.40m:hs],[0.80m:qs],[2.20m:qs],[3.80m:ql],[4.20m:qi]	VC-58	Link
472579	560732.7	Vibrocore	2010	432002	6211990	-23.6	[0.00m:hs],[0.30m:hs],[1.20m:hp],[1.90m:hs],[2.20m:hs],[2.30m:qs],[3.80m:q	VC-59	Link
472580	550704.5	Vibrocore	2010	425994	6205999	-26.9	[0.00m:hs],[0.50m:gs]	VC-61	Link
472581	550704.6	Vibrocore	2010	431997	6205999	-22.8	[0.00m:hs],[0.80m:hp],[0.90m:hg],[1.00m:qi],[2.80m:qi]	VC-62	Link

472582	550704.7	Vibrocore	2010	430004	6204001	-24	[0.00m:hs],[0.50m:gs]	VC-63	Link
472583	550704.8	Vibrocore	2010	426006	6200008	-24.7	[0.00m:hs],[0.40m:hs],[3.60m:ds],[4.20m:ds],[5.50m:qs]	VC-64	Link
472584	550704.9	Vibrocore	2010	432001	6199999	-22.8	[0.00m:hs],[0.40m:qs],[3.90m:ql]	VC-65	Link
472585	550704.10	Vibrocore	2010	435995	6200008	-20.7	[0.00m:hs],[2.80m:hp],[2.90m:hs],[3.10m:qi],[5.40m:ql]	VC-66	Link
472586	550704.11	Vibrocore	2010	427996	6197995	-23.5	[0.00m:hs],[2.60m:hs],[3.50m:ds]	VC-67	Link
472587	550704.12	Vibrocore	2010	425991	6194000	-24.4	[0.00m:hs],[0.40m:hs],[4.90m:hs],[5.00m:ds]	VC-68	Link
472588	550704.13	Vibrocore	2010	431996	6194001	-21.9	[0.00m:hs],[4.60m:hp]	VC-69	Link
472589	550704.14	Vibrocore	2010	435999	6194005	-20.5	[0.00m:hs],[0.70m:hg],[0.80m:hs],[0.90m:hs],[1.10m:hs],[3.50m:hs],[3.70m:ds]	VC-70	Link
472590	550708.13	Vibrocore	2010	423998	6192004	-24.6	[0.00m:hs],[0.10m:hs],[0.30m:ds],[3.50m:dl],[3.51m:ds],[5.30m:ds]	VC-71	Link
472591	550708.14	Vibrocore	2010	426006	6188006	-23.1	[0.00m:qs]	VC-72	Link
472592	550708.15	Vibrocore	2010	431996	6188003	-21	[0.00m:hp]	VC-73	Link
472593	550708.16	Vibrocore	2010	435990	6190002	-19.8	[0.00m:hs],[0.90m:hs],[1.30m:hs],[3.60m:ds]	VC-74	Link
472594	550708.17	Vibrocore	2010	433999	6185996	-20	[0.00m:hs],[0.50m:hs],[2.00m:ds],[3.00m:ds],[5.30m:ds]	VC-75	Link
472595	550704.15	Vibrocore	2011	427979	6205992	-25.8	[0.00m:hs],[1.10m:hs],[3.60m:hs],[4.20m:hs],[4.60m:hs]	VC-1-1-01	Link
472596	550704.16	Vibrocore	2011	429006	6206005	-24.9	[0.00m:hs],[0.30m:gs],[1.60m:gs],[2.60m:gs]	VC-1-1-02	Link
472597	550704.17	Vibrocore	2011	429987	6206002	-23.8	[0.00m:hs],[0.20m:gs]	VC-1-1-03	Link
472598	550704.18	Vibrocore	2011	430980	6206007	-23.3	[0.00m:hs],[0.40m:hs],[2.80m:hs],[3.00m:hs]	VC-1-1-04	Link
472599	550704.19	Vibrocore	2011	432997	6205997	-22.2	[0.00m:hs],[0.40m:hs],[1.40m:qi],[1.50m:ql]	VC-1-1-05	Link
472600	550704.20	Vibrocore	2011	434002	6205995	-21.9	[0.00m:hs],[0.30m:hs],[1.50m:ds],[3.00m:ds],[3.80m:ds]	VC-1-1-06	Link
472601	550704.21	Vibrocore	2011	428484	6204990	-25.4	[0.00m:hs],[0.70m:hs]	VC-1-1-07	Link
472602	550704.22	Vibrocore	2011	429478	6205006	-25.4	[0.00m:gs]	VC-1-1-08	Link
472603	550704.23	Vibrocore	2011	430503	6205015	-23.7	[0.00m:hs],[0.30m:gs]	VC-1-1-09	Link
472604	550704.24	Vibrocore	2011	431499	6205008	-23.1	[0.00m:hs],[0.40m:hs],[4.80m:ql],[5.80m:qi]	VC-1-1-10	Link
472605	550704.25	Vibrocore	2011	432493	6205012	-22.5	[0.00m:hp],[0.10m:hs],[0.80m:hs],[1.60m:hl],[2.00m:hs],[2.10m:ql],[2.80m:ql]	VC-1-1-11	Link
472606	550704.26	Vibrocore	2011	433496	6204999	-22.2	[0.00m:hs],[1.20m:ql]	VC-1-1-12	Link
472607	550704.27	Vibrocore	2011	434520	6205001	-22	[0.00m:hs],[1.30m:hl],[1.90m:hs],[2.60m:ds],[3.60m:ds]	VC-1-1-13	Link
472608	550704.28	Vibrocore	2011	428001	6204008	-25.3	[0.00m:hs],[0.30m:hs],[0.50m:hs],[2.50m:hs],[2.60m:hs],[3.30m:hl],[3.40m:hs]	VC-1-1-14	Link
472609	550704.29	Vibrocore	2011	429000	6204009	-24.7	[0.00m:hs],[0.50m:gs],[3.90m:gs]	VC-1-1-15	Link
472610	550704.30	Vibrocore	2011	430980	6204006	-23.4	[0.00m:hs],[1.80m:gs]	VC-1-1-16B	Link
472611	550704.31	Vibrocore	2011	431988	6204008	-22.8	[0.00m:hs],[4.70m:ql]	VC-1-1-17	Link
472612	550704.32	Vibrocore	2011	433003	6203988	-22.2	[0.00m:hs],[0.20m:hs],[1.20m:qi],[1.70m:ql]	VC-1-1-18	Link
472613	550704.33	Vibrocore	2011	434018	6203991	-21.7	[0.00m:hs],[1.40m:hs],[1.90m:ds]	VC-1-1-19B	Link
472614	550704.34	Vibrocore	2011	428486	6203003	-24.7	[0.00m:hs],[0.50m:hs],[1.80m:hs],[4.10m:hg],[4.40m:hs],[5.10m:hs],[5.30m:h]	VC-1-1-20	Link

472615	550704.35	Vibrocore	2011	429485	6203004	-24.1	[0.00m:gs]	VC-1-1-21	Link
472616	550704.36	Vibrocore	2011	430501	6203013	-23.5	[0.00m:hs],[0.20m:gs]	VC-1-1-22	Link
472617	550704.37	Vibrocore	2011	431518	6202999	-23.1	[0.00m:hs],[4.50m:qi]	VC-1-1-23B	Link
472618	550704.38	Vibrocore	2011	432497	6202982	-22.6	[0.00m:hs],[0.40m:ql],[2.50m:ql],[4.20m:ql]	VC-1-1-24	Link
472619	550704.39	Vibrocore	2011	433515	6202994	-22.3	[0.00m:hs],[0.90m:ql]	VC-1-1-25	Link
472620	550704.40	Vibrocore	2011	434507	6202990	-21.6	[0.00m:hs],[0.90m:hs],[1.10m:ds],[5.30m:ds]	VC-1-1-26	Link
472621	550704.41	Vibrocore	2011	427990	6201999	-24.8	[0.00m:hs],[0.30m:hs],[2.40m:gs],[2.70m:gs]	VC-1-1-27	Link
472622	550704.42	Vibrocore	2011	429001	6201993	-24	[0.00m:hs],[1.30m:hs],[1.80m:gs]	VC-1-1-28	Link
472623	550704.43	Vibrocore	2011	430007	6201991	-23.8	[0.00m:hs],[0.30m:hs],[0.50m:gs]	VC-1-1-29	Link
472624	550704.44	Vibrocore	2011	431009	6202003	-23.1	[0.00m:hs],[0.20m:hs]	VC-1-1-30	Link
472625	550704.45	Vibrocore	2011	432016	6202010	-22.3	[0.00m:hs],[0.30m:hs],[0.80m:qi],[1.00m:ql]	VC-1-1-31	Link
472626	550704.46	Vibrocore	2011	433006	6202007	-22.1	[0.00m:hs],[0.90m:ql]	VC-1-1-32	Link
472627	550704.47	Vibrocore	2011	434022	6201996	-22.2	[0.00m:hs],[0.60m:ql]	VC-1-1-33	Link
472628	550704.48	Vibrocore	2011	430494	6201485	-23.2	[0.00m:hs],[0.40m:gs]	VC-1-1-34	Link
501078	560829.463	Vibrocore	2013	442563	6217138	-10.62	[0.00m:hs],[0.50m:hs],[1.00m:ml]	VHS_CR1_VC+001	Link
501079	560829.464	Vibrocore	2013	443992	6217020	-5.82	[0.00m:hs],[0.60m:ms]	VHS_CR1_VC+003	Link
501080	560829.465	Vibrocore	2013	441138	6217260	-15.4	[0.00m:hs],[0.50m:g],[1.10m:g],[1.40m:g],[1.60m:g],[2.80m:g],[3.30m:g]	VHS_CR1_VC+006	Link
501081	560829.466	Vibrocore	2013	440373	6217326	-15.89	[0.00m:hs],[0.40m:hs],[3.50m:hs]	VHS_CR1_VC+007	Link
501082	560829.467	Vibrocore	2013	443346	6214301	-4.99	[0.00m:hs]	VHS_CR2_VC+000	Link
501083	560829.468	Vibrocore	2013	441493	6213953	-12.78	[0.00m:hs],[0.20m:hs]	VHS_CR2_VC+005	Link
501084	560829.469	Vibrocore	2013	441493	6213955	-12.78	[0.00m:hs],[0.70m:hs]	VHS_CR2_VC+005	Link
501085	560829.470	Vibrocore	2013	440252	6213719	-13.83	[0.00m:hg]	VHS_CR2_VC+006	Link
501086	560829.471	Vibrocore	2013	439489	6213574	-17.8	[0.00m:hs]	VHS_CR2_VC+007	Link
501087	560829.472	Vibrocore	2013	443722	6214373	-2.9	[0.00m:hg]	VHS_CR2_VC-002	Link
662844	560722.8	Vibrocore	2020	403487	6236723	-32	[0.00m:hs],[0.50m:hp],[2.24m:ft],[2.35m:tl],[2.53m:ts],[2.62m:ti],[2.70m:ts]	VKY-09	Link
662847	550701.1	Vibrocore	2020	383404	6206132	-32	[0.00m:hg],[0.20m:hs],[0.32m:hg],[0.51m:hs],[0.60m:ts]	VKY-101	Link
662848	550704.182	Vibrocore	2020	425343	6203055	-26	[0.00m:hs],[0.97m:ts],[1.42m:tg],[1.56m:ts]	VKY-105	Link
662849	550702.1	Vibrocore	2020	394528	6207280	-29	[0.00m:hs],[0.27m:hg],[0.62m:hs],[1.99m:hg],[2.11m:ts]	VKY-106	Link
662851	560729.1	Vibrocore	2020	383131	6210087	-30	[0.00m:hs],[2.63m:hg],[3.15m:ts]	VKY-110	Link
662852	560729.2	Vibrocore	2020	384841	6209967	-30	[0.00m:hs],[0.78m:hs],[2.70m:hg],[2.98m:hs]	VKY-111	Link
662853	560730.2	Vibrocore	2020	396251	6209212	-30	[0.00m:hs],[0.59m:hs],[0.74m:ts]	VKY-112	Link
662854	560731.1	Vibrocore	2020	407393	6208383	-24	[0.00m:hs],[0.73m:hs],[4.98m:ts]	VKY-114	Link
662855	560730.3	Vibrocore	2020	398583	6211894	-24	[0.00m:hs]	VKY-117	Link

662859	560732.44	Vibrocore	2020	423402	6218550	-26	[0.00m:hs],[0.25m:ts]	VKY-124	Link
662870	560728.32	Vibrocore	2020	425051	6231206	-27	[0.00m:hs],[1.25m:ts]	VKY-21	Link
662871	560728.33	Vibrocore	2020	423340	6229320	-27	[0.00m:hs],[0.96m:hs]	VKY-22	Link
662872	560727.3	Vibrocore	2020	417525	6229734	-30	[0.00m:hs],[0.86m:ts]	VKY-23	Link
662873	560727.4	Vibrocore	2020	410184	6230244	-30	[0.00m:hs],[1.64m:ts]	VKY-24	Link
662874	560727.5	Vibrocore	2020	407095	6230461	-30	[0.00m:hs],[1.85m:hl],[2.45m:hv],[2.61m:hl],[3.01m:hv],[3.41m:hs]	VKY-25	Link
662877	560725.6	Vibrocore	2020	387853	6229805	-35	[0.00m:hs],[0.11m:hs],[3.61m:hv]	VKY-28	Link
662878	560725.7	Vibrocore	2020	389719	6229661	-30	[0.00m:hs],[0.78m:hs]	VKY-29	Link
662879	560725.8	Vibrocore	2020	387045	6227869	-34	[0.00m:hs],[0.59m:hs],[2.59m:hi],[3.59m:hl],[5.10m:ts]	VKY-30	Link
662881	560728.34	Vibrocore	2020	424707	6223200	-26	[0.00m:hs],[1.80m:ts]	VKY-32	Link
662883	560727.6	Vibrocore	2020	408025	6221187	-27	[0.00m:hs],[0.40m:ti],[1.00m:tv],[1.70m:tl]	VKY-35	Link
662884	560731.2	Vibrocore	2020	408537	6216331	-26	[0.00m:hs],[1.00m:hs],[1.19m:ts]	VKY-36	Link
662887	560730.5	Vibrocore	2020	405501	6214514	-25	[0.00m:hs],[1.33m:hs],[1.43m:hs],[1.58m:hs],[1.72m:hs],[2.66m:ts]	VKY-39	Link
662887	560730.5	Vibrocore	2020	405501	6214514	-25	[0.00m:hs],[1.33m:hs],[1.43m:hs],[1.58m:hs],[1.72m:hs],[2.66m:ts]	VKY-39	Link
662888	560730.6	Vibrocore	2020	404310	6208594	-24	[0.00m:hs],[0.30m:hs],[4.70m:hv]	VKY-40	Link
662889	560729.3	Vibrocore	2020	386322	6207847	-28	[0.00m:hs],[3.32m:hg],[3.62m:hs]	VKY-41	Link
662890	550702.2	Vibrocore	2020	397114	6207091	-27	[0.00m:hs],[0.28m:hs]	VKY-42	Link
662891	550702.3	Vibrocore	2020	401062	6204838	-24	[0.00m:hg],[0.20m:hs]	VKY-43	Link
662892	550702.4	Vibrocore	2020	399776	6204932	-25	[0.00m:hg],[0.29m:hs]	VKY-44	Link
662893	550604.2	Vibrocore	2020	372671	6204816	-35	[0.00m:hg],[0.08m:ts],[2.48m:ts],[4.78m:tg],[5.23m:ts]	VKY-45	Link
662894	550702.5	Vibrocore	2020	400877	6202843	-25	[0.00m:hg],[1.00m:hs]	VKY-46	Link
662895	550702.6	Vibrocore	2020	404083	6202603	-23	[0.00m:hs],[0.90m:hg],[1.40m:hs]	VKY-47	Link
662896	550704.183	Vibrocore	2020	425053	6198440	-25	[0.00m:hs],[2.60m:ts]	VKY-48	Link
662897	550704.184	Vibrocore	2020	422234	6197332	-26	[0.00m:hs],[1.65m:hs],[5.53m:hs]	VKY-49	Link
662898	550702.7	Vibrocore	2020	403505	6195707	-25	[0.00m:hs],[0.70m:hg],[0.97m:hi],[3.47m:hg]	VKY-50	Link
662899	550703.2	Vibrocore	2020	416092	6194857	-21	[0.00m:hs],[2.44m:hg],[2.58m:hs],[2.75m:hg],[2.92m:ts]	VKY-51	Link
662900	550701.2	Vibrocore	2020	389420	6195599	-31	[0.00m:hg],[0.17m:ms]	VKY-52	Link
662901	550703.3	Vibrocore	2020	413514	6193914	-21	[0.00m:hs],[0.28m:hs]	VKY-53	Link
662902	550703.4	Vibrocore	2020	419111	6193516	-23	[0.00m:hs],[3.65m:hg],[3.72m:hs],[3.77m:hg],[3.83m:hs]	VKY-54	Link
662903	550708.32	Vibrocore	2020	424553	6191708	-25	[0.00m:hs],[0.86m:ts]	VKY-55	Link
662904	550701.3	Vibrocore	2020	388188	6193680	-33	[0.00m:hg],[0.12m:hs],[0.73m:hg],[0.85m:ql],[3.10m:ms]	VKY-56	Link
662905	550707.13	Vibrocore	2020	407134	6192368	-20	[0.00m:hs],[0.23m:hg],[0.33m:hs],[1.30m:hg]	VKY-57	Link
662906	550707.14	Vibrocore	2020	409166	6192217	-20	[0.00m:hs],[1.30m:hg]	VKY-58	Link

662907	550707.15	Vibrocore	2020	415482	6191776	-21	[0.00m:hs],[0.44m:hg],[0.64m:hs],[2.06m:hg],[2.37m:hs],[4.60m:hs]	VKY-59	Link
662908	550708.33	Vibrocore	2020	422247	6191282	-26	[0.00m:hs],[0.93m:hp],[1.00m:ft],[1.44m:ts]	VKY-60	Link
662909	550608.13	Vibrocore	2020	372329	6192805	-36	[0.00m:hs],[1.26m:hg],[1.32m:hs],[1.82m:hg],[1.97m:ts]	VKY-61	Link
662910	550705.23	Vibrocore	2020	378011	6192335	-36	[0.00m:hs],[0.58m:ml],[3.63m:ds],[4.69m:ds]	VKY-62	Link
662911	550705.24	Vibrocore	2020	384262	6191953	-28	[0.00m:hs],[0.50m:hs],[0.60m:hs]	VKY-63	Link
662912	550706.20	Vibrocore	2020	404104	6190551	-23	[0.00m:hs],[0.21m:hs],[0.67m:hg],[0.94m:hs],[4.40m:hp]	VKY-64	Link
662913	550707.16	Vibrocore	2020	412300	6189990	-19	[0.00m:hs]	VKY-65	Link
662914	550708.34	Vibrocore	2020	423716	6189180	-25	[0.00m:hs],[0.50m:ts]	VKY-66	Link
662915	550707.17	Vibrocore	2020	414954	6187807	-20	[0.00m:hs],[3.20m:hg],[3.95m:hs],[4.38m:hg],[4.56m:hs]	VKY-67	Link
662916	550708.35	Vibrocore	2020	422243	6187295	-25	[0.00m:hs]	VKY-68	Link
662917	550608.14	Vibrocore	2020	372325	6188796	-35	[0.00m:hs],[1.70m:hv],[2.13m:ts]	VKY-69	Link
662918	550707.18	Vibrocore	2020	408811	6186217	-18	[0.00m:hg],[0.86m:hs]	VKY-70	Link
662919	550708.36	Vibrocore	2020	423792	6185153	-24	[0.00m:hs],[0.15m:ts]	VKY-71	Link
662935	550604.3	Vibrocore	2020	372176	6198815	-35	[0.00m:hs],[1.45m:hg],[1.90m:ts]	VKY-90	Link
662936	550702.8	Vibrocore	2020	403470	6200625	-23	[0.00m:hg],[0.37m:hs],[0.48m:hg],[0.58m:hs]	VKY-91	Link
662937	550704.185	Vibrocore	2020	422611	6199274	-26	[0.00m:hs],[4.03m:hs]	VKY-94	Link
662938	550701.4	Vibrocore	2020	389409	6201620	-26	[0.00m:hs]	VKY-95	Link
662939	550704.186	Vibrocore	2020	423912	6201212	-26	[0.00m:hs],[2.96m:ts]	VKY-96	Link
662940	550703.5	Vibrocore	2020	410736	6202130	-23	[0.00m:hs],[0.30m:hs]	VKY-98	Link
662941	550703.6	Vibrocore	2020	408512	6202293	-22	[0.00m:hs]	VKY-99	Link